report

Maximum allowable pressures

Maximum allowable pressures during horizontal directional drillings focused on sand

Student: Birgitte Keulen
9431002

Counselling Team: Prof. dr. ir. A. Verruijt
Ir. G. Arends
O.E. Strack B. Sc
Ir. D.R. Mastbergen
Ing. H.H.J. van der Werff

TU Delft
Technische Universiteit Delft

DCA

WL | delft hydraulics

Visser & Smit Hanab

COLOPHON

Graduation research

Title:	Maximum allowable pressure
Subtitle:	Maximum allowable pressures during horizontal directional drillings focused on sand
Document:	report
Status:	final
Institute:	Delft University of Technology Faculty of Civil Engineering and Geosciences Sub faculty Civil Engineering, department Geomechanics
Location:	Delft Hydraulics, Marine & Coastal Management

Graduation student

Birgitte A.M. Keulen 9431002
Brabantse Turfmarkt 20
2611 CN Delft
015-2137031

B.A.M.Keulen@student.tudelft.nl
BirgitteKeulen@hotmail.com
Birgitte.Keulen@horvat.nl

Counselling team

- Prof. dr. ir. A. Verruijt, Professor of Geomechanics (chairman)
  Faculty of Civil Engineering and Geosciences
- Ir. G. Arends, University lecturer of Underground Space Technology
  Faculty of Civil Engineering and Geosciences
- O. Erik Strack B. sc, assistant researcher Geotechnical Laboratory
  Faculty of Civil Engineering and Geosciences
- Ir. D.R. Mastbergen, senior advisor/researcher dredging & slurry technology
  Delft Hydraulics, marine & coastal management
- Ing. H.H.J. van der Werff, Head Engineering Department, Visser & Smit Hanab

Supported by

Drilling Contractors Association, Europe

Contact address

Postal Address:
Geotechnical Laboratory
Delft University of Technology
sub faculty of Civil Engineering
P.O.Box 5048
2600 GA Delft
The Netherlands
Tel: +31 (0)15 278 1880

Visiting Address:
Geotechnical Laboratory
Keverling Buismanweg 1
Delft

PREFACE

This is the report of the thesis research done within the framework of the study of Civil Engineering at Delft University Technology. It is the last subject of the curriculum (duration of five years). The research was performed at the department of Geomechanics in the period of January to September 2001.

I have enjoyed working on this research and for that I would like to thank a few people for their support.

First I would like to thank the DCA (Drilling Contractors Association) for the Sponsorship Award 2000, which I received. I hope that this report will contribute to the industry. Also I would like to thank Delft Hydraulics for providing the facilities of a place to work at the institute. I would like to thank the people at Visser Smit Hanab for their efforts to explain the current approach.

Next, I would like to thank the counselling team with whom it was very pleasant to work. I regard myself lucky to have had such good and reasonable counselling. Also the non-official counsellor, my colleague-student Rob Vos, I would like to thank for listening to my ideas, talking about his, getting coffee and all other activities that made the period very pleasant and relaxed.

I certainly have forgotten to thank people. I hope they will see this apology as a 'thank you'.

Birgitte Keulen
Delft, 5 september 2001

READERS' GUIDE

This document consists of the main report and the appendices. The main report is kept compact in order to make it more pleasant to read. The appendices contain more elaborate information and full mathematical derivations of the equations. The appendices form an integral part of the document.

Report

In the report's first chapter an introduction is given to the technique. The questions regarding the behaviour of soil under fluid pressure during a horizontal directional drilling (HDD) are outlined. Next a problem definition and objective are given and the steps taken in the research are presented.

In the second chapter an inventory is given of how in current practice the maximum allowable pressures are approached, of the research that was done within the framework of BTL and of the available models. From this inventory conclusions are drawn.

In chapter three soil models ('new' models) are presented to describe the behaviour of a cylindrical and a spherical cavity under pressure. These models are compared to the model at the basis of the equations of L&H. In the following chapter it is tried to introduce failure into these models. The new failure criterion (maximum strain) is compared to the failure criterion of L&H (plasticity radius). Finally in the last chapter conclusions and recommendations are presented.

Appendices

In the appendices at first the lists (symbols, literature, etc) are given, followed by a more elaborate description of the HDD technique (appendix B). Appendix B is the background information for chapter one.

Then a more elaborate description of the literature (BTL-research), which is the basis for the thesis research, is given (appendix C). Both tests and models are described. This is the background information for chapter two.

The following appendix (appendix D) contains a full description of the model that stands at the basis of the equations of Luger and Hergarden. Next to that a comparison is made between the failure criterion of maximum radius of the plasticity zone and of maximum strain. This is the background information for chapter two, three and four.

In appendix E the soil models of chapter three are fully described. These soil models stand also at the basis of the derivation of failure criteria. Therefore this appendix is background information for chapter three and four.

Finally in the last appendix (appendix F) the BTL experiment data regarding maximum allowable pressure is used to calculate maximum allowable pressures according to Luger and Hergarden and according to maximum strain. In this appendix reference is made to appendix C. The appendix is background information for chapter four.

Note: The equations that are presented in the report only are placed between round brackets. The equations derived in the appendices are placed between square brackets.

SUMMARY

Horizontal directional drilling (HDD) is a rather simple installation technique for pipes for public infrastructure and it has therefore become increasingly popular. When HDD is started, a pilot drilling is made first; a small borehole is made in the soil along the trajectory. After the pilot drilling the borehole is enlarged with a reamer until the designed diameter is obtained and the product pipe is pulled in.

Drilling fluid or mud is used for the stability of the borehole and to transport the excavated soil. A certain minimum mud pressure is needed to ensure a return flow and to ensure that the borehole does not collapse. In order to prevent soil failure, it is necessary that the pressure will not exceed a certain maximum.

At present in the Netherlands and also abroad, in order to compute the maximum allowable mud pressures, it is assumed that the cavity expansion theory applies in the borehole at greater depth. The equations to calculate this pressure were first presented by Luger and Hergarden (L&H, 1988). This theory assumes plastic deformations, which lead to failure. However, recent research has shown that soil failure due to hydraulic fracturing is an important failure mechanism also.

In the framework of BTL (Boren Tunnels & Leidingen) research was done to look at whether hydraulic fracturing was observed before in the context of liquid injection in softer soils like clay. The process of hydraulic fracturing in soil with cohesion (clay) was recognised in literature indeed and models were developed. However no literature was found on hydraulic fracturing in soils without cohesion (sand).

This thesis research was done to improve the knowledge of the behaviour of sand and bentonite around a borehole in order to better determine the soil failure process under maximum pressures. New soil models to describe soil behaviour were developed for a cylindrical and a spherical cavity under fluid pressure. The soil model for a cylindrical cavity is comparable to the soil model at the basis of the equations derived by L&H. The soil models assume;

- the medium to be homogeneous and isotropic,
- to have infinite dimensions (gravity neglected) and therefore prior to the application of the load the entire soil mass has an isotropic effective stress,
- the soil behaves in the plastic zone as a compressible plastic solid, defined by Mohr-Coulomb shear strength parameters (c, φ). Beyond the plastic zone the soil is assumed to behave as a linearly elastic, isotropic solid defined by a modulus of deformation (E) and a Poisson's ratio (v).

Next to that, in the derived models for this thesis it is possible to take dilatancy into account.

It was tried to introduce failure and especially hydraulic fracturing into these 'new' models. The introduction of the criterion of a maximum strain instead of a maximum radius of plasticity (L&H) seems to satisfy better the results found in the mentioned BTL-experiments. However it is difficult to draw absolute conclusions as the model is not a full representation of the reality due to;

- the assumptions made for the soil model,
- the parameters that are used for calculation are difficult to determine, showing wide ranges of variation,
- stratified soil can not be introduced.

It is therefore recommended to use the equations with a lot of precaution.

TABLE OF CONTENTS

1 INTRODUCTORY

1.1 Background

1.1.1 Horizontal Directional Drilling

Traditional methods of installing pipelines and cables require the excavation of trenches. The trenches are backfilled after the installation of the pipe or cable.

In the early 80's, the first pipelines in The Netherlands were installed with the trenchless technique of horizontal directional drilling (HDD). The technique was commonly used in the oil industry to drill vertical holes (for oil or gas extraction). In the last decades the use of the technique has expanded and is more and more used in urban areas in order to reduce discomfort for local residents.

Research is done to understand the processes during the drilling and to predict the pressures and forces. In the Netherlands research is done within the framework of BTL (Boren van Tunnels en Leidingen). This research program is the basis for this thesis.

A horizontal directional drilling can be separated in three phases; pilot boring, pre-reaming and pipe pull back installation. During the pilot boring a small borehole is made along the design trajectory of the drilling. To enlarge the borehole until the designed size, a reamer is used. The number of reaming phases depends on the size of the designed diameter. The last phase is the pullback operation. The drilling rig is standing at the entry point. The product pipe is prepared at the exit point of the drilling. The drill pipe with the product pipe attached is pulled back through the borehole to the entry point. A more elaborate description of the technique is given in appendix B.

1.1.2 Maximum and minimum pressures

A drilling fluid, usually a bentonite water mixture, is pumped into the borehole through the drill pipes to the nozzles in the drill head or reamer. The drilling fluid is used to secure the stability of the borehole and has to transport the cuttings out of the borehole by the return flow. To secure these functions a certain minimum mud pressure is needed. In order to prevent soil failure, it is necessary that the pressure will not exceed a certain maximum.

In brief, there are limits to the pressures:

- An upper limit – This is the maximum pressure the soil can sustain without failure.
- A lower limit – The minimum pressure has to be kept above a certain limit to ensure a return flow and to ensure that the borehole does not collapse.

However, a flow rate is installed and not a pressure. It should therefore be realised that the occurring pressure can only indirectly be influenced. An example of pressures during a drilling is given in Figure 1.

Exceeding the maximum allowable fluid pressure may result in soil failure. This is generally unacceptable and therefore a more refined knowledge of the process is needed. At present it is assumed that the cavity expansion theory applies to the process that occurs in the borehole in case of failure at deeper parts of the drilling (for shallow parts it is assumed that a wedge is pushed out of the soil). This theory was first developed by Vesic (1972) and further developed by Luger and Hergarden (L&H-1988).

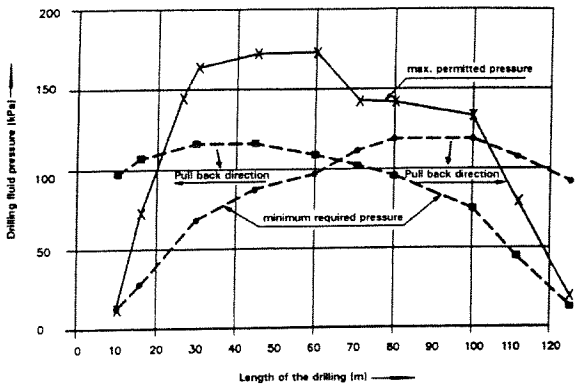

Figure 1: Maximum allowed and minimum required pressure during drilling

This theory assumes that plastic deformations lead to failure. However, recent research has shown that soil failure due to hydraulic fracturing also plays an important role in the failure mechanism.

1.2 Motive and object of thesis research

As stated in the previous paragraph the process of hydraulic fracturing was observed. Literature research showed that hydraulic fracturing was already recognised for cohesive soft soils like clay. Furthermore models were found describing this failure process in cohesive soil. However, models and tests showing hydraulic fracturing in non-cohesive soils, like sand, were not found.

1.2.1 Problem definition thesis

When the maximum allowable pressure of drilling fluid is reached during a HDD in sand, the failure behaviour in sand and the accompanying fluid pressure is unknown.

1.2.2 Object definition thesis

Improve the knowledge of the failure behaviour of sand with bentonite around a borehole in order to better determine the maximum allowable drilling fluid pressure in sand.

1.2.3 Limitations thesis

Although analytic models can only roughly approximate soil behaviour, they can be used as a tool to gain insight into the fundamental nature of the problems they address. Since general understanding of the soil behaviour is the main objective in this research the solutions will be restricted to analytical solutions.

1.3 Structure research*

The successive of the steps taken to approach the objective of the research for this thesis were the following:

- Inventory of literature and research on the subject, and current design and construction practice, in order to describe the current state of the art and to outline the demands on 'new' soil models and failure criteria.
- Definition of soil model to describe in general soil behaviour.
- Possibilities of the introduction of failure into soil model.
- Comparison of 'new' soil models and failure - criteria to current approach.

On the basis of these steps conclusions were drawn and recommendations were made.

* For the structure of the report reference is made to the readers' guide.

2 INVENTORY

In this chapter the current knowledge regarding maximum allowable pressures is inventoried. This comprises the literature on the subject, research done and current design and construction practice. This is done in order to describe the current state of the art and to outline the demands on 'new' soil models and failure criteria.

The descriptions in this chapter are kept brief in general. A more elaborate characterisation of the subjects is given in appendix C.

First, an elaborate description is given of how nowadays in current design and construction practice is dealt with maximum allowable pressures during horizontal directional drilling. This includes also the uncertainties that exist concerning the pressure that actually occurs in the borehole. Next an overview is given of what was learned of the research done by BTL regarding maximum allowable pressures. Finally, the available models describing the behaviour of soil focussed on hydraulic fracturing found within the research by BTL are presented.

2.1 Current Approach

The following paragraph explains how, in practice at present, the maximum allowable pressures are dealt with. Remarks will be made regarding the design and the construction phase.

2.1.1 Calculations – Design phase

In the design phase an estimate is made for the maximum allowable pressure. This is done on the basis of the method recommended by appendix E in NEN 3651. This method is developed by Luger & Hergarden and explained in appendix D.

For a proper assessment and interpretation of the recommended design approach in NEN 3651 a considerable amount of soil parameters have to be established. How these parameters are established, is explained in the following paragraph.

Assumptions & Equations from NEN 3651

The model is based on the assumption of axial symmetry around the borehole and the following four conditions:

- Equilibrium
- Hooke's law for increments of elastic deformation
- Mohr-Coulomb's failure criterion.
- Absence of isotropic deformations in the plastic zone

The following equation applies;

$$p_{max} = p'_{max} + u \qquad (1)$$

$$p'_{max} = (p'_f + c \cdot \cot\varphi) \cdot \{(\frac{R_0}{R_{p,max}})^2 + Q\}^{\frac{-\sin\varphi}{1+\sin\varphi}} - c \cdot \cot\varphi \qquad (2)$$

in which;

$$Q = \frac{(\sigma'_0 \cdot \sin\varphi + c \cdot \cos\varphi)}{G} \qquad (3)$$

and;

$$p'_f = \sigma'_0(1+\sin\varphi) + c\cos\varphi \qquad (4)$$

and;

p_{max}	maximum allowable mud pressure
u	initial in-situ pore pressure
p'_{max}	maximum allowable *effective* mud pressure
σ'_0	the initial effective stress
φ	internal friction angle
c	cohesion
R_0	initial radius of the borehole
$R_{p,\,max}$	maximum allowable radius plastic zone
G	shear modulus

The effective mud pressures are defined as; $p' = p-u$ and $p'_f = p_f - u$

The other criterion is related to the limit pressure. The effective limit pressure p'_{lim} follows from (2) if $R_{p,max}$ approaches infinity:

$$p'_{lim} = (p'_f + c\cdot\cot\varphi)\cdot Q^{\frac{-\sin\varphi}{1+\sin\varphi}} - c\cdot\cot\varphi \qquad (5)$$

A safety factor is used, p'_{lim} is multiplied by 0.9. If this value is lower than p'_{max} then this $0{,}9*p'_{lim}$ should be regarded as the maximum allowable pressure.

Input

The input parameters of the equation for p'_{max} (2) and p'_{lim} (5) are σ'_0, φ, c, R_0, $R_{p,max}$ (only for p_{max}) and G. Not all of these parameters are derived directly from the soil investigation. Below is explained how they are derived nowadays in design practice (Figure 2:).

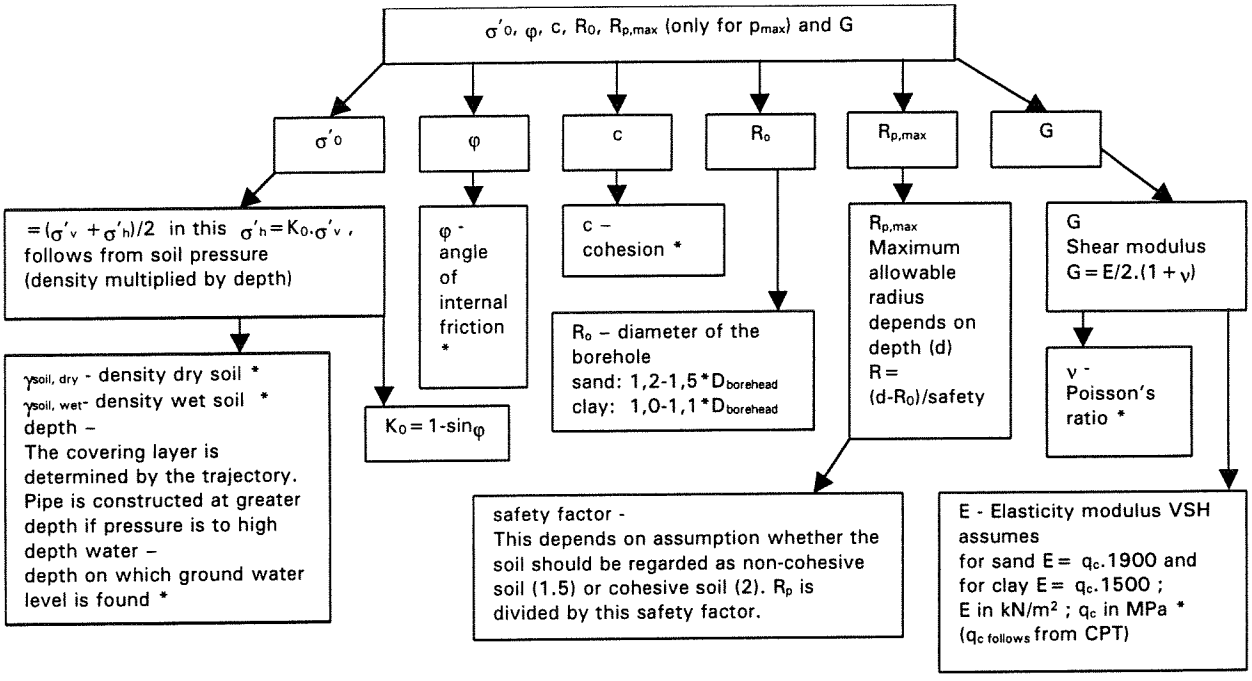

- assumed, on basis of soil investigation. In The Netherlands there are, for a horizontal directional drilling, always some CPT's (cone penetration tests) available and usually a bore log of a soil investigation borehole.

Figure 2: Parameter determination in practice

The most important difficulty occurs when the soil is not homogeneous. To generate output for layered soil, an engineering judgement is made from the soil investigation. Soil characteristics are chosen which are representative for the whole cover. With an educated guess the angle of internal friction (φ), the density of the soil (γ), and the cohesion (c) are determined for a specific cross section. These values are chosen more conservative when the soil is "weaker" (clay or peat) or in the absence of a stronger overlaying strata. When in doubt, the values are varied to determine the sensitivity and the resulting effect.

Output

The output is also interpreted on the basis of experience. The minimum required pressure to maintain the return flow (p_{return}) must be smaller than the maximum allowable pressure (p'_{max} or p'_{lim}). However, the design does not meet the requirements when: $p_{return} = p'_{max}$ or p'_{lim}.

An additional requirement can be found in the appendix of NEN3651. A safety margin of 0.5 bar is recommended. In practice a larger difference is often taken into account. This depends on the rig equipment used. When a larger rig is used the safety margin should be set larger. It is obvious that with a larger rig more damage can be caused due to a larger volume of mud that can be pumped into the ground.

Safety

From the above it can be concluded that safety limits are taken into account in three different ways:

- interpretation of input parameters
- safety factor on R_p
- interpretation of results

2.1.2 Construction practice

This paragraph explains how the maximum allowable pressure is used in the construction practice.

Contemporary procedures in practice

Nowadays the construction practice at drilling contractor, Visser & Smit Hanab (VSH) for controlling the mud pressures is as follows (see also Figure 3):

- A calculation of the maximum allowable pressure is made as described in the previous paragraph (§ 2.1.1).
- On site a pump test is performed (pumping different flows, to measure and determine the pressure losses between the mud pump and downhole assembly).
- The losses due to friction along the drill string are calculated on the basis of roughness and length of the drill string.
- The measured pressure head on the rig minus the losses due to the nozzles and the losses due to pipe friction give an indication of the pressure in the hole. This can be compared to the maximum allowable pressure.

Note: However, it is recognised that the return flow and the borehole pressures are interrelated and mutually in balance (see next subparagraph - Pressure in the borehole).

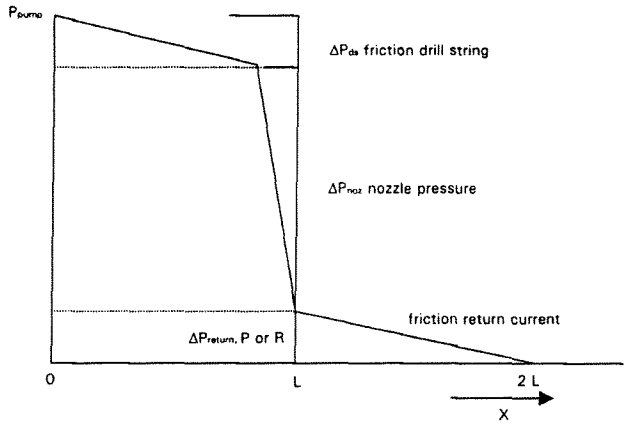

Figure 3: Pressure losses during drilling fluid cycle

It is also possible to measure the mud pressure in the borehole. However, until now, this is only done in research and special projects. In those cases the pressure gauge is not placed directly on the head, but a little bit behind it. It is technical difficult to measure the pressure real time. Transport of data from the head to an above ground location is difficult (small diameter of drill pipe) and only feasible during pilot drillings when a cable in the drill pipe is installed. Therefore the measurements that have been done during the BTL research where all done with a data logger that was read afterwards.

Pressure in the borehole

In the research done by BTL it was learned that the pressure in the borehole is determined by the return flow and not by the pump pressure on the rig. The pressure in the return flow consists of two components; a static and a dynamic.

The density and height of the fluid column determine the static pressure in the borehole. There is usually no influence of the ground water in the borehole due to the sealing of the borehole (plastering). Only when the borehole gets unstable or the sealing is damaged; then the ground water level can have influence on the local pressure in the borehole.

The pressure loss is the dynamic component of the return flow. To transport the mixture to ground surface, there has to be an overpressure in the borehole in relation with the static component. This component depends on the length and diameter of the borehole and the rheology of the drilling fluid. Because the velocity of the mixture is low, the yield stress plays an important role defining the occurring pressure.

2.1.3 Interaction design & construction

At this moment the exchange of information between the drilling contractor and the designers can be improved significantly. Failure, mud outbreak, or loss of return flow is not always reported or when reported analysed. Developments for monitoring the key operational parameters are in progress. Currently there is not a set standard in the industry. Officially, for HDD American oil industry standards are applied, but these are not always suitable. It will take some time before data, concerning pressure measurements and recognised failure, is available and monitoring procedures are applied implemented. It is concluded that, at present, theory can hardly be calibrated against practical data or experience.

2.2 Research done concerning maximum allowable pressures

In this paragraph experiments and research done within the framework of BTL are presented. This is only a brief overview. Reference is made to appendix C in which a more elaborate description is given.

2.2.1 Sight experiment in gelatine (BTL17)

In the framework of BTL (BTL17, 1996) the first experiment regarding maximum allowable pressures was a sight experiment to get qualitative results regarding the failure of cohesive material under fluid pressure. A drilling (scale 1:20) was performed with a coloured liquid in transparent medium, gelatine. Instead of cavity expansion, radial fractures originated in random directions. This resembled hydraulic fracturing, as it is known from rock-mechanics. The question was raised whether the cavity expansion theory gave an adequate description of the failure mechanism. A literature search was started (see § 2.3.2).

Figure 4: Photo blow out in gelatine (BTL17)

2.2.2 Sight experiment in dredging test channel (BTL21)

This sight experiment was followed by a new experiment in the dredging flume of Delft Hydraulics (BTL21, 1997). In this experiment a mini-rig was installed, drilling along a glass wall in order to visualise the processes. Amongst others it was tried to enforce a blow-out by pushing the drill head further in the soil without pumping drilling fluid in order to block the return current. Than the drill head was stopped and the pumping of mud was restarted.

The borehole that was formed, when the return current was blocked, showed an increasing diameter. The hole had more or less a balloon form. The pressure in the borehole enlarged continuously. After some time, bulges occurred on the contours of the bentonite 'balloon'. Especially the upward bulges grew (direction of decreasing soil pressure gradient) and just under the surface a sudden fracture to the surface originated, from which mud spouted with force. After the blow-out the pressure dropped again. Observations showed that on some distance of the borehole dilatancy occurred. This was distinguished by the 'drying' of parts of the sand. The measured soil failure fluid pressure was larger than the calculated pressure with the method of L&H. However it was concluded with post additional calculations with the numerical computer soil model PLAXIS that the measured pressures during the experiments cannot be used for quantitative analysis as the walls had too much influence. But also the high soil stiffness could have played a role.

Figure 5: Photo blow out in dredging test channel (BTL21)

2.2.3 Attempt to enforce blow-out (BTL 47)

On the site of a contractor (Visser & Smit Hanab) a few tests have been done to look whether blow-outs could be enforced and monitored in order to validate the available equations (L&H). The results where published in BTL 47. However a blow out at great depth was not achieved, although a large quantity of drilling fluid was pumped into the soil. It was concluded that the soil was not homogeneous and internal fluid loss occurred.

2.2.4 Blow out experiment (BTL 48)

Furthermore, a scale test was performed in which the main parameter, pressure, was not scaled. The purpose of these tests was to examine how sand fails, when the mud pressure increases until the limit pressure and at which pressure failure occurs.

In all tests fracturing was found. The fracturing was local, as a crack did not develop over the entire injection area. The peak pressure was more or less the same, after that the pressure developed differently. It was concluded that the first crack develops at the observed peak pressure and that the development of the rest of the pattern depended on the thickness of the mud due to plastering effects. The predicted maximum pressures according to the cavity expansion theory were higher than the measured failure pressure. (the calculated pressure was 700 kPa, the measured around 400 kPa, which was about 2.5 times the initial pressure). This is in accordance with the theory that fracturing occurs at lower pressure than cavity expansion.

2.3 Available models

In this paragraph a subdivision is made into models based on plasticity and models which take hydraulic fracturing as failure into account.

2.3.1 Models based on plasticity

In paragraph 2.1 it is explained that in the current design practice the equations derived by H.J. Luger and H.J.A.M. Hergarden (1988) are used. These are based on the introduction of a maximum allowable plastic zone. For further reading on this method reference is made to appendix D. The theory of L&H was based on the theory of cavity expansion, developed by Vesić (further reading appendix C).

These equations were derived from a soil model. This model is based on the assumption of axial symmetry around the borehole and the following conditions;

- the medium is homogeneous, isotropic and has infinite dimensions,

- prior to the application of load the soil has an isotropic effective stress
- there is equilibrium,
- Hooke's law for increments of elastic deformation apply,
- Mohr-Coulomb's failure criterion applies,
- absence of isotropic deformations in the plastic zone.

In the above-mentioned appendix (appendix D) the equations are derived from the soil model on which they are based.

2.3.2 Models for hydraulic fracturing

When became clear during the drilling tests in gelatine (paragraph 2.2.1) that hydraulic fracturing may be an important failure mechanism, a literature search was performed for models describing this behaviour. These were found for cohesive soils but not for non-cohesive soils.

A summary of these models is given in appendix C. The models, presented in this appendix, are based on analytical theories and some are compared to empirical findings. An important difference in the theories is the assumption at which fracturing occurs. As a result of;

- tensile stresses, divided into two groups, assumption of;
  - linear elastic material,
  - non-linear elastic material,
- shear stresses.

As stated before the models were not very useful as they apply only for cohesive soils. Next to that the models apply for vertical holes. All tests, to which is referred, were carried out with water, except for the tests executed by Andersen et al.

2.4 Conclusions inventory

2.4.1 Current design practice

From current practice the conclusion can be drawn that within the equations used to calculate the maximum allowable pressures a lot of safety is hidden. The actual fluid pressures occurring in the borehole are, in general, not exactly known as they can not be derived from the measured pump pressures and as limited or no measurements are performed in the borehole. Therefore little data is available regarding pressures in the borehole at the moment of failure.

The soil research that is executed nowadays in The Netherlands for a horizontal directional drilling contains always some CPT's and mostly a boring test. From a sounding (CPT) the only parameter that can be derived directly is q_c. An indication of the type of soil can be derived from the friction number and boring. Water pressures in permeable soil are known. Furthermore with an educated guess, based on experience in Dutch soil, the following parameters can be determined: σ, σ', u, φ, c, E, ν, G. Preferable is to take only these parameters into account in a new model.

2.4.2 BTL research

The research done by BTL gave the following clues for factors that could play a role in the failure process of soil.

- speed of pressure build up could play a role
- dilatancy or contractant behaviour could play a role
- When the return current is blocked the injected volume of mud determines the pressure in the borehole.
- 'Bulges' mainly grew upward
- Dilatancy occurred on some distance (it should be noted that the sand was densely packed). It could be that also sand reacts undrained.
- Fractures occurred locally.
- In the tests described in BTL 48 the failure pressure was $2.5*\sigma'_0$. Values in the same range were also found during other research.*

* The remark refers to what was written in the report BTL 48. In this report reference is made to conclusions that were drawn after evaluation of the blow-out that occurred during the drilling of the 2nd Heinenoord tunnel (A. Bezuijen & H. Brassinga).

3 DERIVATION OF SOIL MODELS*

In this chapter the soil models are presented which were developed within the framework of this thesis to describe the soil behaviour in case of cavity expansion due to an increasing internal pressure. Such an increasing internal pressure in a cavity is the representation of the injection of mud into the soil in case of horizontal directional drilling. It was necessary to develop such a model to be able to introduce failure (see next chapter).

First a general description is given of the assumptions on which the model is based on and a brief description of the soil model will be given.

Next the two types of deformation, which are largely the same, will be presented.
1. Soil model of a cylindrical expansion cavity
Represents the soil behaviour under normal drilling conditions. A long 'pipe' is drilled.
2. Soil model of a spherical expansion cavity
Represents the soil behaviour when the return flow is blocked. A kind of 'balloon' will be formed in the soil.
The characterisation will contain only a brief overview of the equations. The soil model of a cylindrical cavity will be discussed most extensively.

After the presentation of the two soil models, remarks will be made regarding the relation between these 'new' models and the model on which the equations of Luger & Hergarden are based. Finally an overview will be given on the merits and demerits of these soil models and the possibilities to improve the models.

* In this chapter only the main equations are presented. The complete mathematical description, on which the equations are based, can be found in appendix E.

3.1 Overview 'new' soil models

In this paragraph the assumptions on which the soil models are based are explained and a description of the soil models is given in 'words'.

3.1.1 Assumptions

The models contain elasto-plastic solutions for stresses and strains around a cylindrical or spherical cavity. For both deformation models (cylindrical and spherical) the following assumptions were used:

- The material is supposed to be elastic up to a certain limit, defined by Coulomb's failure criterion, depending on cohesion 'c' and angle of internal friction 'φ' of the material.
- Beyond the coulomb failure criterion the material is plastic, with a constant ratio between the volume change (dilatancy) and the shear deformation.
- The material has an initial homogeneous state of stress, up to infinity (gravity is neglected).
- Plasticity may occur in a zone around the cavity, the material further from the cavity remains in the elastic state.

3.1.2 Brief description model

The soil model assumes the following;

- Initially

There is a hole in a medium of infinite extent. In each direction, and in each location this soil has the same characteristics and the same initial stress.

- Enlarged pressure

If there is an enlarged pressure there are basically two states possible;

- The pressure is enlarged, but the medium remains entirely in the elastic state.
- The pressure is enlarged above a certain limit (Mohr-Coulomb criterion). The medium becomes plastic around the hole. Further away from the hole the pressure is still under the limit and remains elastic. (see Figure 7 and figures regarding stresses e.g. Figure 9)

3.1.3 Acknowledgement

The soil models presented in this chapter were developed on the basis of the work of Prof. dr. ir. A. Verruijt. He described, earlier, a solution for the problem of a cylindrical cavity in an infinite elasto-plastic material. This solution concerned the underpressure in a cavity, as it was the approximation of the excavation of a tunnel in a soil mass. During this research, in March 2001, the models were rewritten for the purpose of describing an overpressure in a soil mass.

3.2 Cylindrical cavity*

In this paragraph the main equations regarding the soil model of a cylindrical cavity are presented.

Figure 6 shows an element of material in a cylindrical co-ordinate system. It is assumed that the displacement field is cylindrically symmetrical. The stresses acting upon the element are indicated in the figure.

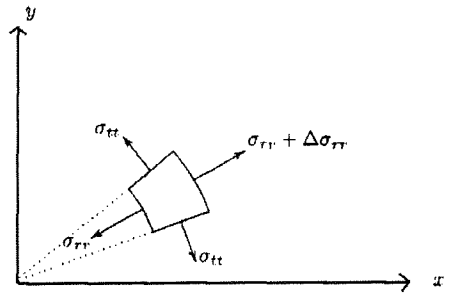

Figure 6: Element, cylindrical cavity

Stresses are considered *positive for tension*.
Strains are considered *positive for extension*.

The only non-trivial equation of equilibrium now is the one in radial direction;

$$\frac{d\sigma_{rr}}{dr} + \frac{\sigma_{rr} - \sigma_{tt}}{r} = 0 \qquad [E.1.1]$$

This equation must be satisfied in the elastic region and in the plastic region.

3.2.1 Elastic region

In the elastic region the stresses can be related to the strains by Hooke's law.

The solution for a cavity in an infinite elastic field applies to the cavity expansion problem in the outer region, for $r_e < r < r_\infty$ (see Figure 7)

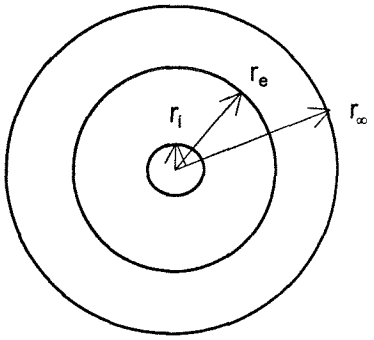

Figure 7: definition of radii

* In this chapter only the main equations are presented. The complete mathematical description, on which the equations are based, can be found in appendix E.

The solution is considered to consist of two parts;

- The initial state, uniform stresses in the entire medium (p_0 = initial stress)

$$\sigma_{rr} = -p_0 \qquad [E.1.15]$$

and $$\sigma_{tt} = -p_0 \qquad [E.1.16]$$

- Solution for the increase of the stresses due to expansion of the cavity (incremental)

The total stresses are the *sum* of the *initial* stresses and the *incremental* elastic stresses. The solutions for stresses in the elastic zone are;

$$\sigma_{rr} = -p_0 - (p_e - p_0)\frac{r_e^2}{r^2} \qquad [E.1.25]$$

$$\sigma_{tt} = -p_0 + (p_e - p_0)\frac{r_e^2}{r^2} \qquad [E.1.26]$$

p_e is the final pressure at the boundary of the elastic region, which is supposed to be greater than the initial pressure p_o.

3.2.2 Plastic region

In the interior region, $r_i < r < r_e$, the soil may be in the plastic state (see Figure 7). It is assumed that in this region the radial stress σ_{rr} is the major principal stress, and the tangential stress σ_{tt} is the minor principal stress. The basis of this assumption is the notion that the cause for stress increase is the fact that the radial pressure at the cavity boundary is increased.

Two parameters are defined;

$$a = c\cot\varphi \qquad [E.1.30]$$

and $$m = \frac{1-\sin\varphi}{1+\sin\varphi} \qquad [E.1.31]$$

The last is the active soil pressure coefficient (K_a).

The pressure at the wall of the borehole is

$$r = r_i \;:\; \sigma_{rr} = -p_i \qquad [E.1.34]$$

The solutions for stresses in the plastic zone are

$$\sigma_{rr} - a = -(p_i + a)\left(\frac{r}{r_i}\right)^{-(1-m)} \qquad [E.1.36]$$

$$\sigma_{tt} - a = -m(p_i + a)\left(\frac{r}{r_i}\right)^{-(1-m)} \qquad [E.1.37]$$

There is a radial equilibrium at the interface between the plastic and elastic regions. Next to that the usual assumption in elasto-plastic problems that the stresses in the elastic region must approach the Mohr- Coulomb yield condition at the interface is used.

This determines the radial stress at the boundary between the plastic and the elastic regions.

$$p_e + a = \frac{2}{1+m}(p_0 + a) = (1+\sin\varphi)(p_0 + a) \qquad [E.1.42]$$

Furthermore the radius of the plastic region is determined.

$$(\frac{r_e}{r_i})^{(1-m)} = \frac{1+m}{2}\frac{p_i + a}{p_0 + a} \qquad [E.1.43]$$

A plastic region will develop when the right hand side of this equation is greater than 1. For smaller values of the pressure at the cavity boundary the entire field will remain elastic.

$$p_i + a > \frac{2}{1+m}(p_0 + a) = (1+\sin\varphi)(p_0 + a) \qquad [E.1.44]$$

3.2.3 Displacements

The displacements in the elastic zone are;

$$r > r_e : u = \frac{(p_e - p_0)r_e^2}{2\mu r} \qquad [E.1.45]$$

This is an isochoric displacement (displacement without volume change).

For the deformations in the plastic region it is assumed that there can be a certain volume change (by dilatancy), proportional to the shear strain. ψ is the dilatancy angle, positive for volume expansion. If $\psi = 0$ the deformations will be isochoric. The parameter 'k' represents

$$k = \frac{1-\sin\psi}{1+\sin\psi} \qquad [E.1.51]$$

The displacement at the cavity boundary now is;

$$\frac{u_i}{r_i} = \frac{p_0 + a}{2\mu}\frac{1-m}{1+m}[\frac{1+m}{2}\frac{p_i + a}{p_0 + a}]^{(k+1)/(1-m)} \qquad [E.1.53]$$

This solution applies if the pressure at the cavity boundary is sufficiently high, so that a certain plastic region develops around the cavity. If this is not the case, the elastic solution remains.

3.2.4 Graphical representation

For the construction of a graphical representation of the equations dimensionless values were introduced. For further reading reference is made to appendix E.

$$P = \frac{p_i + a}{p_0 + a},\ U = \frac{u_i}{r_i}\frac{2\mu}{p_0 + a},\ S = \frac{s_{rr} + a}{p_0 + a} \text{ and } T = \frac{s_{tt} + a}{p_0 + a}$$

The parameters $s_{rr} = -\sigma_{rr}$ and $s_{tt} = -\sigma_{tt}$ were introduced to ensure positive parameters for pressure.

Figure 8 shows the relation between the dimensionless pressure P and the dimensionless displacement U, for the case that $\varphi = 30^0$, and for three values of dilatancy angle ψ.

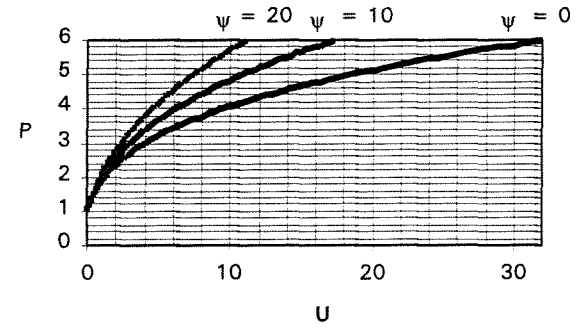

Figure 8: Expansion versus pressure, cylindrical cavity in infinite space

To give a graphical representation of the stresses, distinction must be made between the pressure in the cavity below the limit that produces plastic deformations, and above that limit. The limiting value of the pressure is $P = 2/(1+m)$. Below this limit all deformations will be elastic.

Above this limit there will be two regions, a plastic region immediately around the cavity, and an elastic region outside, up to infinity. The boundary between these two regions is the radius r_e (see Figure 7).

For the case $\varphi = 30^0$ the radial stresses are shown in Figure 9 for increasing values of the stress inside the cavity. The radial stress at the cavity boundary increases from p_o to $6p_o$.

The tangential stresses for the same values of the radial stress at the cavity boundary are shown in Figure 10.

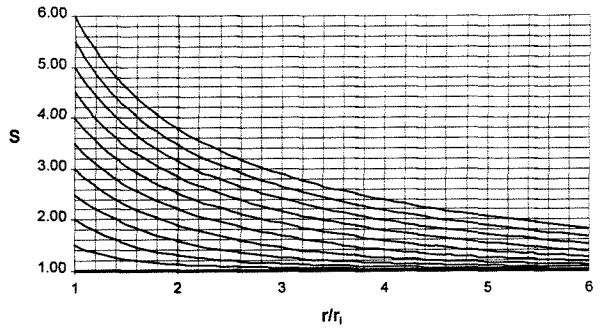

Figure 9: Cylindrical cavity in infinite space: radial stresses: S

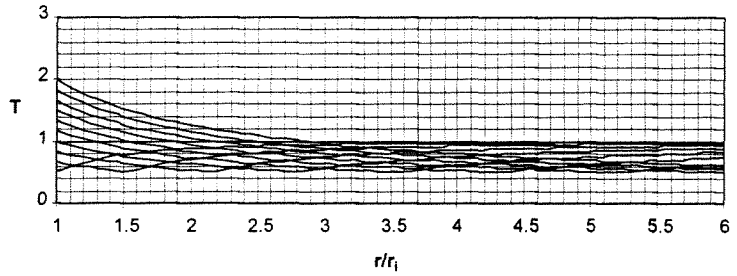

Figure 10: Cylindrical cavity in infinite space: tangential stresses: T

The stresses at the interface between the plastic and elastic zone, i.e. for $r = r_e$, are $S = 2/(1+m)$ and $T = 2m/(1+m)$. These values are always positive, and they are independent of the pressure in the cavity.

3.3 Spherical cavity*

The main equations named in the previous paragraph for a cylindrical solution will be presented here for a spherical solution. For explanation on certain steps reference is made to the previous paragraph or to appendix E.

3.3.1 Elastic region

Solution for the stresses due to expansion of the cavity (incremental) is the *sum* of the *initial* stresses and the *incremental* elastic stresses. The solutions are;

$$\sigma_{rr} = -p_0 - (p_e - p_0)\frac{r_e^3}{r^3} \qquad \text{[E.2.25]}$$

$$\sigma_{tt} = -p_0 + \frac{1}{2}(p_e - p_0)\frac{r_e^3}{r^3} \qquad \text{[E.2.26]}$$

3.3.2 Plastic region

The solutions for stresses in the plastic zone are;

$$\sigma_{rr} - a = -(p_i + a)\left(\frac{r}{r_i}\right)^{-2(1-m)} \qquad \text{[E.2.36]}$$

$$\sigma_{tt} - a = -m(p_i + a)\left(\frac{r}{r_i}\right)^{-2(1-m)} \qquad \text{[E.2.37]}$$

The radial stress at the boundary between the plastic and the elastic regions is;

$$p_e + a = \frac{3}{1+2m}(p_0 + a) \qquad \text{[E.2.42]}$$

Furthermore the radius of the plastic region is determined;

* In this chapter only the main equations are presented. The complete mathematical description, on which the equations are based, can be found in appendix E.

$$(\frac{r_e}{r_i})^{2(1-m)} = \frac{1+2m}{3}\frac{p_i+a}{p_0+a} \qquad [E.2.43]$$

$$p_i + a > \frac{3}{1+2m}(p_0+a) = \frac{1+\sin\varphi}{1-\frac{1}{3}\sin\varphi}(p_0+a) \qquad [E.2.44]$$

3.3.3 Displacements

The displacements in the elastic zone;

$$r > r_e : u = \frac{(p_e - p_0)r_e^3}{4\mu r^2} \qquad [E.2.45]$$

The parameter 'k' taking dilatancy into account has the following relation to ψ;

$$k = \frac{2-\sin\psi}{1+\sin\psi} \qquad [E.2.51]$$

The displacements in the plastic zone;

$$\frac{u_i}{r_i} = \frac{p_0+a}{2\mu}\frac{1-m}{1+2m}[\frac{1+2m}{3}\frac{p_i+a}{p_0+a}]^{(k+1)/2(1-m)} \qquad [E.2.53]$$

3.3.4 Graphical representation

For the construction of a graphical representation of the equations dimensionless values were introduced as in the previous paragraph.

Figure 11 shows the relation between the dimensionless pressure P and the dimensionless displacement U, for the case that φ = 30°, and for three values of dilatancy angle ψ.

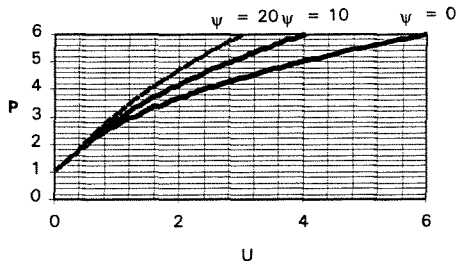

Figure 11: Expansion versus pressure, spherical cavity in infinite space

For the case $\varphi = 30^0$ the radial stresses are shown in Figure 12 for increasing values of the stress inside the cavity. The radial stress at the cavity boundary increases from p_0 to $6p_0$.

The tangential stresses for the same values of the radial stress at the cavity boundary are shown in Figure 13.

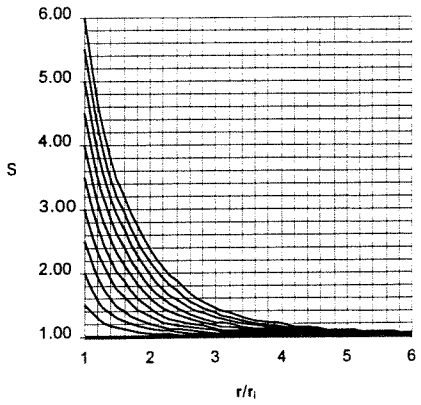

Figure 12: Spherical cavity in infinite space: radial stresses: S

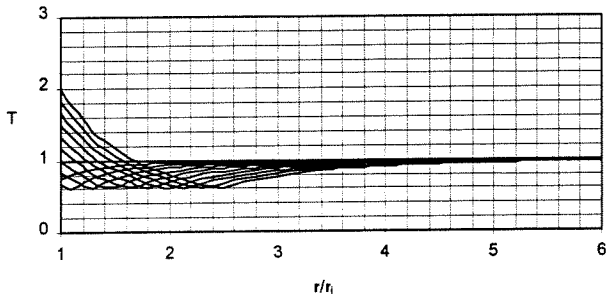

Figure 13: Spherical cavity in infinite space: tangential stresses: T

3.4 Evaluation of 'new' soil models

In this paragraph first a comparison will be drawn between the model on which the equations of Luger and Hergarden are based and the 'new' model for a cylindrical cavity (derived in §3.2).

Next some remarks will be made regarding the soil models pointing out the merits and demerits of these models. This is done in order to give an overview of possible improvements, or other solutions to describe soil behaviour and shortcomings of the models.

3.4.1 Comparison to model of Luger & Hergarden

The exact parameters of the equations proposed by L&H differ from the 'new' models hence a different impression can be obtained. In appendix D the equations presented by Luger and Hergarden have been derived anew to compare the model of Luger and Hergarden and the 'new' model. It was concluded from this derivation that the models are more or less the same. In the model of L&H and the 'new' model not only the same assumptions regarding the soil behaviour are used, actually the whole approach is similar. In the model at the basis of the equations of Luger & Hergarden the only 'real' differences are;

- The pressures are written as a function of time, but speed-factors do not play a role in the analysis. This approach results in the same solutions, though the 'steps' that have to be taken seem more complicated.
- Displacements are only written as changes in radii and not in strains.
- The assumption is used that no volume change occurs in the plastic zone. Dilatancy is therefore not taken into account.

The differences between the models are only minor. The 'new' model is slightly better as it has the possibility to introduce dilatancy in the plastic region and as it is a little bit clearer because it does not use the detour of the 'incremental' approach. Next to that, a spherical cavity model was presented, which represents better the soil behaviour of a blocked return flow.

3.4.2 Merits and demerits of models

As stated in the previous subparagraph both models are more or less the same. Therefore, in this subparagraph, to both will be referred (to the 'new' models and the model used by L&H).

Merits

The merits are in the field of 'rather easy to use'

- Required parameters can be determined from simple soil investigation and by engineering judgement.
- In current practice these are the models to be used (as they are recommended in the appendix of NEN 3651:1994), therefore a lot of experience and 'feeling' is gained. In general they are used cautiously.

Demerits

The demerits are in the field of the assumptions, which are at the basis of the models.

- The soil is regarded to be of infinite extent having the same characteristics in each direction. Therefore gravitation, heterogeneity and stratification are not taken into account. e.g.;

- The in- and decreasing soil pressure is not taken into account as if a vertical hole is regarded instead of a horizontal.
- The model assumes isotropic soil pressure.
- The different behaviour of the area where mud has infiltrated into the pore skeleton (sand) cannot be taken into account.
- Stratified soil cannot be described without arbitrary assumptions on the soil characteristics.

- The models assume a perfect cylinder or sphere. Deviations cannot easily be introduced.
- The Mohr-Coulomb criterion is used to describe the transition from elastic to plastic. This criterion is a simplification of the reality.
- The models use a representation of the characteristics
- Drained / undrained behaviour cannot be taken into account, except for changing the material parameters.
- An interpretation is needed of the soil data. It depends on the professional skills of the engineer how good the input and therefore the output (representation of the soil) is.

Possibilities / Challenges

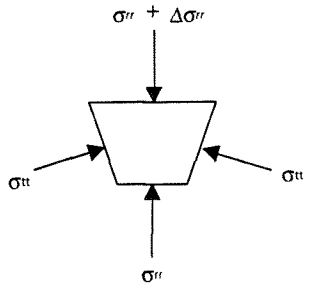

Figure 14: Stresses on element (general)

At this moment stress distribution is assumed to be quite simple (see Figure 14). If e.g. gravity is introduced, also shear stresses should be taken into account. Solving this problem analytical is far from simple. Also introducing other properties such as mudspurt or stratification* would be quite complicated. It is therefore concluded that this soil model cannot be improved easily.

* Recently within the framework of a thesis research at Delft University of Technology a soil model is developed which can model a softer overlying layer while drilling in a stronger layer. (Drilling fluid losses, Rob Vos, September 2001)

4 INTRODUCING FAILURE INTO 'NEW' MODELS

In this chapter the soil models described in the previous chapter (3 Derivation of soil models) are used to introduce a soil failure mode. Several ideas have been worked out. The proposed approaches do not pretend to be the only ones. They are merely some possibilities.

First the possibility is presented to introduce failure assuming that the borehole fails when the soil becomes plastic instead of elastic according to the Mohr-Coulomb criterion. The second possibility that is presented looks into the ways in which tensile forces can be introduced into the soil models. Finally failure is introduced by assuming a maximum allowable strain. Except for the 'strain criterion' the ideas presented here are only elaborated for the cylindrical cavity model. In the last paragraph the merits and demerits of the proposed failure criteria are discussed.

4.1 Soil fails when in transition from elastic to plastic

Equation [E.1.44] states that the soil becomes plastic if the right hand of the equation becomes larger than 1. If the sides are equated the soil remains fully elastic;

$$p_i + a > \frac{2}{1+m}(p_0 + a) = (1+\sin\varphi)(p_0 + a) \qquad \text{[E.1.44]}$$

$$p_i = (1+\sin\varphi)p_0 + a\sin\varphi \qquad (6)$$

For c = o (sand) -> a = 0. The equation reduces to;

$$p_i = (1+\sin\varphi)p_0 \qquad (7)$$

If this is regarded as the maximum allowable pressure then it is a very conservative approach, because the plastic state is neglected.

4.2 Introducing tensile forces

In general a cohesive soil is regarded to be able to sustain small tensile forces and non-cohesive soils are regarded to be able to take none.

Therefore a possibility to introduce failure could be the introduction of tensile forces. The radial stress is larger than the tangential stress. It was tried to introduce failure by assuming that failure occurs when the tangential stress becomes zero. This was tried in the elastic state and in the plastic state.

Elastic state

The equation found in appendix E;

$$\sigma_{tt} = -p_0 + (p_e - p_0)\frac{r_e^2}{r^2} = 0 \qquad \text{[E.1.26]}$$

and $r_i = r_e$;

$$\sigma_{tt} = -p_0 + (p_e - p_0) = 0 \qquad (8)$$

$$p_e = 2p_0 \qquad (9)$$

However, before the tangential stress is reduced to zero (in the elastic state) the soil has become plastic around the borehole. In the previous paragraph (4.1) was derived;

$$p_i + a > \frac{2}{1+m}(p_0 + a) = (1+\sin\varphi)(p_0 + a) \qquad [E.1.44]$$

A plastic region will develop when the right hand side of this equation is greater than 1. For smaller values of the pressure at the borehole boundary the entire field will remain elastic. In general for sand $a=0$ ($c=0$) and $\varphi = 30^0 - 40^0$ then if p_i is larger plastic zone starts to develop; $p_i > 1.5p_0 - 1.65p_0$. These values are lower than $2p_0$.

Plastic state

The equation found in appendix E;

$$\sigma_{tt} - a = -m(p_i + a)\left(\frac{r}{r_i}\right)^{-(1-m)} = 0 \qquad [E.1.37]$$

$r = r_i$;

$$\sigma_{tt} - a = -m(p_i + a) = 0 \qquad (10)$$

$$p_i = \frac{(1-m)a}{m} \qquad (11)$$

This would be the maximum allowable pressure. In equation (11) the parameter for the initial stress (p_0) is not found anymore. If there is no cohesion (assumption for sand) the soil cannot fail in this way. If the circle of Mohr is reminded it can easily be seen that in sand the tangential stress can not reduce to zero (see Figure 15).

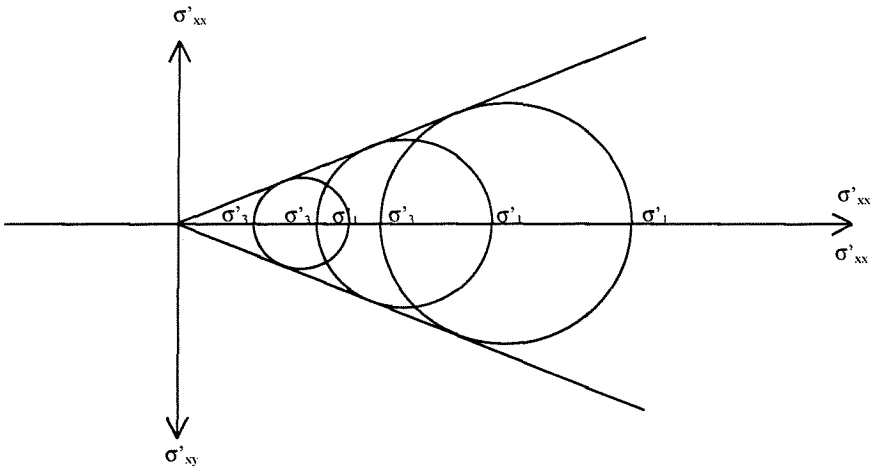

Figure 15: Circle of Mohr of a non-cohesive soil (e.g. sand)

This can also be seen from Figure 9, Figure 10, Figure 12, and Figure 13 in chapter 3 that neither radial nor tangential negative stresses can be introduced into the model. If the pressure of the mud enlarges the counter pressure enlarges too (both the tangential and radial stresses).

Also some cases with cohesive soils are calculated. It is reminded that the focus of the research was on non-cohesive soil (sand).

If cohesion is assumed; the following case is presented - moderate clay;

σ_{tt}	= 0 kPa	c	=10 kPa	φ	$=17.5^0$
		a	=31.7 kPa	m	=0.54

Resulting in; p_i = 27 kPa

In case a negative tangential stress is allowed; σ_{tt}=-5 kPa -> p_i = 36.3 kPa

Case of stiff clay;

σ_{tt}	= 0 kPa	c	=30 kPa	φ	$=17.5^0$
		a	=95.1 kPa	m	=0.54

Resulting in; p_i = 81 kPa

In case a negative tangential stress is allowed; σ_{tt}=-5 kPa -> p_i = 90.3 kPa

4.3 Failure due to maximum strain

In this chapter the introduction of failure by introducing an upper limit for strain is presented. The models presented in the previous chapter are used to the describe the soil behaviour.

Basic concept

It is possible that when the strain becomes too large the integrity of the borehole is threatened.

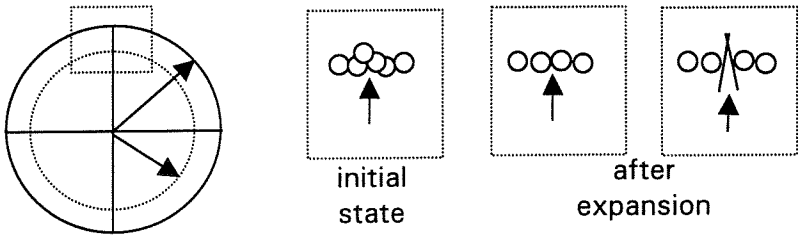

Figure 16: Influence of expansion – strain of the soil

It could be that the mud pushes (the already due to expansion of the borehole pushed aside) grains further aside. The mud finally can form a kind of wedge that can be the start of a crack.

Introducing maximum tangential strain in the defined elastic plastic soil model can describe this failure criterion. In the following subparagraph this failure criterion is introduced.

Equations

Tangential strain can be described with the following equation;

$$\varepsilon_{tt} = \frac{u_r}{r} \qquad [E.1.8]$$

This relation was already defined;

$$\frac{u_i}{r_i} = \varepsilon_{tt} = \frac{p_0 + a}{2\mu} \cdot \frac{1-m}{r_i} \cdot \left[\frac{1+m}{2} \cdot \frac{p_i + a}{p_0 + a} \right]^{\frac{k+1}{1-m}} \qquad [E.1.53]$$

It is reminded that in this:

a	$c \cot\varphi$
m	$(1-\sin\varphi)/(1+\sin\varphi)$
$k_{cyl.}$	$(1-\sin\psi)/(1+\sin\psi)$

A failure criterion can be introduced by assuming that there is a maximum strain:

$$\varepsilon_{tt,max} = \frac{p_0 + a}{2\mu} \cdot \frac{1-m}{r_i} \cdot \left[\frac{1+m}{2} \cdot \frac{p_{i,max} + a}{p_0 + a} \right]^{\frac{k+1}{1-m}} \qquad (12)$$

This can be rewritten in the following form:

$$p_{i,max,cyl.} = \left\{ \left[\varepsilon_{tt,max} \cdot \frac{2\mu}{p_0 + a} \cdot \frac{1+m}{1-m} \right]^{\frac{1-m}{k_{cyl.}+1}} \cdot \frac{2}{1+m} \cdot (p_0 + a) \right\} - a \qquad (13)$$

This equation describes a maximum allowable pressure in the borehole (p_i) based on maximum allowable strain ($\varepsilon_{tt,\,max}$) for a cylindrical cavity. For a spherical cavity the expression reads;

$$p_{i,max,sphere} = \left\{ \left[\varepsilon_{tt,max} \cdot \frac{2\mu}{p_0 + a} \cdot \frac{1+2m}{1-m} \right]^{\frac{2(1-m)}{k_{sphere}+1}} \cdot \frac{3}{1+2m} \cdot (p_0 + a) \right\} - a \qquad (14)$$

It is reminded that parameters 'a' and 'm' are the same for the cylindrical and spherical cavity model, however 'k' differs ($k_{sphere} = (2-\sin\psi)/(1+\sin\psi)$).

In the following paragraphs and in appendix F this failure criterion is compared to the failure criterion defined by Luger and Hergarden.

4.4 Conclusions regarding the introduction of failure

In this paragraph the failure criteria described in this chapter are discussed first, followed by a comparison of the failure criterion of Luger and Hergarden to the failure criterion of strain. A comparison is made of the equations (see also appendix D) and some cases are computed (reference: appendix F) for comparison.

4.4.1 The presented failure criteria

The conclusions drawn in the paragraphs (4.1- 4.3) in which the failure criteria are presented are repeated here;

- If it is assumed that soil fails when the elastic state goes to the plastic state then it is a very conservative approach. The plastic state is then neglected.
- The introduction of tensile forces could be done in the elastic and plastic state;
  - Elastic state; before the tangential stress reduces to zero in the elastic state the soil has become plastic around the borehole.
  - Plastic state; in the derived equation the parameter for the initial stress (p_0) is not found anymore. If there is no cohesion (assumption for sand) the soil cannot fail in this way.
- Failure due to maximum strain; a failure criterion both for the cylindrical cavity as for the spherical cavity was defined.

It is concluded that the only new failure criterion for non-cohesive soils defined in this research is the failure criterion related to maximum strain. This seems a probable approach as the sight experiments agree with this (first expansion than a fracture). For cohesive soils a criterion is presented using the criterion of tensile forces. This last criterion will not be worked out as this is out of the scope of this research.

4.4.2 Comparison to failure criterion of Luger & Hergarden and strain criterion

The maximum strain criterion will be compared to the criterion of Luger and Hergarden (maximum radius of plastic zone). First the equations are rewritten in the parameters used by the other model (see also appendix D). Next some tests of BTL are calculated with both criteria (reference is made to appendix F).

Equations

First the equations of Luger and Hergarden are presented in the parameters of the 'new' soil models. For symbols and conversion reference is made to appendix A.

$$R_p^2 = \left(\frac{1+m}{2} \frac{p_i + a}{p_0 + a} \right)^{\frac{2}{1-m}} \cdot r_i^2 \qquad [D.3.8]$$

$$R_p^2 = \varepsilon_{rr} \cdot \frac{2\mu}{p_0 \cdot \sin\varphi + c\cos\varphi} \cdot r_i^2 \qquad [D.3.16]$$

Now the following equation;

$$p' = (p'_f + c\cot\varphi) \cdot ((R_0 / R_p)^2 + Q)^{\frac{-\sin\varphi}{1+\sin\varphi}} - c\cot\varphi \qquad [D.1.7]$$

can be written as;

$$p' = ((p_0 \cdot (1+\sin\varphi) + c\cos\varphi) + a) \cdot \left((1+\frac{1}{2\varepsilon_{rr}}) \cdot \frac{p_0 \cdot \sin\varphi + c\cos\varphi}{\mu} \right)^{\frac{-\sin\varphi}{1+\sin\varphi}} - a \qquad [D.3.19]$$

The equations for maximum strain are rewritten (ε_{rr} equals in the 'new' models ε_{tt}). Strain can be expressed in the radius of the plastic zone;

$$\varepsilon_{rr} = \varepsilon_{tt} = \frac{R_p^{\,2}}{R_0^{\,2}} \cdot \frac{\sigma'_0 \cdot \sin\varphi + c\cos\varphi}{2G} \qquad [D.3.21]$$

For maximum allowable pressure related to maximum strain the following expression was found (in §4.3):

$$p_i = \left\{ \left[\varepsilon_{tt} \cdot \frac{2\mu}{p_0 + a} \cdot \frac{1+m}{1-m} \right]^{\frac{1-m}{k+1}} \cdot \frac{2}{1+m} \cdot (p_0 + a) \right\} - a \qquad (13)$$

If $\psi = 0$ and therefore $k = 1$. the expression becomes:

$$p_i = \left(\left(\frac{R_p}{R_0}\right)^{\frac{2\sin\varphi}{1+\sin\varphi}} \cdot (1+\sin\varphi) \cdot (\sigma'_0 + c\cot\varphi) \right) - c\cot\varphi \qquad [D.3.23]$$

Numerical values

Both criteria are tested on cases from the BTL research (reference is made to appendix F).

In chapter 3 of this report the shortcomings of the soil models at the basis of the criteria are outlined. It is therefore emphasised that the conclusions drawn should be treated carefully.

For the following cases a comparison is made;

- *Standard cases to see the influence of parameters.* As the strain criterion was chosen rather small, the values were much more conservative for the standard case. This is logical as the strain criterion can be seen as an 'extra' demand. The variation of the parameters showed that influence of different parameters in both models was more or less the same (except for φ).
- *BTL 21 – sight experiment.* It is difficult to compare the values as the return flow was blocked and therefore the spherical cavity approach is better (the L&H criterion assumes a cylindrical cavity). It seems that a larger strain than 2% and / or some dilatancy should be introduced. The volume pumped into the soil was also compared to the strain it should give. This gave excessive results.
- *BTL 48 – Blow out experiments.* The results in of the equations of L&H were too high (conclusion of BTL 48). The pressure computed with the equation for maximum strain (cylindrical cavity) gives better results, which is logical as an extra more conservative demand can be introduced. Some dilatancy could play a role, but does not have a large influence.
- *BTL 47 – Attempt to enforce blow out.* This field experiment consisted of five attempts for blowouts (no failure occurred). For the first two tests (deep drillings) the results were comparable with maximum strain criterion (spherical cavity – 2%). For the shallower drillings the results found with the assumption of a maximum strain of 2% were too high compared to the measured values. However if a smaller strain is allowed the measured

pressures can be better approached. During the experiment there were doubts about the stratification of the soil. It is therefore difficult to draw conclusions.

- *BTL 46 – Monitoring projects HDD, monitoring three projects* (Noordzeekanaal, Ringvaart and Blerick). Three practical projects were compared. The approach of maximum allowable strain is more conservative. From the graphs it could be seen that the 'lines' for maximum strain seem to be above the calculated occurring pressure – lines (see as example Figure 17 – for more graphs reference is made to appendix F). If it is assumed that the occurring pressure was higher (in accordance with measurements) than the strain criterion of 2% would be too conservative as no blow-outs have occurred.

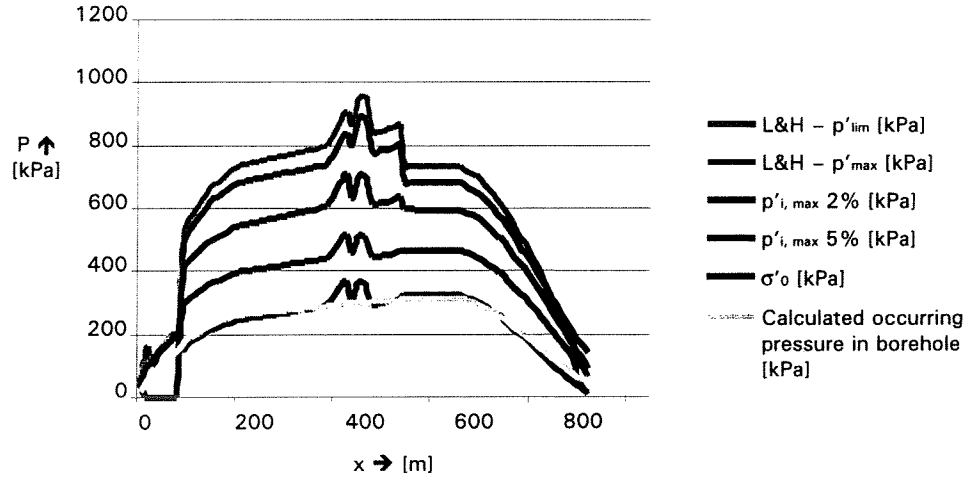

Figure 17: Maximum allowable pressures Ringvaart (reference is made to appendix F)

Conclusion comparison failure criteria (L&H - maximum strain)

As stated in the previous subparagraph the comparison of values should be treated carefully. The model at the basis of both failure criteria (L&H and 'new' model) has shortcomings, which directly influence the outcome of the failure equations (see chapter 3).

The following conclusions can be drawn;

- It was showed that it is possible to rewrite the criteria (L&H failure criterion in 'new' model-parameters and vice versa).
- The spherical cavity model approaches better the blocked return flow.
- The failure criterion of maximum strain is more conservative, as small values for maximum strain are chosen. But this is logical as it introduces an extra demand.
- A maximum strain of 2% seems to be too conservative. A maximum strain of 5% could be more a reasonable value. However, values remain arbitrary. Also dilatancy can play a role.

It remains difficult to draw conclusions. There are a lot of uncertainties;

- in the used models,
- the soil parameters that are substituted,
- and in the measured failure values.

More data to compare is therefore recommendable. However the shortcomings should always be reminded and therefore no absolute conclusions should be made from the results of these equations, but they can give an impression.

5 CONCLUSIONS & RECOMMENDATIONS

Inventory

From current practice the conclusion can be drawn that within the equations used to calculate the maximum allowable pressures safety is hidden. The actual fluid pressures occurring in the borehole are, in general, not exactly known as they cannot be derived from the pump pressures and as little measurements are performed in the borehole. Therefore limited or no data is available regarding pressures in the borehole at the moment of failure.

It is therefore recommended that the developments for monitoring the key operational parameters continue and that available systems are implemented. This should include the drill fluid pressure in the borehole. It would already be an improvement if this would be done with a data logger (not online recording). This would create the possibility to analyse data in case of failure and would give the opportunity to learn from these cases.

'New' soil models

It was concluded that the model at the basis of the equations of L&H is more or less the same as the cylindrical cavity model ('new' model). The differences between the models are only minor. The 'new' model is slightly better as it has the possibility to introduce dilatancy in the plastic region and as it is a little bit clearer because it does not use the detour of the 'incremental' approach. Next to that, a spherical cavity model was presented, which represents better the soil behaviour of a blocked return flow.

For all soil models the following applies;

- Parameters can be determined from simple soil investigation and by engineering judgement. Therefore they are rather easy to use. Next to that, in current practice these are the models used, therefore a lot of experience and 'feeling' is gained. In general they are used cautiously.
- The soil models are based on assumptions that are not in accordance with reality. The main deviations are that the soil that is regarded to be of infinite extent with the same characteristics in each direction, and that the Mohr-Coulomb criterion applies.

Therefore an interpretation is needed of the soil data. It depends on the professional skills of the engineer how good the input and therefore the output (representation of the soil) is.

At this moment stress distribution is assumed to be quite simple. If e.g. gravity is introduced, also shear stresses should be taken into account. Solving this problem analytical is far from simple. Also introducing other properties such as mudspurt or stratification would be quite complicated. It is therefore concluded that this soil model cannot be improved easily.

Failure criteria (in general)

It was concluded that the new failure criterion for non-cohesive soils defined in this research is the failure criterion related to maximum strain. This seems a probable approach as the sight experiments agree with this (first expansion than a fracture).

For cohesive soils a criterion is presented using the criterion of tensile forces. This last criterion will not be worked out as this is outside the scope of this research.

Comparison of maximum strain and L&H

The comparison of values should be treated carefully. The model at the basis of both failure criteria (L&H and 'new' model) has shortcomings, which directly influence the outcome of the failure equations.

The following improvements can be mentioned;

- The spherical cavity model approaches better the situation of a blocked return flow.
- The measured values in the BTL research can in general be better approached.
- A maximum strain of 2% seems to be too conservative. A maximum strain of 5% could be more a reasonable value. However, values remain arbitrary. Also dilatancy can play a role. It is reminded that the failure criterion of maximum strain is more conservative than L&H, as small values for maximum strain are chosen. The strain criterion can be regarded as an extra demand.

Next to that it was showed that it was possible to rewrite the criteria. The failure criterion proposed by Luger and Hergarden (maximum allowable radius of plastic zone) can be rewritten in the parameters of the 'new' soil models.

It is reminded that there are a lot of uncertainties; (i) in the models used, (ii) the parameters that are filled in, (iii) and in the measured values. Therefore it remains difficult to draw conclusions. More data to make comparisons is therefore recommendable. However the shortcomings should always be remembered and therefore no absolute conclusions should be made from the results of these equations. It has no use to fill in very detailed values in a rather 'rough' model.

It is recommended to start using the maximum strain criterion. However the demand for the maximum strain (which percentage) should be further defined.

The ostensible accuracy of an equation depends on the length of the equation, the number of parameters needed and the institute that has developed it. However the ostensible accuracy should not be confused with the actual accuracy!

conclusion of meeting June, 27th 2001

Appendices

Maximum allowable pressures during horizontal directional drillings focused on sand

Student: Birgitte Keulen
9431002

Counselling Team: Prof. dr. ir. A. Verruijt
Ir. G. Arends
O.E. Strack B. Sc
Ir. D.R. Mastbergen
Ir. H.H.J. van der Werff

TU Delft
Technische Universiteit Delft

DCA

Visser & Smit Hanab

WL | delft hydraulics

COLOPHON

Graduation research

Title:	Maximum allowable pressure
Subtitle:	Maximum allowable pressures during horizontal directional drillings focused on sand
Document:	report
Status:	final
Institute:	Delft University of Technology Faculty of Civil Engineering and Geosciences Sub faculty Civil Engineering, department Geomechanics
Location:	Delft Hydraulics, Marine & Coastal Management

Graduation student

Birgitte A.M. Keulen
Brabantse Turfmarkt 20
2611 CN Delft
015-2137031

9431002
B.A.M.Keulen@student.tudelft.nl
BirgitteKeulen@hotmail.com
Birgitte.Keulen@horvat.nl

Counselling team

- Prof. dr. ir. A. Verruijt, Professor of Geomechanics (chairman)
  Faculty of Civil Engineering and Geosciences
- Ir. G. Arends, University lecturer of Underground Space Technology
  Faculty of Civil Engineering and Geosciences
- O. Erik Strack B. sc, assistant researcher Geotechnical Laboratory
  Faculty of Civil Engineering and Geosciences
- Ir. D.R. Mastbergen, senior advisor/researcher dredging & slurry technology
  Delft Hydraulics, marine & coastal management
- Ing. H.H.J. van der Werff, Head Engineering Department, Visser & Smit Hanab

Supported by

Drilling Contractors Association, Europe

Contact address

Postal Address:
Geotechnical Laboratory
Delft University of Technology
sub faculty of Civil Engineering
P.O.Box 5048
2600 GA Delft
The Netherlands
Tel: +31 (0)15 278 1880

Visiting Address:
Geotechnical Laboratory
Keverling Buismanweg 1
Delft

READERS' GUIDE

This document consists of the main report and the appendices. The main report is kept compact in order to make it more pleasant to read. The appendices contain more elaborate information and full mathematical derivations of the equations. The appendices form an integral part of the document.

Report

In the report's first chapter an introduction is given to the technique. The questions regarding the behaviour of soil under fluid pressure during a horizontal directional drilling (HDD) are outlined. Next a problem definition and objective are given and the steps taken in the research are presented.

In the second chapter an inventory is given of how in current practice the maximum allowable pressures are approached, of the research that was done within the framework of BTL and of the available models. From this inventory conclusions are drawn.

In chapter three soil models ('new' models) are presented to describe the behaviour of a cylindrical and a spherical cavity under pressure. These models are compared to the model at the basis of the equations of L&H. In the following chapter it is tried to introduce failure into these models. The new failure criterion (maximum strain) is compared to the failure criterion of L&H (plasticity radius). Finally in the last chapter conclusions and recommendations are presented.

Appendices

In the appendices at first the lists (symbols, literature, etc) are given, followed by a more elaborate description of the HDD technique (appendix B). Appendix B is the background information for chapter one.

Then a more elaborate description of the literature (BTL-research), which is the basis for the thesis research, is given (appendix C). Both tests and models are described. This is the background information for chapter two.

The following appendix (appendix D) contains a full description of the model that stands at the basis of the equations of Luger and Hergarden. Next to that a comparison is made between the failure criterion of maximum radius of the plasticity zone and of maximum strain. This is the background information for chapter two, three and four.

In appendix E the soil models of chapter three are fully described. These soil models stand also at the basis of the derivation of failure criteria. Therefore this appendix is background information for chapter three and four.

Finally in the last appendix (appendix F) the BTL experiment data regarding maximum allowable pressure is used to calculate maximum allowable pressures according to Luger and Hergarden and according to maximum strain. In this appendix reference is made to appendix C. The appendix is background information for chapter four.

Note: The equations that are presented in the report only are placed between round brackets. The equations derived in the appendices are placed between square brackets.

TABLE OF CONTENTS APPENDICES

A LISTS

A.1 Symbols, abbreviations, etc

The symbols used in appendix C are not mentioned here, but only in the appendix.

Greek symbols

γ	specific gravity
$\gamma_{soil,\ dry}$	density dry soil
$\gamma_{soil,\ wet}$	density wet soil
ε	strain -'new model'
ε_{rr}	radial strain -'new model'
ε_{tt}	tangential strain -'new model'
$\varepsilon_{tt,\ max}$	maximum tangential strain -'new model'
λ	Lamé constant = $\nu E/((1+\nu)(1-2\nu)$ - 'new model'
μ	Lamé constant = $E/(2(1+\nu))=G$ - 'new model'
ν	Poisson's ratio
σ	stress
σ'	effective stress ($=\sigma$-u)
σ'_0	initial effective stress - L&H - – often assumed; $=(\sigma'_v+\sigma'_h)/2$
σ'_h	horizontal effective stress – often assumed; $=\sigma'_v*K_0$
σ'_r	radial effective stress - L&H
σ_{rr}	radial stress - 'new model'
σ_{tt}	tangential stress - 'new model'
σ'_v	vertical effective stress
φ	internal friction angle
ψ	dilatancy angle - 'new model'

Other symbols and abbreviations

a	c cot φ - 'new model'
BTL	Boren tunnels en Leidingen
c	cohesion
Cyl.	reference to cylindrical cavity model
d	depth of the drilling
E	elasticity modulus - 'new model'
e	volume strain -'new model'
G	shear modulus $=E/(2(1+\nu))=\mu$ - L&H
k	proportional parameter for angle of dilatancy - 'new model' cylinder: $=(1-\sin\psi)/(1+\sin\psi)$ sphere: $=(2-\sin\psi)/(1+\sin\psi)$
K_0	neutral soil coefficient $=1-\sin\varphi$
K_a	active soil pressure $=(1-\sin\varphi)/(1+\sin\varphi)$
L&H	reference to Luger and Hergarden (appendix D)
m	$=(1-\sin\varphi)/(1+\sin\varphi)=K_a$ - 'new model'
'new model'	reference to new developed models (chapter 3 and 4, appendix E)
Q	$=(\sigma'_0*\sin\varphi+c\cos\varphi)/G$ - L&H
p_0	the initial stress in the soil (used as effective stress) – 'new model'
p'_f	$\sigma'_0*(1+\sin\varphi)+c\cos\varphi$ - L&H
p_e	pressure at the boundary of the elastic region
p_i	mud pressure in the borehole - 'new model'

$p_{i,\,max}$	maximum allowable mud pressure in the borehole - 'new model'
p'_{lim}	effective limit pressure - L&H
p'_{max}	*maximum allowable effective mud pressure* - L&H
p_{return}	pressure needed to maintain return flow
r	radius (coordinate) - 'new model'
r_{∞}	radius extends to infinity - 'new model'
R_0	initial radius of the borehole - L&H
r_e	radius elastic zone - 'new model'
R_g	radius of the borehole - L&H
r_i	initial radius borehole - 'new model'
R_{p-}	radius plastic zone – L&H
$R_{p,\,max-}$	maximum radius plastic zone – L&H
s	actual position of particle - L&H
s_0	initial position of particle - L&H
s_{rr}	$=-\sigma_{rr}$ - 'new model'
s_{tt}	$=-\sigma_{tt}$ - 'new model'
Sphere.	reference to spherical cavity model
u	displacement
u	water pressure
u_e	displacement at the boundary of the elastic region - 'new model'
u_i	displacement at the cavity boundary - 'new model'

Conversion symbols 'new' model <-> Luger & Hergarden

$\mu \leftrightarrow G$

$p'_0 \leftrightarrow \sigma'_0$

$p'_{i,max} \leftrightarrow p'_{max}$ or p'_{lim}

$r_i = R_0$

$r_i + u_i = R_g \rightarrow r_i + r_i \cdot \varepsilon_{rr} = R_g$

$r_e = R_p$

A.2 Figures

Report

Appendices

A.3 Tables

Report

-

Appendices

A.4 Literature

last name, initials (affiliation)
title and subtitle
edition, affiliation, year

Adel, den H. (GeoDelft)
BTL 48 Blow out proeven, Feitenrapport
BTL, 2000

Arends, G. (TU Delft)
ctip4790 Ondergrondse Bouwen deel 2 Sleufloze technieken
lecture notes TU Delft, 1997

Bezuijen, A. (GeoDelft)
BTL 3 Stabiliteit van het boorfront
BTL, 1995

Bezuijen, A. (GeoDelft), Huisman, M. (Delft Hydraulics), Mastbergen, D.R. (Delft Hydraulics)
BTL 17 Verdringingsprocessen bij gestuurd boren, modelproeven en berekeningen
BTL, 1996

Bezuijen, A. (GeoDelft), Brassinga, H.E. (GeoDelft)
Blow-put pressures measured in a centrifuge model and in the field
article

Bjerrum, L. (Norwegian Geotechnical Institute), Nash, J.K.T.L. (King's College), Kennard, R.M. (Harris & Sutherland), Gibson, R.E. (King's College)
Hydraulic fracturing in field permeability testing
Géotechnique, vol. 22, 1972, nr. 2, pp. 319-332

Dutch regulations
Aanvullende eisen voor stalen leidingen in kruising met belangrijke waterstaatswerken (Nederlandse norm)
NEN 3651:1994 ,

Dutch regulations
Ondergrondse pijpleiding, Grondslag voor de sterkteberekening (Nederlandse Praktijkrichtlijn)
NPR 3659:1996

Grontmij, RWS-DWW, GeoDelft, Gasunie, Delft Hydraulics, NACAP, 3D Drilling
BTL 50 Handboek Horizontaal Gestuurd Boren
BTL, 2000

Hergarden, H.J.A.M. (GeoDelft). Huisman M. (Delft Hydraulics), Knibbeler, A.G.M. (Mos Grondmechanica)
BTL 41 part 1 & 2 Rekenmodellen voor grondgedrag bij horizontaal gestuurde boringen
BTL, 1998

Hergarden, H.J.A.M. (GeoDelft)
BTL 54 Bepaling randeffecten bij blow-out proef in Baggergoot
BTL, 1999

Luger, H.J. (GeoDelft)
BAGT 347 Voorspelling en interpretatie van penetratieweerstand in zand, Inpassing en analyse van de ruimte-expansietheorie
CO-256401, 1982

Luger, H.J. (Geodelft), Hergarden, H.J.A.M. (GeoDelft)
Directional Drilling in soft soil; influence of mud pressures
Proceedings No-Dig, 1988

Mastbergen, D.R.(Delft Hydraulics), Ten Broeke, C.J.(Grontmij), Bezuijen, A.(GeoDelft)
BTL 21 part 1 & 2 Proeven Directional Drilling in Baggergoot
BTL, 1997

Mastbergen, D.R. (Delft Hydraulics), Huisman, M. (Delft Hydraulics), Kuyper, H. (Gasunie)
BTL 46 part 1 & 2 Monitoring praktijkprojecten Horizontaal Gestuurd Boren
BTL, 1999

Mastbergen, D.R. (Delft Hydraulics)
BTL 47 Veldproeven Blow-out
BTL, 1999

Mastbergen, D.R. (Delft Hydraulics)
BTL 51 Computermodel "Geboor" vs. 2.01
BTL, 1999

Schrieck, van der G.L.M. (TU Delft)
ctwa5300 Baggertechniek
lecture notes TU Delft, 1998

Sitters, C.M.W. (TU Delft)
ctma4360 Material models for soil and rock
lecture notes TU Delft, 1998

Tol van, A.F. (TU Delft), Everts, H.J. (TU Delft)
ctco5331 Grond en grondkerende constructies CUR 162 Construeren met grond
lecture notes TU Delft, 1999

Verruijt, A. (TU Delft)
Grondmechanica
fourth edition, Delftse Uitgevers Maatschappij, 1993

Vesic, A.S. (Duke University, Durham)
Expansion of cavities in infinite soil mass
ASCE Journal of the Soil Mechanics and Foundations Division, vol. 98, 1972, SM3, pp. 265-290

B HORIZONTAL DIRECTIONAL DRILLING

A description of the execution of a horizontal directional drilling is given in this appendix. The stages needed for the execution of a drilling are; the pilot drilling, the reaming phase and the pull back operation. These will be presented consecutively.

Pilot drilling

A pilot hole is drilled beginning at a prescribed angle from horizontal and continues under and across the obstacle along a design profile made up of straight tangents and long radius arcs. A schematic of the technique is shown in Figure 1.

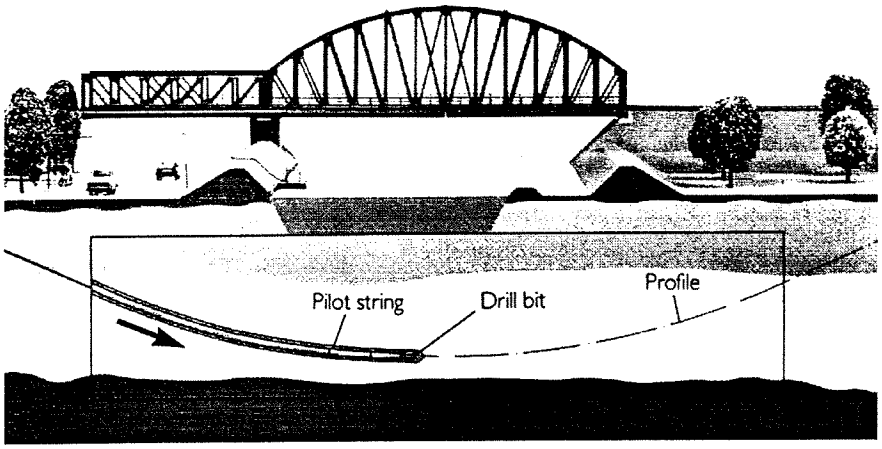

Figure 1: Pilot drilling

The steering possibility is enabled by a small bend in the drill string just behind the cutting head. The pilot drill string is not rotated except to orient the bend. If the bend is oriented to the right, the drill path then proceeds in a smooth radius bend to the right. A steering tool in the pilot drill string near the cutting head monitors the drill path. Two electric cables are laid on the ground level. The steering tool detects the relation of the drill string to the magnetic field that is generated by the electric cables and its inclination. The location of the drill head will be calculated with the transmitted data from the steering tool. Shallow drillings can be followed with a man-hold instrument on the surface.

Reaming phase

Once the pilot hole is complete, the borehole must be enlarged to a suitable diameter for the product pipeline. This is accomplished by reaming the hole to successively larger diameters. Generally, the reamer is attached to the drill string on the bank opposite the drilling rig and pulled back into the pilot hole. See Figure 2. Joints of drill pipe are added as the reamer makes its way back to the drilling rig. Large quantities of drilling fluid are pumped into the hole to maintain the integrity of the hole and to transport out cuttings.

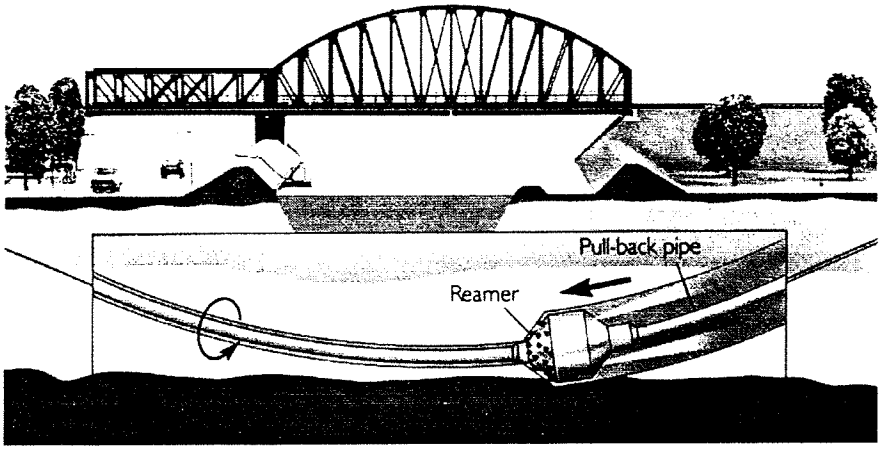

Figure 2: Reaming phase

Pull back operation

Once the drilled hole is enlarged, the product pipeline can be pulled through it. The pipeline is prefabricated on the bank opposite the drilling rig. A barrel reamer is attached to the drill string, and then connected to the pipeline pull head via a swivel. The swivel prevents any translation of the reamer's rotation into the pipeline string allowing for a smooth pull into the drilled hole. The drilling rig then begins the pullback operation, rotating and pulling on the drill string and once again circulating high volumes of drilling fluid. The pullback continues until the pipeline is completely pulled in.

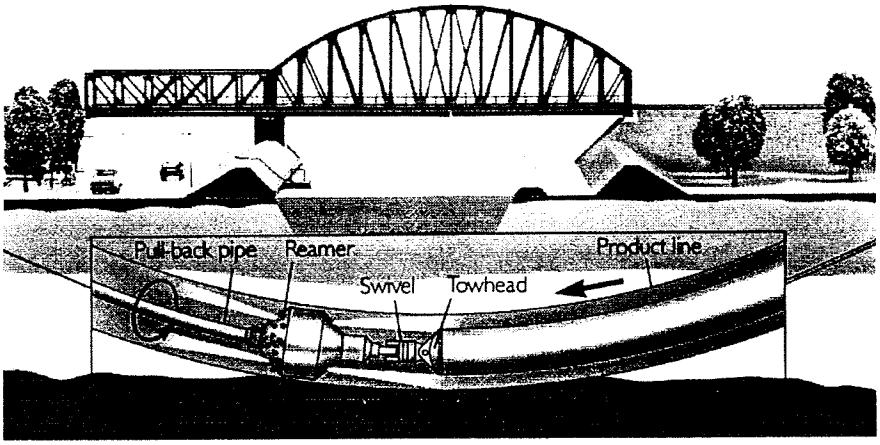

Figure 3: Pull back operation

C LITERATURE

In this appendix the literature found on the subject of maximum pressures is described. The information about this literature can be found in appendix A (author, publication date, etc)

The information in this appendix can be subdivided into two categories:

- Tests – In this paragraph tests that where done in the framework of BTL are described.
- Models – In this paragraph the soil models that are found are described. These can be subdivided into two categories; introduction of failure due to a plastic zone and due to fracturing.

Not only the literature described in the paragraph 'Tests' is derived from BTL reports, most literature described in this appendix was found in these reports.

C.1 Tests in the framework of BTL

In this paragraph the experiments and field measurements, carried out within the framework of the research of BTL, are presented. Some of these tests and measurements have enhanced the understanding of how soil reacts if it is subjected to increasing fluid pressures.

C.1.1 Laboratory test, Drilling in transparent medium (BTL 17)

A small-scale sight experiment was executed to visualise and to get qualitative results regarding the failure of material under fluid pressure. A drilling (scale 1:20) was performed with a coloured liquid in gelatine. No cavity expansion was observed, instead radial fractures originated in random directions. This resembled hydraulic fracturing, as it is known from rock-mechanics. The limit-pressure, which was found, showed coherence with the undrained peak shear strength of the gelatine.

The question was raised whether the cavity expansion theory gives an adequate description of the failure mechanism. A brief literature search was performed to look whether hydraulic fracturing was seen before in the context of liquid injection in softer soils like clay and sand. The results of this research can be found in paragraph C.2.2 and following paragraphs.

C.1.2 Laboratory test, Sight experiment (BTL 21)

This experiment took place in the flume of Delft Hydraulics. A drilling was performed along wall of glass in sand and clay, prepared under controlled circumstances. Operational parameters were measured and the process was recorded on video. The purpose of the tests was to get a better idea of the processes: excavation, plastering, transportation, and stability of the borehole.

A pilot drilling was performed just along the wall of glass with a so-called mini-drilling rig. The tests were performed in solidly packed fine sand and in sand in which blocks of soft clay were placed.

The procedure to enforce a blow-out was the following:

- Pump was turned off to be able to push the drill head carefully away without excavation. (return flow blocked)
- Pressure measure equipment was put in the soil near the drill head.
- The pump was turned on again. The drill head was not moved. Mud was pumped in the soil.
- The pressure was measured and the process was recorded on video.
- This was done until failure or a blow-out occurred.

It was not in all "sand" tests possible to enforce a blow-out. Sometimes the borehole was re-opened along the drill string and the return flow restarted. In none of the 'clay' tests it was possible to enforce a blow-out. Each time the return current restarted.

The following was remarked:

- The borehole that was formed, when the return current was blocked, showed an increasing diameter. The hole had more or less a balloon form. The pressure in the borehole increased continuously. This pressure was determined by the total amount of injected mud and therefore, the deformations of the soil. Time and flow therefore determined the pressure.
- After some time, bulges occurred on the contours of the bentonite 'balloon'. Especially the upward bulges grew (direction of decreasing soil pressure

gradient). When a bulge had grown to about 30cm under the surface a sudden fracture to the surface arose, from which mud spouted with force and the pressure dropped immediately.

- Observations showed that on some distance of the borehole dilatancy and therefore shear occurred. This was distinguished by the 'drying' of parts of the sand and is an indication that the sand was densely packed.
- The soil conditions in sand, on short distance of the borehole, seemed to be influenced. Soundings showed a decrease of resistance on one diameter distance. In clay no influence was found.
- The calculated allowable maximum pressures were lower than the values measured. However it was concluded during extra calculations with a numerical model, Plaxis that the measured pressures during the experiments are not representative for quantitative analysis. (§ C.1.7)

C.1.3 Field test, Monitoring projects HDD (BTL 46)

Monitoring projects - Noordzeekanaal, Haarlemmerringvaart and Blerick

These three projects were meant to test earlier gained theoretical knowledge in practice. The research concerned the processes in the drill string, the borehole and in the soil. The operational parameters were as good as possible measured, with the installation of pressure and flow meters and compared with the calculated parameters.

Al three projects were mainly in Pleistocene solid packed middle fine sand. The soil of the project in Blerick also contained some gravel.

In the projects the following was examined:

1. Noordzeekanaal – A measure PC was installed to collect data and analyses were done on the drilling fluid.
2. Ringvaart – Pressure measurements in the drill trajectory were done and sand contents were analysed.
3. Blerick – pressure measurements were executed and total volume- and mass balance of soil and fluid was measured.

There did not occur irregularities that indicated that the maximum allowable pressure was exceeded except for the last metres of the drilling under the Ringvaart.

C.1.4 Field test, Attempt to enforce blow-out (BTL 47)

On the site of Visser & Smit Hanab a few tests have been done to compare the calculated soil failure pressure to the measured in order to validate the calculation method. The results where published in BTL 47. A blow out at great depth has not been achieved. Five tests have been executed. The result were the following:

Test	Depth drill head	Flow l/min	Pumped on location	Pressure	Remark
1	9.40m –GL	111	4.88 m^3	>2.1 bar	displacement
2	9.20m –GL	105	0.47m^3	2.0 bar	return current
3	3.35m –GL	109.1	4.29m^3	0.5 bar	displacement
4	-	0	-		no flow
5	1.04m –GL	107.6	1.26m^3	0.2 bar	blow-out

Table 1: Results tests BTL 47

In each test the drill head (after having drilled until more or less to the right depth) was pushed further in the soil without pumping drilling fluid to block the return current

1. In the first test the return current was successfully blocked. However, the supply of drilling fluid was insufficient to enforce a blow-out to ground level. In spite of the large volume of 4.88 m^3 of drilling fluid that was pumped in the ground, no blow-out occurred. The proposed explanation for this fact was that the volume was pushed under a weak layer due to inhomogeneous soil composition. In that case the fluid has pushed the soil away or the fluid has lifted the entire surface over a certain area.
2. During the second test a blockage of the return current was not achieved.
3. In the third test the return current was blocked just as in the first test. No large pressure increase has been registered. Therefore the same explanation was made as for the first test.
4. In this test the nozzle was blocked. A fluid pressure of 110 bar was not enough to reopen the nozzle.
5. In this last test a blow-out was achieved. However this was a "shallow" blow-out for which case the cavity expansion theory is not valid.

With these results the required validation of the soil failure pressure calculation is still not achieved. It was therefore recommended to perform new tests in strictly homogeneous sandy soil.

C.1.5 Laboratory test, Blow out experiments (BTL 48)

The purpose of these tests was to examine how an at which pressure sand fails, when the mud pressure is increased beyond the failure value of the soil. A scale test was performed in a laboratory installation in which the main parameter, pressure, was not scaled.

In a cylindrical reservoir a sand-soil was prepared. The effective pressure in the soil was put on 200 kPa using a draining upper plate. The water tension was atmospheric. In the soil a horizontal pipe was installed, which contained bentonite. This represented the borehole. The wall of this pipe could be removed by removing an inner pipe (by turning a spindle) over a length of 0.15 m. The bentonite then came into contact with the soil. The next step was to increase the bentonite pressure to above the expected limit pressure. The amount of bentonite pumped into the soil was measured. At the same time the stressed and water tension in the soil were measured. After the test the soil was carefully excavated to research the cracks that occurred.

Five tests were executed. The first test (test 101) had no expansion reservoir. The intention was to put pressure on the central pipe by carefully pressing the plunger. However when the spindle was turned only a little, the volume of bentonite was enlarged and the pressure reduced. This could not be handled with the plunger. The hole 'collapsed'. Therefore a system with an expansion reservoir was used.

The results found are presented in Table 2 below;

Test	Time [s] 1)	concentration [g/l] 2)	Volume [l]	flow [l/s] 3)	Pressure calculated [kPa] L&H 4)	Pressure calculated [kPa] Y&KP 5)	Peak Pressure [kPa] 6)
101		125	1	$6.8*10^{-4}$	700	330	312
102	1400	125	0.9	$6.8*10^{-4}$	700	330	250
103	15	125	1	0.076	700	330	404
104	15	150	1	0.076	700	330	391
105	15	100	1.1	0.076	700	330	375

Table 2: Test results BTL 48 – Blow out tests

Remarks regarding parameters in Table 2;

1) The speed of opening the pipe was increased in later tests.
2) The concentration of the bentonite was varied (drilling fluid rheological properties)
3) Flow = volume/time
4) Pressure calculated with the formulas of Luger and Hergarden (assumed E=15MPa). – L&H
5) Pressure calculated with the theory of Yanagisawa and Komak Panah. –Y&KP
6) The pressure was measured in the initial opening. The pressure at the start in the first test was to low. The peak pressure was more or less the same in the last three tests. However the development after this peak pressure differed for each test.

The following conclusions were drawn from these tests:

- In all tests fracturing was found.
- Fracturing was local. A crack did not develop over the entire injection area.

- The peak pressure was more or less the same after that the pressure developed differently. It was concluded that the first crack develops at the measured peak pressure and that the development of the rest of the pattern depended on the thickness of the mud (intrusion and penetration of drilling fluid).
- The predicted maximum pressures according to the cavity expansion theory are too high. The calculations according to Yanagisawa and Komak Panah seem to match better. Both theories are based on the start of plasticity. However the observed failure mechanism is fracturing.
- The difference between the calculation of the maximum pressure according to the cavity expansion theory and according to Yanagisawa and Komak Panah is the way in which the drilling fluid intrusion is taken into account. In the theory of cavity expansion it is assumed that the pressure works directly on the wall (no penetration). In the theory of Y&KP it is assumed that the mud flows through a cylindrical soil sample. There is a hydraulic gradient. The forces work on a larger area.
- it was expected that the penetration of mud in the sample would depend on the concentration (thickness) of the mud. This was not found in the test results. This could be a result of the small number of tests done and the fact that during each test the same volume was put in the soil.

C.1.6 Numerical and analytical calculation models for soil failure (BTL 41)

In BTL 41 Numerical tests were done. With the help of Plaxis, a finite element method computer program, a simulation of a blow-out was established. Two different material models were used: Mohr Coulomb and Soft Soil (Cam-Clay). By means of interfaces a possibility is put in the numerical model to simulate discontinuities (fracturing). These discontinuities are the start of a fracture. The strength parameter of the interface was therefore reduced. The reduction factor was chosen arbitrarily.

It was seen in these tests that failure (blow-out) without an interface occurred. When it occurred it was due to the development of large plastic areas. When an interface was introduced the failure occurred due to wedges above the borehole. With the help of interfaces it was not possible to simulate the hydraulic fracturing process. Only the final situation when the fracture is established could be approached.

C.1.7 Influence of wall during blow-out experiments in dredging flume (BTL 54)

Calculations were made with Plaxis to determine the influence of the walls in the test channel during the performed experiments (paragraph C.1.2). The maximum pressure of the drilling fluid when the soil fails was calculated. From the simulation by Plaxis it appears that the limited width of the test channel and the wall friction probably cannot be neglected. This could be the reason why the measured pressures where relatively high. However, the high elasticity modulus and dilatancy effects due to the very densely-packed sand, may also have been a reason for the relative high failure pressure.

C.2 Models*

In reports published by BTL several models can be found on the maximum allowable pressure. These models are presented in this paragraph. The models are based on analytical theories and some are compared to empirical findings. They can be divided into two categories:

1. Models based on expansion theory
This consists of the theory of Vesic and the theory developed by Luger and Hergarden (which is based on the theory of Vesic) is described in appendix D.

2. Models based on hydraulic fracturing
In the framework of the research performed by BTL a sight experiment was carried out (BTL 17 – see §C.1.1). A hole was drilled through gelatine. No cavity expansion was observed, instead randomly radial fractures originated. Coherence was found in the limit pressure and the undrained peak shear strength of gelatine. This aroused the question whether hydraulic fracturing as known from rock mechanics also was found for softer soils injected with a fluid. A restricted literature research showed that this was indeed found for fluid injection in soft clay (both in the field, mostly offshore, as in laboratory tests). An important difference in the theories is the assumption at which fracturing occurs:

- As a result of tensile stresses. A subdivision applies here:
  - assumption of linear elastic material (C.2.3)
  - assumption of non-linear elastic material (C.2.4)
- As a result of shear stresses (C.2.5 and C.2.6)

All tests have been carried out with water, except for the tests executed by Andersen et al. (C.2.7).

* Models presented in this paragraph are mostly found in BTL 17

C.2.1 Vesic *

Vesic first introduced the expansion theory for cavities in soil mass in 1972. Luger & Hergarden developed the theory further in 1988 to able to use it for calculations of maximum allowable pressure during a horizontal directional drilling. In this paragraph the model of Vesic is explained. The model developed by Luger and Hergarden is explained in appendix D.

The method developed by Vesic determines the size of the plastic zone that is assumed to originate from increased fluid pressures in a borehole. The following assumptions are made:

- The medium is homogeneous and isotropic and has infinite dimensions.
- In the cavity there is a uniformly distributed internal pressure 'p'.
- The soil behaves in the plastic zone as a compressible plastic solid, defined by Coulomb-Mohr shear strength parameters (c, φ), as well as by an average volumetric strain (Δ).
- Beyond the plastic zone the soil is assumed to behave as a linearly deformable, isotropic solid defined by a modulus of deformation (E) and a Poisson's ratio (ν).
- Prior to the application of the load the entire soil mass has an isotropic effective stress q
- The body forces within the plastic zone are negligible when compared with existing and newly applied stresses.

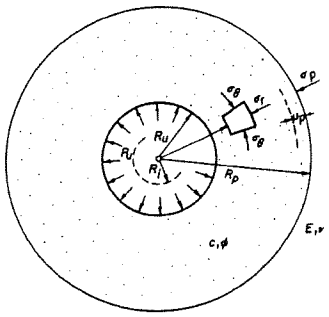

Figure 4: Representation of cavity

Thus, a cylindrical symmetrical problem of a gravity free medium is considered. The shearing stresses acting on an element, such as shown in Figure 4, vanish. The equations of equilibrium are reduced to;

$$\frac{\partial \sigma_r}{\partial r} + \frac{\sigma_r - \sigma_\theta}{r} = 0 \qquad [C.1.1]$$

In which 'r' is the distance to the centre of the cavity. The condition of rupture, according to Mohr, becomes;

$$(\sigma_r - \sigma_\theta) = (\sigma_r + \sigma_\theta)\sin\varphi + 2c\cos\varphi \qquad [C.1.2]$$

Introducing [C.1.2] into [C.1.1], and keeping in mind that, at limit equilibrium;

$$\frac{\sigma_\theta + c\cot\varphi}{\sigma_r + c\cot\varphi} = \frac{1-\sin\varphi}{1+\sin\varphi} \qquad [C.1.3]$$

* Text is mainly derived from; Expansion of cavities in infinite soil mass, Aleksandar Sedmak Vesić, Journal of the soil mechanics and foundation division, Proceedings of the American Society of Civil Engineers, March 1972

as well as that $\sigma_r = p_u$ for $r = R_u$, the solution of the differential equation [C.1.1] can be obtained;

$$\sigma_r = (p_u + c\cot\varphi)\left(\frac{R_u}{r}\right)^{2\sin\varphi/(1+\sin\varphi)} - c\cot\varphi \qquad [C.1.4]$$

The expression shows the rate of decrease of stress with distance within the plastic zone depends on the slope of the Mohr's envelope. It can be shown that, if $\varphi = 0$, equation [C.1.4] transforms into;

$$\sigma_r = p_u - 2c\,\ln\left(\frac{r}{R_u}\right) \qquad [C.1.5]$$

To determine the ultimate pressure, p_u, and the radius of the plastic zone, R_p, a relationship stating that the change of volume of the cavity is equal to the change of volume of the elastic zone plus the change of volume of the plastic zone is used. Denoting the radial displacement of the limit of plastic zone by u_p, this relationship can be written as follows;

$$R_u^2 - R_i^2 = -[(R_p - u_p)^2 - R_p^2 + (R_p^2 - R_u^2)\Delta \qquad [C.1.6]$$

The radial displacement, u_p, can be computed from the well-known Lamé's solution;

$$u_p = \frac{1+\nu}{E} R_p(\sigma_p - q) \qquad [C.1.7]$$

In which σ_p is the value of σ_r at $r = R_p$

$$\sigma_p = (p_u + c\cot\varphi)\left(\frac{R_u}{R_p}\right)^{2\sin\varphi/(1+\sin\varphi)} - c\cot\varphi \qquad [C.1.8]$$

Combining equation [C.1.7] with equation [C.1.8] and neglecting the higher powers of u_p as well as R_u^3, Equation [C.1.6] becomes;

$$2\frac{R_p^2}{R_u^2}\frac{1+\nu}{E}\left[(p_u + c\cot\varphi)\left(\frac{R_u}{R_p}\right)^{\frac{2\sin\varphi}{1+\sin\varphi}} - (q + c\cot\varphi)\right] + \frac{R_p^2}{R_u^2}\Delta = 1 + \Delta \qquad [C.1.9]$$

The equilibrium of stress components at $r = R_p$ requires that;

$$(p_u + c\cot\varphi)\left(\frac{R_u}{R_p}\right)^{\frac{2\sin\varphi}{1+\sin\varphi}} = (q + c\cot\varphi)(1 + \sin\varphi) \qquad [C.1.10]$$

The radius of the plastic zone, R_p, is found from the expression;

$$\frac{R_p}{R_u} = \sqrt{I'_{rr}\cdot\sec\varphi} \qquad [C.1.11]$$

In which;

$$I'_{rr} = \frac{I_r}{1 + \Delta\cdot I_r\cdot\sec\varphi} = \zeta_v' I_r \qquad [C.1.12]$$

and ζ_v' is the volume change factor for a cylindrical cavity.

In [C.1.12] I_r is the following:

$$I_r = \frac{E}{2\cdot(1+\nu)\cdot(c + q\cdot\tan\varphi)} = \frac{G}{s} \qquad [C.1.13]$$

In which:

E Elasticity modulus
ν Poisson's coefficient
c cohesion
q isotropic stress
φ angle of internal friction

The quantity, I_r, called the rigidity index, has a physical meaning: it represents the ratio of the shear modulus, G, of the soil to its initial shear strength, $s = c + q \tan \varphi$. Typical values of rigidity indexes for different known media have been computed and assembled in Table 3, together with the typical resulting values of the R_p/R_u ratio.

Medium	Rigidity index I_r [C.1.13]	Relative radius of plastic zone R_p/R_u (if $\Delta = 0$) cylindrical cavity
Rock	100 to 500	12 to 25
Sand (loose tot dense) $q = 1$ kg/cm²	70 to 150	9 to 15
saturated clay (soft to stiff)	10 to 300	3 to 17
Micaceous silt	10 to 30	3 to 6
Mild steel	300	17

Table 3: Typical values of rigidity index I_r

Knowing R_p/R_u the ultimate cavity pressure can be computed from equation [C.1.10]. The result can be put into the following from;

$$p_u = c \cdot F_c + q \cdot F_q \qquad [C.1.14]$$

In which:
p_u = effective failure pressure of the soil
q = effective isotropic stress

F_c and F_q are dimensionless factors, which are calculated in the following way:

$$F_q = (1 + \sin\varphi) \cdot (I'_{rr} \cdot \sec\varphi)^{\frac{\sin\varphi}{1+\sin\varphi}} \qquad [C.1.15]$$

$$F_c = (F_q - 1) \cdot \cot an\varphi \qquad [C.1.16]$$

For $\varphi = 0$ and $\Delta = 0$;

$$F_c = \ln I_r + \qquad [C.1.17]$$

C.2.2 Comparison to test results (BTL 17)

Mori and Tamura (1987) conducted experiments that both looked at the hydraulic fracturing process, and at the process of expansion. They did this by filling up a balloon in a borehole. The limit pressures they found almost perfectly matched the results found with the equations based on the expansion theory. Mori and Tamura stated that expansion is an upper limit for fracturing, which is valid for liquids with a very high viscosity (no intrusion into the soil).

C.2.3 Start fracturing due to tensile stress, linear elastic (Bjerrum, BTL17)

In the following paragraph the approach presented by Bjerrum et al. (1972) is explained. Their theory is based on a situation where in practice the permeability of a clay layer has to be determined. The permeability that was found in an in-situ test was larger than the calculated permeability. For a better understanding they performed additional laboratory tests and developed a theory.

In Bjerrum's approach the following is assumed:

- Hydraulic fracturing caused by tensile stresses. Fracturing starts when the tensile strength of the material (soil pressure) is exceeded.
- Elastic material – The material deforms elastically until collapse. The E-modulus is constant.
- The pore pressure in clay is constant and independent of the deformation of the hole.
- The hole is vertical.

In the equations presented by Bjerrum soil expansion is taken into account but the approach differs from Luger and Hergarden. Bjerrum acknowledges three different types of deformation; direct fracturing (a), cylindrical expansion (b), and fracturing after expansion (c) (see Figure 5). In this approach he takes a maximum deformation into account.

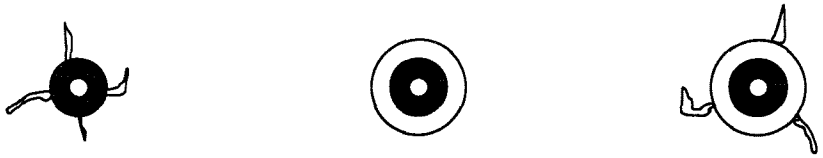

a) direct fracturing | b) cylindrical expansion | c) fracturing after expansion

Figure 5: Possible processes according to Bjerrum et al.

a. Fracturing before cylindrical expansion is achieved

$$\frac{\Delta u_{lim}}{\sigma'_v} = \left(\frac{1}{\nu} - 1\right) \cdot \left((1-\alpha) \cdot K_0 + \frac{\sigma'_{tmax}}{\sigma^t_v}\right) \qquad [C.3.1]$$

if $0 \le \frac{\Delta u_{lim}}{\sigma'_v} \le (1+\beta) \cdot K_0$ no expansion

b. Cylindrical expansion without fracturing

$$0 \le \frac{\Delta u_{lim}}{\sigma'_v} \le (1+\beta) \cdot K_0 \qquad [C.3.2]$$

if $\left(\frac{1}{\nu} - 1\right) \cdot \left((1-\alpha) \cdot K_0 + \frac{\sigma'_{tmax}}{\sigma^t_v}\right) > (1+\beta) \cdot K_0$ no fracturing type a

and $(1-\nu) \cdot \left((2-\alpha+\beta) \cdot K_0 + \frac{\sigma'_{tmax}}{\sigma^t_v}\right) > \frac{\Delta u}{\sigma'_v}$ no fracturing type c

c. Fracturing after limited expansion

$$\frac{\Delta u_{lim}}{\sigma'_v} = (1-\nu)\cdot((2-\alpha+\beta)\cdot K_0 + \frac{\sigma'_{tmax}}{\sigma'^{t}_{v}}) \qquad [C.3.3]$$

if $(\frac{1}{\nu}-1)\cdot((1-\alpha)\cdot K_0 + \frac{\sigma'_{tmax}}{\sigma'^{t}_{v}}) > (1+\beta)\cdot K_0$ no fracturing type a

and $(1+\beta)\cdot K_0 < \frac{\Delta u}{\sigma'_v}$ no expansion

In this:

Δu_{lim}	overpressure limit of fluid in hole (water) = p'_{lim} = imposed pressure difference during in-situ permeability test
Δu	overpressure of fluid in hole (water)
ν	Poisson's ratio
σ'_v	effective vertical ground pressure (previous to test boring)
$\sigma'_{t,max}$	maximum effective tensile tension that soil can take
α	constant of material $-1.1 < \alpha < 4$
β	constant of material $0.5 < \beta < 4$
K_0	ratio horizontal / vertical effective strength

Bjerrum et al. suppose, in contrast to other theories, that the cavity expansion limit pressure is not an absolute upper limit. The explanation for this could be that Bjerrum et al. not only consider a maximum allowable pressure, but also a maximum allowable deformation. The latter is also an upper limit for cavity expansion.

The theory has also been compared to test results of other researchers. However, it appeared that the theory does not adequately describe the physical process. When the support pressure tends to zero, according to the theory the failure pressure should also be zero. This is not supported by the test results. Moreover, it is a disadvantage that the influence of the material characteristics is so large. These characteristics depend on the compressibility of the material and are difficult to determine.

C.2.4 *Initiation of fracturing due to tensile stress, not linear elastic (BTL17)*

Andersen et al. (1994) developed a more sophisticated model. It is based on the following assumptions:

- shear modulus is not linear (G) and depends on τ (shear stress)
- pore pressure is not linear
  Pore pressure: $u = u_0 + \Delta u$
  In which:
  u = actual pore pressure
  u_0 = pore pressure previous to drilling
  Δu = change of pore pressure due to for example the drilling of the hole and the connected deformations of the soil, and due to changes in the fluid pressure in the borehole.
- due to Δu the effective stresses changes (in general smaller)

Fracturing occurs when:

$$\Delta p_m = p_{lim} - \sigma'_{r0} \qquad [C.4.1]$$

And the following conditions are met:

$\Delta\sigma'_\theta = -(K_0.\ \sigma'_{v0} + \sigma_{t,max})$ vertical fracture [C.4.2]

$\Delta\sigma'_z = -(\sigma'_{v0} + \sigma_{t,max})$ horizontal fracture [C.4.3]

$p_{lim} = u_0 + \sigma'_{h_0}$ or $\sigma'_{v_0} + \Delta p_m$ [C.4.4]

if $\Delta\sigma'_\theta$ determines then σ'_{h0} otherwise (if $\Delta\sigma'_z$ determines) then σ'_{v0}

In which:

Δp_m	overpressure in borehole compared to soil massif
$\Delta\sigma'_\theta$	change in effective tangential stress
$\Delta\sigma'_z$	change in effective vertical stress
σ'_{r0}	effective radial stress prior to boring
σ'_{v0}	effective vertical stress prior to boring
$\sigma_{t,max}$	tensile strength, can possibly be put on '0'.

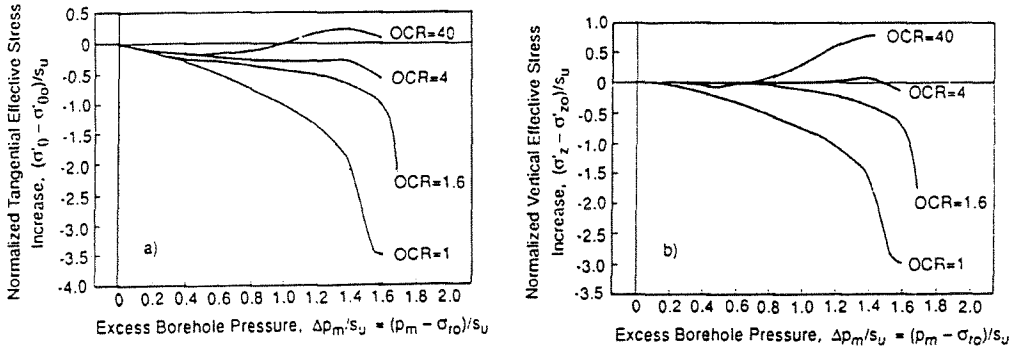

Figure 6: Changes in tangential and vertical stresses as a function of overpressure in a borehole

This theory requires that additional shear tests and FEM analysis are done to be able to use the mentioned equations. The theoretical calculated limit pressures seem to correspond to the measured pressures. However there is the disadvantage of complicated tests and calculations.

C.2.5 Initiation of fracturing due to shear, method 1 (Komak Panah and Yanagisawa, BTL17)

In this approach it is assumed that fracturing occurs due to shear and not due to tensile stresses. Laboratory test results seem to support the equations presented in this paragraph.

A model can be made based on the Mohr-Coulomb criterion. Komak Panah and Yanagisawa developed a theory, based on this assumption, for a hollow cylindrical sample (geometry is shown in Figure 7), which is fully saturated, to calculate total stresses in this sample.

$$\sigma_r = p_{lim} \qquad [C.5.1]$$

$$\sigma_\theta = \frac{2\sigma_h b^2 - p_{lim}(b^2 + a^2)}{b^2 - a^2} \qquad [C.5.2]$$

In which:

σ_r radial stresses
σ_θ tangential stresses
σ_h horizontal stresses
a radius borehole (internal radius)
b radius sample (external radius)

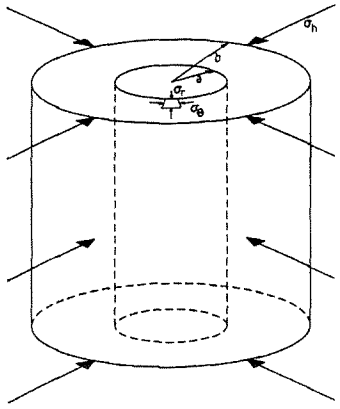

Figure 7: Definitions used by Komak Panah and Yanagisawa

Fracturing occurs, when $\sigma_r > \sigma_\theta$. The Mohr-Coulomb failure criterion can now be written as:

$$(\sigma_r - \sigma_\theta) = (\sigma_r + \sigma_\theta)\sin\varphi_u + 2c_u\cos\varphi_u \qquad [C.5.3]$$

In which;

φ_u undrained angle of internal friction

The combination of the equations [C.5.2] and [C.5.3] leads to the following:

$$p_{lim} = \frac{b^2(1+\sin\varphi_u)}{b^2 + a^2\sin\varphi_u}\sigma_h + \frac{(b^2 - a^2)\cos\varphi_u}{b^2 + a^2\sin\varphi_u}c_u \qquad [C.5.4]$$

When taking into account (in the same way as in the theory of Andersen et al. § C.2.7):

- The influence of overpressure of the groundwater in the pores.

- Instead of the horizontal stresses (σ_h) the minimal stresses (σ_0) (are usually the same).

Then the equation can be rewritten as:

$$p_{lim} = \frac{b^2(1+\sin\varphi_u)}{b^2+a^2\sin\varphi_u}\sigma_{min} - \frac{(b^2-a^2)\cos\varphi_u}{b^2+a^2\sin\varphi_u}\Delta u + \frac{(b^2-a^2)\cos\varphi_u}{b^2+a^2\sin\varphi_u}c_u \quad [C.5.5]$$

For $b >> a$ the equation can be simplified:

$$p_{lim} = \sigma_{min}(1+\sin\varphi_u) - \Delta u\sin\varphi_u + c_u\cos\varphi_u \quad [C.5.6]$$

For clay it can be assumed $\varphi_u = 0°$:

$$p_{lim} = \sigma_{min} + c_u \quad [C.5.7]$$

The equation (non-simplified) has been compared to the results of experiments on clay samples. The results matched well. Therefore it was concluded that the theory is valid for saturated clay samples under laboratory conditions (controlled speed of build-up of pressure 0.1 kPa/s).

Mori and Tamura (1987 – earlier mentioned in § C.2.2) performed experiments on samples with the same form (hollow cylinders), but with different speeds of built up of pressure. Equation [C.5.7] seemed to be accurate for:

0.1 kPa/s $\rightarrow p_{lim} = \sigma_{min} + c_u$

However for a faster pressure build-up the following was found.

2 kPa/s $\rightarrow p_{lim} = \sigma_{min} + 2c_u$ [C.5.8]

The fact that the borehole is not saturated anymore could possibly explain the difference in the results.

C.2.6 Start fracturing due to shear, method 2 (Overy and Dean, BTL17)

Overy and Dean also expected fracturing due to shear. They derived another equation. When the radial and tangential stresses around the borehole are considered (σ_r and σ_θ), for a liquid injection it appears that radial stresses become larger (compression) and tangential stresses become smaller (tensile forces).

Shear occurs when:

$$\sigma_r - \sigma_\theta = 2c_u \quad [C.6.1]$$

Overy and Dean made two assumptions:

- The fluid pressure in the borehole is at the moment of failure larger than the radial stress σ_r.
- The reduction of tangential stress σ_θ can be neglected.

The following equation can then be derived:

$$p_{lim} = \sigma_{min} + 2c_u \quad [C.6.2]$$

This equation is the same as found during he empirical tests with fast pressure build-up (Mori and Tamura, 1987). This theory predicted the limit pressure reasonably well in two out of three investigated cases of practice tests in vertical boreholes in the North Sea

C.2.7 Calculation methods (Andersen and Lunne, BTL 17)

Andersen and Lunne (1994) made a comparison between several analytical and empirical methods. According to them too large tensile forces introduce fracturing and not shear. As a representation of their comparison they made the following figure (Figure 8):

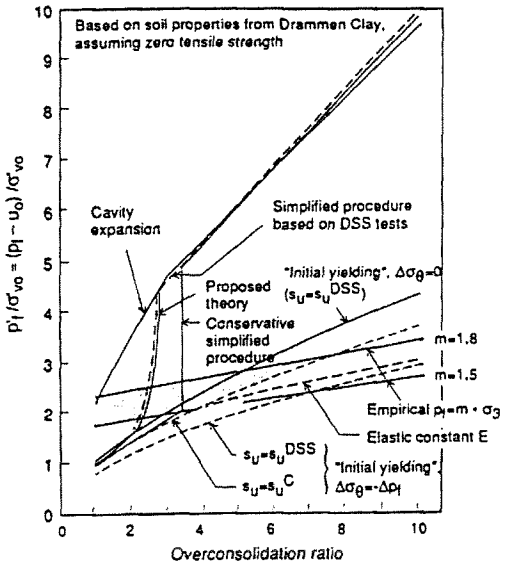

Figure 8: comparison between new theory Andersen et al. simplified version, and other theories

In this figure the failure pressure (p_{lim}) is divided by the effective vertical stress (σ'_{vo}) and is showed as a function of OCR (over consolidation ratio*). The differences between the various methods are not the main issue. Apparently there are great differences and the cavity expansion theory results in an upper limit for the failure pressure.

On the basis of measurements Andersen et al. propose a new method incorporating the behaviour of clay. They do this by simulating stress-deformation behaviour in a finite element method (FEM) calculation where parameters are derived from a direct simple shear test. In practice this is not always possible, therefore, they also propose simplified methods:

- This simple method shows that hydraulic fracturing occurs with a OCR smaller than 3.5.

$$\frac{p'_{lim}}{\sigma'_{v0}} = K_0 + 1.2\frac{c_u}{\sigma'_{v0}} \qquad [C.7.1]$$

- However when the value of OCR is larger than 3.5 cavity expansion will be the failure mechanism. Then the following applies:

$$\frac{p'_{lim}}{\sigma'_{v0}} = K_0 + 4.5\frac{c_u}{\sigma'_{v0}} \qquad [C.7.2]$$

This simple method is based on a correlation. When clay has an OCR<3.5 then contraction behaviour applies. The tangential stresses are <0 and hydraulic fracturing occurs. If the clay has an OCR >3.5 then dilatancy will prevent hydraulic fracturing.

* The OCR is an value that indicates what maximum pressure has been put on the clay in the past in comparison with current vertical effective stress

C.2.8 Probability fracturing (Massarsch, BTL41)

Massarsch (1978) looked at the problem in a slightly different way. He assumed plastic deformation (cavity expansion) which could, perhaps, change into hydraulic fracturing. Massarsch defined the following criterion for the occurrence of hydraulic fracturing:

If the criterion is valid [C.8.1], fracturing is likely

$$\frac{\sigma'_{min\,0}}{c_u} < 1.73 \cdot \bar{A}_f + 0.43 \qquad [C.8.1]$$

In which:
$\bar{A}_f$ Skempton's pore pressure parameter*

	$\bar{A}_f$
active clay	1.0 – 1.5
normal consolidated 'weak' clay	0.8 – 1.0
lightly overconsolidated clay	0.6 – 0.8
overconsolidated clay	0.3 – 0.6

Table 4: values that can be taken for $\bar{A}_f$

Massarsch takes as limit-pressure the cylindrical expansion limit pressure. The condition mentioned above should be read: "IF deformations occur, fracturing is or is not probable...".

Whether a vertical or horizontal pressure originates is determined by the following condition:

$$C_r = \frac{1.73\bar{A}_f + 0.43}{K_0(1.73\bar{A}_f - 0.577)} \qquad [C.8.2]$$

If $C_r < 1$ then horizontal fractures
If $C_r > 1$ then vertical fractures
It appeared that C_r is larger than 1 for most clays. Therefore, in practically all clays vertical fractures occur.

Next to this, Massarsch gives, on the basis of the radius of the plastic zone, an estimate for the length of the occurring fractures that depend on the diameter of the borehole (D):

$$L = 0.3D\sqrt{\frac{2(1+\nu)G}{c_u}} \qquad [C.8.3]$$

These equations have not been verified in practice. Equation [C.8.3] is the only equation found that describes the length of the fracture. According to Massarsch soil characteristics and the diameter of the drilling determine the length of fractures. In the test in gelatine (BTL17) it is found that these also depend on flow and progress velocity.

* $\bar{A}_f$ is a relation between the increase in pore pressure and the increase in deviator stress during shear. $\bar{A}_f$ refers to the value of failure.

C.2.9 *Comparison*

In the table below the different parameters used by the models are mentioned (Table 5: Overview models). In all models the following is assumed:

- isotropic stresses
- homogeneous soil conditions

It is repeated that most models are based on the behaviour of clay.

Mechanism:	**§**	**Remarks**
Cavity expansion – Vesic	C.2.1	No volume change R_0 (= R_{bh}) , R_p, φ, E, ν, c, q
Cavity expansion – *Luger & Hergarden*	appendix D	Absence isotropic deformations in plastic zone R_0, R_p, φ, G (E, ν) c, σ'_0
Fracturing due to tensile stresses – linear elastic – Bjerrum	C.2.3	Maximum allowable deformations Three possible processes Assumes upper limit for cavity expansion ν, Δu, σ'_v, $\sigma'_{t,max}$, α, β, K_0 (not supported by test results)
Fracturing due to tensile stresses – not linear elastic – Andersen & Lunne	C.2.4	pore pressures not linear effective stresses change additional FEM and shear tests necessary G (τ), Δp_m, σ'_0, K_0, $\sigma_{t,max}$ simple equations on the basis of OCR
Fracturing due to shear – Komak Panah and Yanagisawa	C.2.5	Tests on hollow cylindrical sample Mohr Coulomb φ_u, Δu, σ_{min}, c_u (seems to be supported by test results – slow pressure build up)
Fracturing due to shear – Overy and Dean	C.2.6	Fluid pressure > σ_r when soil fails Reduction tangential σ neglected σ_{min}, c_u (seems to be supported by test results – fast pressure build up)
Probability fracturing – Massarsch	C.2.8	Plastic deformation which can change into hydraulic fracturing Probability of occurrence Also equation for length fracture σ_{min}, c_u, K_0,$\bar{A}_f$

Table 5: *Overview models*

Next to that, it is expected that:

- speed of pressure build up plays a role
- dilatancy or contractant behaviour plays a role

D SOIL MODEL OF LUGER & HERGARDEN AND COMPARISON WITH 'NEW' MODEL

In this appendix the approach to maximum allowable pressures developed by Luger and Hergarden is described. First the initial presentation of the approach is given. This consists of the theory and the equations used.

At the start of the thesis research it was not clear what the basis of these equations were. Therefore these equations were anew derived. The model that forms the basis for these equations is based on a cylindrical cavity. This derivation is presented in § D.2.

To complete the comparison the failure criterion as presented by Luger & Hergarden is rewritten in the parameters used for the new failure criterion and vice versa (§ D.3).

From this derivation and comparison it will become clear that both models are actually very much alike.

D.1 Initial presentation of approach*

In this paragraph a description of the theory as it is known from the article for the No-Dig conference in Washington 1988 is presented. More or less the same text was published in the Dutch norms (Appendix E of NEN3651and NPR3659)

D.1.1 Theory

The theory of H.J. Luger and H.J.A.M. Hergarden was first presented on the No-Dig conference in Washington 1988. It was based on the theory of cavity expansion, developed by Vesic. Luger and Hergarden compared their theory to finite element calculations and mud pressure measurements in the borehole (pull back operation drilling under canal "Windaassloot"). The results were in accordance with the theory. In their article they recognise two failure mechanisms of collapse at high pressures: uncontrolled expansion and hydraulic fracturing.

The basis of their theory is the following. The mud in the soil will exert pressure on the soil. When this pressure exceeds a certain value plastic deformation of the soil will result. Initially this will be adjacent to the borehole. When the pressure is increased beyond this value the zone with plastic deformations will enlarge itself as well. In order to prevent blowouts or other damage the plastic zone must remain within a safe radius around the hole. The pressure has to be determined that creates a plastic zone, which does not exceed the established safe radius.

* Large parts of the text in this paragraph are directly derived from the conference paper: No-Dig 1988, Directional Drilling in soft soil: Influence of Mud Pressures

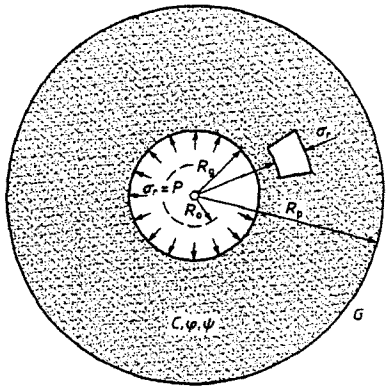

Figure 9: Schematisation of the borehole

A hole is drilled with an initial radius R_o (Figure 9). Under influence of the drill mud pressure (p) the radius of the hole increases, as is shown by line A (Figure 10). When a maximum allowable radius ($R_{p,max}$) of the plastic zone is chosen one can derive the radial stress (σ_r) as a function of the distance to the hole (r), which is shown as line B. At the boundary of hole and soil the mud pressure and radial stress are equal. The intersection of lines A and B gives the maximum allowable pressure in the hole.

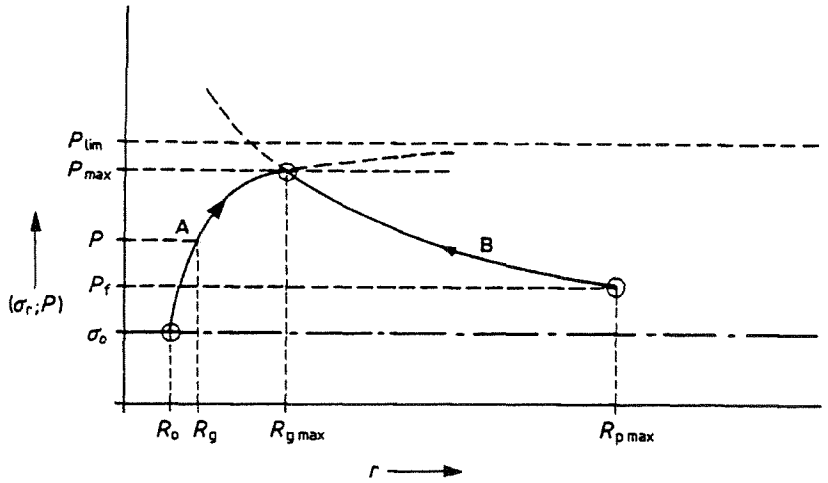

Figure 10: borehole mud pressure versus borehole radius (line A) and radial total stress versus r-co-ordinate

Another criterion is provided by the notion of the so-called "limit pressure" (well known from cavity expansion theories). This is the highest pressure, which can be sustained by a cavity. This forms the upper boundary for the mud pressure in the borehole. It is assumed that one would like to restrict the maximum allowable borehole pressure to less than ninety percent of the limit pressure (p_{lim}).

D.1.2 Equations

The theory mentioned above has resulted in a set of equations. This model is based on the assumption of axial symmetry around the borehole and the following four conditions:

- Equilibrium
- Hooke's law for increments of elastic deformation

- Mohr-Coulomb's failure criterion.
- Absence of isotropic deformations in the plastic zone

First plasticity occurs when the mud-pressure (p) reaches a value (p_f) which is equal to;

$$p_f = \sigma'_0 \cdot (1 + \sin\varphi) + c \cdot \cos\varphi + u \qquad [D.1.1]$$

Where;

σ'_0 the initial effective stress
φ internal friction angle
c cohesion
u initial in-situ pore pressure

The effective mud pressures are defined as; $p' = p\text{-}u$ and $p'_f = p_f - u$
Effective mud pressures, which have not exceeded p'_f the radius of the borehole is described by;

$$R_g = R_0 \cdot [1 \cdot \{(p' - \sigma'_0)/G\}]^{-0.5} \qquad [D.1.2]$$

Where;

R_g radius of the borehole
R_0 initial radius of the borehole
G shear modulus

Equation [D.1.2] describes the form of line A (Figure 10) for mud pressures, which have not exceeded p_f. The equation is the result of the application of Hooke's law on the increments of stresses and strains. For $R_g \approx R_0$ the expression is equivalent to the usual expression for the expansion of a cavity in an elastic material.

Consider a soil particle at the transition between the elastic and plastic zone (position $s = R_p$). Its original position can be determined using equation [D.1.1] and [D.1.2];

$$s_0 = s \cdot [1 - \{(\sigma'_0 \cdot \sin\varphi + c \cdot \cos\varphi)/G\}]^{0.5} \qquad [D.1.3]$$

Where;

s_0 initial position of particle
s actual position of particle

The assumption that in the plastic zone no volume change occurs is used.
The volume between $r = s_0$ and $r = s$ ($= R_p$) is equal to the volume $r = R_0$ and $r = R_g$.
The current radius of the borehole can be expressed as a function of the initial radius and the radius of the plastic zone.

$$R_g^2 = R_0^2 + R_p^2 \cdot \{(\sigma'_0 \cdot \sin\varphi + c \cdot \cos\varphi)/G\} \qquad [D.1.4]$$

Equation [D.1.4] describes the geometry of the hole and the plastic zone. Using the value of the radial stress at the transition from elastic and to plastic behaviour, the equilibrium condition, and using the Mohr-Coulomb failure criterion it is possible to determine the radial stress as a function of the r-co-ordinate;

$$\sigma'_r = (p'_f + c \cdot \cot\varphi) \cdot \left(\frac{R_p}{r}\right)^{\frac{2 \cdot \sin\varphi}{1+\sin\varphi}} - c \cdot \cot\varphi \qquad [D.1.5]$$

where;

σ'_r radial effective stress

Equation [D.1.5] describes line B (Figure 10) when R_p is substituted by $R_{p,max}$. From equation [D.1.4] and [D.1.5] one can derive the relation between the pressure in the hole and the actual radius of the hole, considering that the radial effective stress at the borehole wall is equal to the effective mud pressure: $p' = \sigma'_r$ $(r = R_g)$. It can be concluded that;

$$p' = (p'_f + c \cdot \cot\varphi) \cdot [\{1 - (\frac{R_0}{R_g})^2\} / Q]^{\frac{-\sin\varphi}{1+\sin\varphi}} - c \cdot \cot\varphi \qquad [D.1.6]$$

where;

$$Q = \frac{(\sigma'_0 \cdot \sin\varphi + c \cdot \cos\varphi)}{G}$$

Equation [D.1.6] describes line A in (Figure 10) for mud pressures exceeding p_f.

The maximum allowable value of the mud pressure (intersection of line A and B) equals;

$$p'_{max} = (p'_f + c \cdot \cot\varphi) \cdot \{(\frac{R_0}{R_{p,max}})^2 + Q\}^{\frac{-\sin\varphi}{1+\sin\varphi}} - c \cdot \cot\varphi \qquad [D.1.7]$$

The other criterion mentioned before is related to the limit pressure. The effective limit pressure p'_{lim} follows from equation [D.1.6] if R_g approaches infinity and from equation [D.1.7] if $R_{p,max}$ approaches infinity;

$$p'_{lim} = (p'_f + c \cdot \cot\varphi) \cdot Q^{\frac{-\sin\varphi}{1+\sin\varphi}} - c \cdot \cot\varphi \qquad [D.1.8]$$

D.2 Mathematical description

In this paragraph the model described in the previous paragraph is derived from the basic assumptions. The equations are compared to the new model developed. This model for a cylindrical cavity is presented in appendix E. It is recommended to keep the conversion table with the 'translation' of the symbols used in the 'new' models and in the model of Luger and Hergarden at hand (appendix A).

D.2.1 First plasticity

Luger and Hergarden state that first plasticity occurs when the mud pressure reaches a value (p_f) which is equal to;

$$p'_f = \sigma'_0 \cdot (1 + \sin\varphi) + c \cdot \cos\phi \qquad [D.1.1]$$

This equation is comparable to equation [E.1.44];

$$p_i + a > (1 + \sin\varphi)(p_0 + a) \qquad [D.2.1]$$

where;

a c cotφ

This can be rewritten as;

$$p_i = p_0 \cdot (1 + \sin\varphi) + (1 + \sin\varphi - 1) \cdot a \qquad [D.2.2]$$

$$p_i = p_0 \cdot (1 + \sin\varphi) + c\cos\varphi \qquad [D.2.3]$$

Now the equation has the same form as equation [D.1.1].
(it is reminded that; $p'_f = p_i$ and $\sigma'_0 = p_0$)

D.2.2 Radius of the borehole before first plasticity

According to Luger and Hergarden the radius of the hole for effective mud pressures which have not exceeded p'_f is described by;

$$R_g = R_0 \cdot [1 - \{(p' - \sigma'_0)/G\}]^{-0.5} \qquad [D.1.2]$$

In Report BAGT 347 H.J. Luger (1982) described the following approach to come to this equation;

The equilibrium of an element is described as follows (increments are used in stead of total stresses);

$$\frac{\partial \dot{\sigma}_{rr}}{\partial r} + \frac{\dot{\sigma}_{rr} - \dot{\sigma}_{tt}}{r} = 0 \qquad [D.2.4]$$

$$\dot{\varepsilon}_{rr} = -\frac{\partial \dot{u}_{rr}}{\partial r} \; ; \; \dot{\varepsilon}_{tt} = -\frac{\dot{u}_{rr}}{r} \; ; \; \dot{\varepsilon}_z = 0 \qquad [D.2.5]$$

$$\begin{bmatrix} 1 & -\nu & -\nu \\ -\nu & 1 & -\nu \\ -\nu & -\nu & 1 \end{bmatrix} \begin{bmatrix} \dot{\sigma}_{rr} \\ \dot{\sigma}_{tt} \\ \dot{\sigma}_{zz} \end{bmatrix} = E \begin{bmatrix} \dot{\varepsilon}_{rr} \\ \dot{\varepsilon}_{tt} \\ \dot{\varepsilon}_{zz} \end{bmatrix} \qquad [D.2.6]$$

Inversion;

$$\begin{bmatrix} 1-\nu & \nu & \nu \\ \nu & 1-\nu & \nu \\ \nu & \nu & 1-\nu \end{bmatrix} \begin{bmatrix} \dot{\varepsilon}_{rr} \\ \dot{\varepsilon}_{tt} \\ \dot{\varepsilon}_{zz} \end{bmatrix} = \frac{(1+\nu)(1-2\nu)}{E} \begin{bmatrix} \dot{\sigma}_{rr} \\ \dot{\sigma}_{tt} \\ \dot{\sigma}_{zz} \end{bmatrix} \qquad [D.2.7]$$

Substitution of [D.2.5] in [D.2.7] in [D.2.4];

$$\frac{\partial^2 \dot{u}_{rr}}{\partial r^2} + \frac{1}{r}\frac{\partial \dot{u}_{rr}}{\partial r} - \frac{\dot{u}_{rr}}{r} = 0 \qquad [D.2.8]$$

The solution is of the form;

$$\dot{u}_{rr} = Ar + \frac{B}{r} \qquad [D.2.9]$$

Solution;

$$\dot{\sigma}_{rr}(r,t) = -\frac{2G}{1-2\nu} A(t) + 2G \cdot B(t) \cdot r^{-2} \qquad [D.2.10]$$

The equation [E.1.13] derived in appendix E has the same from;

$$\sigma_{rr} = -2(\lambda + \mu)A + 2\mu B r^{-2} \qquad [D.2.11]$$

$$\dot{\sigma}_{tt}(r,t) = -\frac{2G}{1-2\nu} A(t) - 2G \cdot B(t) \cdot r^{-2} \qquad [D.2.12]$$

Equation [E.1.14] derived in appendix E has the same from;

$$\sigma_{tt} = -2(\lambda + \mu)A - 2\mu B r^{-2} \qquad [D.2.13]$$

$$\dot{\sigma}_z(r,t) = -\frac{4\nu G}{1-2\nu} A(t) \qquad [D.2.14]$$

It is assumed that the stresses on $r = \infty$ do not change. This implies that $A = 0$. The equations then become;

$$\dot{u}_{rr} = Br^{-1} \qquad [D.2.15]$$

$$\dot{\varepsilon}_{rr} = Br^{-2} \; ; \; \dot{\varepsilon}_{tt} = -Br^{-2} \; ; \; \dot{\varepsilon}_{z} = 0 \qquad [D.2.16]$$

$$\dot{\sigma}_{rr} = 2GBr^{-2} \; ; \; \dot{\sigma}_{tt} = -2GBr^{-2} \qquad [D.2.17]$$

As stated before R_g is the radius of the borehole. p is the pressure in the borehole. Therefore the following boundary condition applies;

$$\sigma_{rr}(R_g) = p \qquad [D.2.18]$$

The start conditions are the following;

$$\sigma_{rr}(t_0) = \sigma'_0 \; ; \; \sigma_{tt}(t_0) = \sigma'_0 \qquad [D.2.19]$$

The general expression for σ_{rr} is;

$$\sigma_{rr} = \sigma_{rr}(t_0) + \int_{t_0}^{t} \dot{\sigma}_{rr} dt = \sigma'_0 + 2Gr^{-2} \int_{t_0}^{t} B \, dt \qquad [D.2.20]$$

With boundary condition [D.2.18];

$$\int_{t_0}^{t} B \, dt = \frac{p - \sigma'_0}{2G} R_g^{\,2} \qquad [D.2.21]$$

The complete equations then become;

$$\sigma_{rr} = \sigma'_0 + (p - \sigma'_0)\left(\frac{R_g}{r}\right)^2 \qquad [D.2.22]$$

$$\sigma_{tt} = \sigma'_0 - (p - \sigma'_0)\left(\frac{R_g}{r}\right)^2 \qquad [D.2.23]$$

The equation for the displacement;

$$u_{rr} = u_{rr}(t_0) + \int_{t_0}^{t} \dot{u}_{rr} dt = u_{rr}(t_0) + r^{-1} \int_{t_0}^{t} B \, dt \qquad [D.2.24]$$

The initial displacement is zero; $u(t_0) = 0$. The equation;

$$u_{rr} = r^{-1} \frac{p - \sigma'_0}{2G} R_g^{\,2} \qquad [D.2.25]$$

On the borehole wall the following has to apply;

$$\left(\frac{\partial u_{rr}}{\partial t}\right)_{r=R_g} = \frac{\partial R_g}{\partial t} \qquad [D.2.26]$$

'r' is not a moving co-ordinate, therefore $\delta r/\delta t = 0$. The denomination R_g is a position of a soil particle on the wall of the borehole and therefore it depends on the time scale. The pressure can be written as a function of time but speed-factors do not play a role in the analysis. Equation [D.2.26] becomes;

$$\left(\frac{\partial u_r}{\partial p}\right)_{r=R_g} = \frac{\partial R_g}{\partial p} \qquad [D.2.27]$$

The first term can be determined by differentiation of equation [D.2.25];

$$\left(r^{-1}\left(\frac{R_g^{\,2}}{2G} + \frac{p - \sigma'_0}{G} \cdot R_g \cdot \frac{\partial R_g}{\partial p}\right)\right)_{r=R_g} = \frac{\partial R_g}{\partial p} \qquad [D.2.28]$$

$$\frac{R_g}{2G} + \frac{p - \sigma'_0}{G} \cdot \frac{\partial R_g}{\partial p} = \frac{\partial R_g}{\partial p} \qquad [D.2.29]$$

The solution has the form;

$$R_g = \frac{C}{\sqrt{2G}} \cdot (1 - \frac{p - \sigma'_0}{G})^{-\frac{1}{2}} \qquad [D.2.30]$$

With boundary condition $R_g(t_0) = R_0$ and $p(t_0) = \sigma'_0$ the equation reads;

$$R_g = R_0(1 - \frac{p - \sigma'_0}{G})^{-\frac{1}{2}} \Rightarrow R_g^2 = R_0^2(1 - \frac{p - \sigma'_0}{G})^{-1} \qquad [D.2.31]$$

The above-mentioned equation is equal to equation [D.1.2].

D.2.3 Soil particle at transition

Now consider a soil particle at the transition between the elastic and the plastic zone (position $S = R_p$). Its original position can be determined using equations [D.1.1] and [D.1.5];

$$S_0 = S \cdot (1 - ((\sigma'_0 \cdot \sin\varphi + c\cos\varphi)/G))^{\frac{1}{2}}$$
$$S_0^2 = S^2 \cdot (1 - ((\sigma'_0 \cdot \sin\varphi + c\cos\varphi)/G)) \qquad [D.2.32]$$

Now equation [D.1.3] is derived.

D.2.4 Current radius as function of initial radius and plastic zone

Luger and Hergarden have determined the following relation;

$$R_g^2 = R_0^2 + R_p^2((\sigma'_0 \cdot \sin\varphi + c\cos\varphi)/G) \qquad [D.1.4]$$

This equation can be derived using the assumption that no volume change occurs in the plastic zone. The volume between $r = S_0$ and $r = S(= R_p)$ must then be equal to the volume between $r = R_0$ and $r = R_g$.

Volume circle ring;

$$2\pi r_2^2 - 2\pi r_1^2 = 2\pi(r_2^2 - r_1^2) \qquad [D.2.33]$$

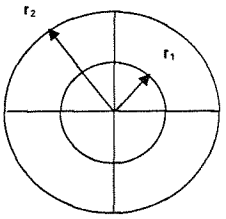

Figure 11: determination radii

$$(S^2 - S_0^2) \cdot 2\pi = (R_g^2 - R_0^2) \cdot 2\pi \qquad [D.2.34]$$

$$R_p^2 - S_0^2 = R_g^2 - R_0^2 \qquad [D.2.35]$$

$$R_g^2 = R_0^2 + (1 - 1 + \frac{\sigma'_0 \sin\varphi + c\cos\varphi}{G})R_p^2 \qquad [D.2.36]$$

This equation is the same as equation [D.1.4].

Now the geometry of the hole and the plastic zone are described.

D.2.5 Radial effective stress

Luger and Hergarden state that the effective stress is now described by;

$$\sigma'_{rr} = (p'_f + c\cot\varphi) \cdot (R_p/r)^{\frac{2\sin\varphi}{1+\sin\varphi}} - c\cot\varphi \qquad [D.1.5]$$

They come to this equation using the value of the radial stress at the transition from elastic to plastic behaviour, the equilibrium condition and the Mohr-Coulomb failure condition.

Mohr Coulomb can be written as;

$$\frac{\sigma'_{tt}+c\cot\varphi}{\sigma'_{rr}+c\cot\varphi}=\frac{1-\sin\varphi}{1+\sin\varphi} \qquad [D.2.37]$$

Equation [D.2.4] now becomes;

$$\frac{\partial\sigma_{rr}}{\partial r}=(\sigma_{rr}+c\cot\varphi)\cdot\frac{2\sin\varphi}{1+\sin\varphi}\cdot\frac{1}{r} \qquad [D.2.38]$$

The form of the solution of the differential equation is;

$$\sigma'_{rr}+c\cot\varphi=C_2\left(\frac{1}{r}\right)^{\frac{2\sin\varphi}{1+\sin\varphi}} \qquad [D.2.39]$$

With the boundary condition $\sigma'_{rr}=p'_f$ for $r=R_p$. C_2 becomes;

$$C_2=(p'_f+c\cot\varphi)R_p^{\frac{2\sin\varphi}{1+\sin\varphi}} \qquad [D.2.40]$$

The equation [D.1.5] is now found.

D.2.6 Pressure in the hole and radius of the borehole

Luger and Hergarden derive the following relation between the pressure in the hole and the actual radius of the hole.

$$p'=(p'_f+c\cot\varphi)\cdot((1-(R_0/R_g)^2)/Q)^{\frac{\sin\varphi}{1+\sin\varphi}}-c\cot\varphi \qquad [D.1.6]$$

where;

$$Q=(\sigma'_0\cdot\sin\varphi+c\cos\varphi)/G \qquad [D.2.41]$$

This can be found considering that $\sigma'_{rr}(r=R_g)=p'$;

$$p'=(p'_f+c\cot\varphi)\left(\frac{R_p}{R_g}\right)^{\frac{2\sin\varphi}{1+\sin\varphi}}-c\cot\varphi \qquad [D.2.42]$$

and using equation [D.1.2];

$$R_g^2=R_0^2+Q\cdot R_p^2 \qquad [D.2.43]$$

$$\Rightarrow\left[\frac{R_p}{R_g}\right]^{\frac{2\sin\varphi}{1+\sin\varphi}}=\left[\frac{R_p^2}{R_g^2}\right]^{\frac{\sin\varphi}{1+\sin\varphi}}=\left[\frac{\frac{R_g^2-R_0^2}{Q}}{R_g^2}\right]^{\frac{\sin\varphi}{1+\sin\varphi}}=\left[\frac{1-\frac{R_0^2}{R_g^2}}{Q}\right]^{\frac{\sin\varphi}{1+\sin\varphi}}$$

This results in equation [D.1.6].

D.2.7 Maximum allowable mud pressure

Luger and Hergarden state that the maximum allowable pressure is attained when the maximum allowable plastic radius is attained. This results in the following equation;

$$p'_{max}=(p'_f+c\cot\varphi)\cdot((R_0/R_{p,max})^2+Q)^{\frac{-\sin\varphi}{1+\sin\varphi}}-c\cot\varphi \qquad [D.1.7]$$

This equation can be derived considering the boundary condition;

$$p'_{max} = \sigma'_{(r=R_{g,max})} \qquad [D.2.44]$$

The radii are defined by;

$$R_{g,max}^{\ 2} = R_0^{\ 2} + R_{p,max}^{\ 2} \cdot Q \qquad [D.2.45]$$

$$\Rightarrow \left[\frac{R_{p,max}^{\ 2}}{R_0^{\ 2} + QR_{p,max}^{\ 2}}\right]^{\frac{\sin\varphi}{1+\sin\varphi}} = \left[\frac{R_0^{\ 2} + QR_{p,max}^{\ 2}}{R_{p,max}^{\ 2}}\right]^{\frac{-\sin\varphi}{1+\sin\varphi}} = \left[\frac{R_0^{\ 2}}{R_{p,max}^{\ 2}} + Q\right]^{\frac{-\sin\varphi}{1+\sin\varphi}}$$

With equation [D.1.5] results this in equation [D.1.7].

D.2.8 Limit pressure

The limit pressure is found if $R_{p,\,max}$ approaches infinity then the ratio $R_0^2 / R_{p,max}^{\ 2}$ approaches 0. This results in the following equation;

$$p'_{lim} = (p'_f + c\cot\varphi)(Q)^{\frac{-\sin\varphi}{1+\sin\varphi}} - c\cot\varphi \qquad [D.1.8]$$

D.3 Rewrite radius plastic zone

In this paragraph the failure criterion proposed by Luger & Hergarden is rewritten in the form of the 'new' developed criterion and vice versa.

First the parameters are compared. For a complete overview of the parameter comparison reference is made to the table conversion with the 'translation' of the symbols used in the 'new' models and in the model of Luger and Hergarden (appendix A).

Then the following relations are rewritten:

- The radii of L&H are rewritten in the form of strains of the 'new' model.
- The failure criterion of L&H of maximum allowable plastic radius is rewritten with the parameters used in the 'new' model.
- The failure criterion based on strain is rewritten in the parameters used by L&H.

D.3.1 Comparison parameters

r_i ('new') $= R_0$ (L & H) [D.3.1]

$r_i + u_i$ ('new') $= R_g$ (L & H) $\rightarrow$ $r_i + r_i \cdot \varepsilon_{rr} = R_g$ [D.3.2]

r_e ('new') $= R_p$ (L & H) [D.3.3]

D.3.2 Radii & strain

Luger and Hergarden state the following relation:

$$R_g^2 = R_0^2 + R_p^2((\sigma'_0 \cdot \sin\varphi + c\cos\varphi)/G) \quad [D.1.4]$$

In the basic model is stated:

-> tangential strain

$$\varepsilon_{tt} = \frac{u_i}{r_i} = \frac{p_0 + a}{2\mu}\frac{1-m}{1+m}\left[\frac{1+m}{2}\frac{p_i + a}{p_0 + a}\right]^{(k+1)/(1-m)} \text{ ([E.1.53])} \quad [D.3.4]$$

-> radial strain

$$\varepsilon_{rr} = \frac{du_i}{dr_i} = \frac{p_0 + a}{2\mu}\frac{1-m}{1+m}\left[\frac{1+m}{2}\frac{p_i + a}{p_0 + a}\right]^{(k+1)/(1-m)} \quad [D.3.5]$$

The expressions for the tangential [D.3.4] and radial [D.3.5] strain are the same.

If $\psi = 0$ then $k = 1$ (isochoric displacement). The expression for radial strain reads then:

$$\varepsilon_{rr} = \frac{du_i}{dr_i} = \frac{p_0 + a}{2\mu}\frac{1-m}{1+m}\left[\frac{1+m}{2}\frac{p_i + a}{p_0 + a}\right]^{2/(1-m)} \quad [D.3.6]$$

Expression [E.1.66] can be rewritten in the form;

$$r_e = \left(\frac{1+m}{2}\frac{p_i + a}{p_0 + a}\right)^{\frac{1}{1-m}} \cdot r_i \quad [D.3.7]$$

Using equations [D.3.1] and [D.3.3], this can be rewritten in the form:

$$R_p^2 = \left(\frac{1+m}{2}\frac{p_i+a}{p_0+a}\right)^{\frac{2}{1-m}} \cdot R_0^2 \quad \text{or} \quad R_p^2 = \left(\frac{1+m}{2}\frac{p_i+a}{p_0+a}\right)^{\frac{2}{1-m}} \cdot r_i^2 \quad [D.3.8]$$

Now equation [D.1.4] is rewritten:

$$R_g = R_0 \cdot (1+\varepsilon_{rr}) \rightarrow R_g^2 = R_0^2 \cdot (1+\varepsilon_{rr})^2 = R_0^2 \cdot (1+2\varepsilon_{rr}+\cancel{\varepsilon_{rr}^2}) \quad [D.3.9]$$

The last term is neglected as the strains are very small and the power of a small number becomes even smaller. The expression reads then:

$$R_g^2 = R_0^2 + 2R_0^2\varepsilon_{rr} = r_i^2 + 2r_i^2\varepsilon_{rr} \quad [D.3.10]$$

This can be rewritten with [D.3.6]:

$$R_g^2 = R_0^2 + \cancel{2}R_0^2 \cdot \frac{p_0+a}{\cancel{2}\mu}\frac{1-m}{1+m}\left[\frac{1+m}{2}\frac{p_i+a}{p_0+a}\right]^{2/(1-m)} \quad [D.3.11]$$

This can be rewritten with [D.3.8]:

$$R_g^2 = R_0^2 + R_p^2 \cdot \frac{p_0+a}{\mu}\frac{1-m}{1+m} = r_i^2 + r_e^2 \cdot \frac{p_0+a}{\mu}\frac{1-m}{1+m} \quad [D.3.12]$$

It is recalled that

$$a = c\cot\varphi \quad [D.3.13]$$

$$m = \frac{1-\sin\varphi}{1+\sin\varphi} \rightarrow \frac{1-m}{1+m} = \sin\varphi \quad [D.3.14]$$

$$\mu = G \quad [D.3.15]$$

It is now clear that equations [D.3.10] and [D.3.12] are the same as equation [D.1.4].

D.3.3 Pressures & Strain – Luger&Hergarden

Equation [D.3.8] can be rewritten with the expression for radial strain [D.3.6];

$$R_p^2 = \varepsilon_{rr} \cdot \frac{2\mu}{p_0+a}\cdot\frac{1+m}{1-m}\cdot R_0^2 = \varepsilon_{rr} \cdot \frac{2\mu}{p_0\cdot\sin\varphi + c\cos\varphi}\cdot R_0^2 \quad [D.3.16]$$

The expression for maximum pressure using the maximum allowable radius was;

$$p' = (p'_f + c\cot\varphi)\cdot((R_0/R_p)^2 + Q)^{\frac{-\sin\varphi}{1+\sin\varphi}} - c\cot\varphi \quad [D.1.7]$$

In this;

$$p'_f = \sigma'_0\cdot(1+\sin\varphi) + c\cdot\cos\phi \quad [D.1.1]$$

and;

$$Q = (\sigma'_0\cdot\sin\varphi + c\cos\varphi)/G \quad [D.2.41]$$

The radii are rewritten:

$$\Rightarrow \frac{R_0^2}{R_p^2} + Q = \frac{\cancel{R_0^2}}{\cancel{R_0^2}\cdot\varepsilon_{rr}}\cdot\frac{p_0\sin\varphi + c\cos\varphi}{2G} + \frac{p_0\sin\varphi + c\cos\varphi}{G} = \left(1+\frac{1}{2\varepsilon_{rr}}\right)\cdot Q \quad [D.3.17]$$

Equation [D.1.7] now reads:

$$p' = (p'_f + c\cot\varphi)\cdot\left((1+\frac{1}{2\varepsilon_{rr}})\cdot Q\right)^{\frac{-\sin\varphi}{1+\sin\varphi}} - c\cot\varphi \qquad [D.3.18]$$

Equation [D.1.7] written with the parameters used in the 'new' model:

$$p' = ((p_0\cdot(1+\sin\varphi)+c\cos\varphi)+a)\cdot\left((1+\frac{1}{2\varepsilon_{rr}})\cdot\frac{p_0\cdot\sin\varphi+c\cos\varphi}{\mu}\right)^{\frac{-\sin\varphi}{1+\sin\varphi}} - a \qquad [D.3.19]$$

D.3.4 Pressures & Strain – New model

It is reminded that ε_{rr} equals in this case ε_{tt}. For maximum allowable pressure related to maximum strain the following expression was found:

$$p_i = \left\{\left[\varepsilon_{tt}\cdot\frac{2\mu}{p_0+a}\cdot\frac{1+m}{1-m}\right]^{\frac{1-m}{k+1}}\cdot\frac{2}{1+m}\cdot(p_0+a)\right\} - a \qquad [D.3.20]$$

Strain can be expressed in the radius of the plastic zone by rewriting equation [D.3.16];

$$\varepsilon_{rr} = \varepsilon_{tt} = \frac{R_p^2}{R_0^2}\cdot\frac{p_0\cdot\sin\varphi+c\cos\varphi}{2\mu} = \frac{R_p^2}{R_0^2}\cdot\frac{\sigma'_0\cdot\sin\varphi+c\cos\varphi}{2G} \qquad [D.3.21]$$

Now equation [D.3.20] can be rewritten;

$$p_i = \left\{\left[\frac{R_p^2}{R_0^2}\cdot\frac{p_0\cdot\sin\varphi+c\cos\varphi}{2\mu}\cdot\frac{2\mu}{(p_0+a)\cdot\sin\varphi}\right]^{\frac{1-m}{k+1}}\cdot\frac{2}{1+m}\cdot(p_0+a)\right\} - a \qquad [D.3.22]$$

If $\psi = 0$ and therefore $k = 1$. The expression becomes:

$$p_i = \left((\frac{R_p}{R_0})^{\frac{2(1-m)}{2}}\cdot\frac{2}{1+m}\cdot(p_0+a)\right) - a = \left((\frac{R_p}{R_0})^{\frac{2\sin\varphi}{1+\sin\varphi}}\cdot(1+\sin\varphi)\cdot(\sigma'_0+c\cot\varphi)\right) - c\cot\varphi \qquad [D.3.23]$$

This is the representation of equation [D.3.20] in parameters used by L&H.

E 'NEW' SOIL MODELS

In this appendix the soil models are presented which were developed to able to describe the soil behaviour in case of cavity expansion due to an increasing internal pressure. Such an increasing internal pressure in a cavity is the representation of the injection of mud into soil in case of horizontal directional drilling. It concerns elasto-plastic solutions for stresses and strains around a cylindrical or spherical cavity.

The following assumptions were used:

- The material is supposed to be elastic up to a certain limit, defined by Coulomb's failure criterion, depending on cohesion 'c' and angle 'φ' of the material.
- Beyond the coulomb failure criterion the material is plastic, with a constant ratio between the volume change (dilatancy) and the shear deformation.
- The material has an initial homogeneous state of stress, up to infinity (gravity is neglected).
- Plasticity may occur in a zone around the cavity, the material further from the cavity remains in the plastic state.

The soil models presented in this appendix originate from the text from Prof. dr. ir. A. Verruijt, Cavity expansion, March 2001.

E.1 Cylindrical cavity

This represents injection of mud or another heavy fluid into a very long cylindrical inclusion in a soil mass of infinite extent, under high pressure.

E.1.1 Basic equations

Figure 12 shows an element of material in a cylindrical co-ordinate system. If the radial co-ordinate is denoted by r and the angle in the x,y-plane by θ, then the volume of the element is r·dr·dθ·dz. It is assumed that the displacement field is cylindrically symmetrical, so that there are no shear stresses acting upon the element, and the tangential stress $d\sigma_{tt}$ is independent of the orientation of the plane. The stresses acting upon the element are indicated in Figure 12.

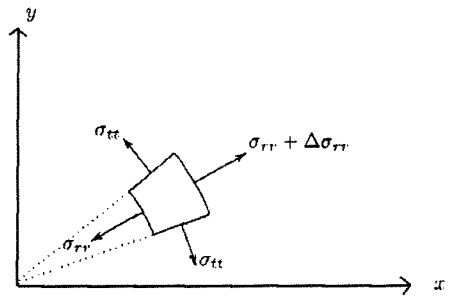

Figure 12: Element, cylindrical cavity

The only non-trivial equation of equilibrium now is the one in radial direction;

$$\frac{d\sigma_{rr}}{dr} + \frac{\sigma_{rr} - \sigma_{tt}}{r} = 0 \qquad [E.1.1]$$

This equation must be satisfied in the elastic region and in the plastic region. The two regions will be considered separately.

E.1.2 Elastic region

Differential equation

In the elastic region the stresses can be related to the strains by Hooke's law;

$$\sigma_{rr} = \lambda e + 2\mu\varepsilon_{rr} \qquad [E.1.2]$$

$$\sigma_{tt} = \lambda e + 2\mu\varepsilon_{tt} \qquad [E.1.3]$$

Where e is the volume strain;

$$e = \varepsilon_{rr} + \varepsilon_{tt} \qquad [E.1.4]$$

and λ and μ are the elastic coefficients (Lamé constants);

$$\lambda = \frac{\nu E}{(1+\nu)(1-2\nu)} \qquad [E.1.5]$$

$$\mu = \frac{E}{2(1+\nu)} \qquad [E.1.6]$$

Stresses are considered *positive for tension*.
Strains are considered *positive for extension*.

The strains ε_{rr} and ε_{tt} can be related to the radial displacement u_r by the relations;

$$\varepsilon_{rr} = \frac{du_r}{dr} \qquad [E.1.7]$$

$$\varepsilon_{tt} = \frac{u_r}{r} \qquad [E.1.8]$$

The volume strain can now be written as;

$$e = \frac{du_r}{dr} + \frac{u_r}{r} \qquad [E.1.9]$$

Substitution of equations [E.1.2] till [E.1.8] into [E.1.1] gives;

$$\frac{d^2u}{dr^2} + \frac{1}{r}\frac{du}{dr} - \frac{u}{r^2} = 0 \qquad [E.1.10]$$

This is the basic differential equation for spherically symmetric elastic deformations. The elastic properties of the material do not appear in this equation.

General solution

The general solution of the differential equation [E.1.10] is;

$$u = Ar + \frac{B}{r} \qquad [E.1.11]$$

Where A and B are integration constants, to be determined from the boundary conditions. The general expression for the volume strain, corresponding to the solution [E.1.11] is;

$$e = 2A \qquad [E.1.12]$$

The stresses σ_{rr} and σ_{tt} can be expressed as;

$$\sigma_{rr} = 2(\lambda + \mu)A - 2\mu\frac{B}{r^2} \qquad [E.1.13]$$

$$\sigma_{tt} = 2(\lambda + \mu)A + 2\mu\frac{B}{r^2} \qquad [E.1.14]$$

This solution will be elaborated in the next section.

Elastic region

The solution for a cavity in an infinite elastic field applies to the cavity expansion problem in the outer region, for $r_e < r < r_\infty$ (see Figure 13)

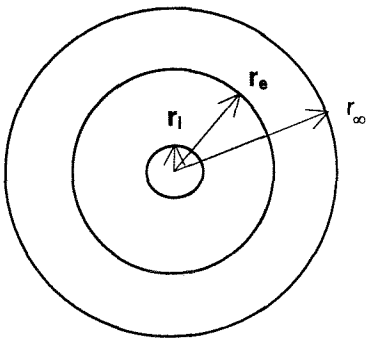

Figure 13: definition of radii

The solution is considered to consist of two parts;

- The initial state, uniform stresses in the entire medium
- Solution for the increase of the stresses due to expansion of the cavity (incremental)

The first part, the initial stress, is supposed to be;

$$\sigma_{rr} = -p_0 \qquad [E.1.15]$$

$$\sigma_{tt} = -p_0 \qquad [E.1.16]$$

The second part of the solution, increase due to expansion, is supposed to have the following boundary condition;

$$r \to \infty \; : \; \sigma_{rr} = 0 \qquad [E.1.17]$$

$$r = r_e \; : \; \sigma_{rr} = -(p_e - p_0) \qquad [E.1.18]$$

Where p_e is the final pressure at the boundary of the elastic region, which is supposed to be greater than the initial pressure p_o.

The constants A and B of the elastic solution are now found to be;

$$A = 0 \qquad [E.1.19]$$

$$B = \frac{(p_e - p_0)r_e^2}{2\mu} \qquad [E.1.20]$$

The stresses for this part of the solution are;

$$\sigma_{rr} = -(p_e - p_0)\frac{r_e^2}{r^2} \qquad [E.1.21]$$

$$\sigma_{tt} = (p_e - p_0)\frac{r_e^2}{r^2} \qquad [E.1.22]$$

The displacement field corresponding to this part of the solution is;

$$u = \frac{(p_e - p_0)r_e^2}{2\mu r} \qquad [E.1.23]$$

The displacement field [E.1.23] represents the total displacements due to stress increase caused by the expansion of the cavity.
The displacement at the boundary of the cavity is of particular interest;

$$u_e = \frac{(p_e - p_0)r_e}{2\mu} \qquad [E.1.24]$$

The total stresses are the *sum* of the *initial* stresses and the *incremental* elastic stresses;

$$\sigma_{rr} = -p_0 - (p_e - p_0)\frac{r_e^2}{r^2} \qquad [E.1.25]$$

$$\sigma_{tt} = -p_0 + (p_e - p_0)\frac{r_e^2}{r^2} \qquad [E.1.26]$$

It can easily be verified that this solution satisfies the boundary conditions;

$$r \to \infty \; : \; \sigma_{rr} = -p_0 \qquad [E.1.27]$$

$$r = r_e \; : \; \sigma_{rr} = -p_e \qquad [E.1.28]$$

The values of r_e and p_e are still unknown at this stage.

E.1.3 Plastic region

Differential equation

The interior region, $r_i < r < r_e$, the soil may be in the plastic state (see Figure 13). It is assumed that in this region the radial stress σ_{rr} is the major principal stress, and the tangential stress σ_{tt} is the minor principal stress. The basis of this assumption is the notion that the cause for stress increase is the fact that the radial pressure at the cavity boundary is increased.

In this case the Mohr-Coulomb criterion can be written as;

$$\sigma_{tt} - a = m(\sigma_{rr} - a) \qquad \text{[E.1.29]}$$

Where;

$$a = c\cot\varphi \qquad \text{[E.1.30]}$$

And;

$$m = \frac{1-\sin\varphi}{1+\sin\varphi} \qquad \text{[E.1.31]}$$

This is the active soil pressure coefficient (K_a). It should be noted that both σ_{rr} and σ_{tt} are negative (pressure), with $\sigma_{rr} < \sigma_{tt} < 0$

Substitution of [E.1.29] into the general equation [E.1.1] now gives;

$$\frac{d(\sigma_{rr} - a)}{dr} + (1-m)\frac{\sigma_{rr} - a}{r} = 0 \qquad \text{[E.1.32]}$$

This is the differential equation in the plastic region.

Solution in the plastic region

The differential equation [E.1.32] can be solved by;

$$\sigma_{rr} - a = Cr^{-(1-m)} \qquad \text{[E.1.33]}$$

Where C is an unknown integration constant. Using the boundary condition;

$$r = r_i \;:\; \sigma_{rr} = -p_i \qquad \text{[E.1.34]}$$

It follows that;

$$-(p_i + a) = Cr_i^{-(1-m)} \qquad \text{[E.1.35]}$$

Elimination of C now gives the final solution in the plastic region;

$$\sigma_{rr} - a = -(p_i + a)\left(\frac{r}{r_i}\right)^{-(1-m)} \qquad \text{[E.1.36]}$$

The tangential stress then is, with [E.1.29];

$$\sigma_{tt} - a = -m(p_i + a)\left(\frac{r}{r_i}\right)^{-(1-m)} \qquad \text{[E.1.37]}$$

If the value of the pressure p_i is given, the stresses in the plastic region are completely determined. However, how far the plastic region extends is not yet known.

E.1.4 Completion of the solution

Determination of constants

To complete the solution the plastic and elastic region must be linked. The conditions are;

$$r = r_e : \sigma_{rr|pl} = \sigma_{rr|el} \qquad [E.1.38]$$

$$r = r_e : \sigma_{tt|pl} = \sigma_{tt|el} \qquad [E.1.39]$$

The first condition is a direct consequence of radial equilibrium at the interface between the plastic and elastic regions. The second condition follows from the usual assumption in elasto-plastic problems that the stresses in the elastic region must approach the Mohr- Coulomb yield condition at the interface.

The first condition [E.1.38], gives with [E.1.28] and [E.1.36];

$$p_e + a = (p_i + a)\left(\frac{r_e}{r_i}\right)^{-(1-m)} \qquad [E.1.40]$$

Similarly, the second condition, equation [E.1.39], gives with [E.1.26] and [E.1.37];

$$2(p_0 + a) - p_e + a = m(p_i + a)\left(\frac{r_e}{r_i}\right)^{-(1-m)} \qquad [E.1.41]$$

From these two equations it follows that;

$$p_e + a = \frac{2}{1+m}(p_0 + a) = (1 + \sin\varphi)(p_0 + a) \qquad [E.1.42]$$

This determines the radial stress at the boundary between the plastic and the elastic regions.

Furthermore, it follows from [E.1.42] and [E.1.40] that;

$$\left(\frac{r_e}{r_i}\right)^{(1-m)} = \frac{1+m}{2}\frac{p_i + a}{p_0 + a} \qquad [E.1.43]$$

This determines the radius of the plastic region.

A plastic region will develop when the right hand side of this equation is greater than 1.

$$p_i + a > \frac{2}{1+m}(p_0 + a) = (1 + \sin\varphi)(p_0 + a) \qquad [E.1.44]$$

For smaller values of the pressure at the cavity boundary the entire field will be elastic.

Displacements

The displacements can be determined by starting from the solution in the elastic region, see [E.1.23];

$$r > r_e : u = \frac{(p_e - p_0)r_e^2}{2\mu r} \qquad [E.1.45]$$

This is an isochoric displacement (displacement without volume change – volume = $2\pi ru$, radial displacement u [E.1.45] is inversely proportional to r).

The displacement at the inner boundary of the elastic region is;

$$u_e = \frac{(p_e - p_0)r_e}{2\mu} \qquad [E.1.46]$$

With [E.1.42] and [E.1.43] this can also be written as;

$$u_e = \frac{(p_0 + a)r_i}{2\mu}\frac{1-m}{1+m}\left[\frac{1+m}{2}\left(\frac{p_i + a}{p_0 + a}\right)\right]^{1/(1-m)} \qquad [E.1.47]$$

For the deformations in the plastic region it is assumed that there can be a certain volume change (by dilatancy), proportional to the shear strain. It can be expected that in this case of cavity expansion the radial displacement u will be positive, and that its magnitude will decrease as the distance r increases. (u/r- positive; du/dr – negative)

$$|\gamma| = |\varepsilon_{rr} - \varepsilon_{tt}| = \left|\frac{du}{dr} - \frac{u}{r}\right| = \frac{u}{r} - \frac{du}{dr} \qquad [E.1.48]$$

The volume change is now supposed to be;

$$e = \frac{du}{dr} + \frac{u}{r} = \left(\frac{u}{r} - \frac{du}{dr}\right)\sin\psi \qquad [E.1.49]$$

Where ψ is the dilatancy angle, positive for volume expansion. If $\psi = o$ the deformations will be isochoric. For positive values of ψ the right hand side of [E.1.49] will be positive, indicating a volume expansion.

The differential equation [E.1.49] can be integrated to give;

$$\frac{u}{u_e} = \left(\frac{r_e}{r}\right)^k \qquad [E.1.50]$$

Where the integration constant has been chosen such that $u = u_e$ for $r = r_e$ and where;

$$k = \frac{1 - \sin\psi}{1 + \sin\psi} \qquad [E.1.51]$$

The displacement of the cavity boundary now is, with [E.1.43];

$$\frac{u_i}{u_e} = \left(\frac{r_e}{r_i}\right)^k = \left[\frac{1+m}{2}\frac{p_i + a}{p_0 + a}\right]^{k/(1-m)} \qquad [E.1.52]$$

With [E.1.47] this gives finally;

$$\frac{u_i}{r_i} = \frac{p_0 + a}{2\mu}\frac{1-m}{1+m}\left[\frac{1+m}{2}\frac{p_i + a}{p_0 + a}\right]^{(k+1)/(1-m)} \qquad [E.1.53]$$

This solution applies if the pressure at the cavity boundary is sufficiently high, so that a certain plastic region develops around the cavity. If this is not the case (factor between brackets is < 1), the elastic solution remains;

$$p_i + a < \frac{2}{1+m}(p_0 + a) \;:\; \frac{u_i}{r_i} = \frac{p_i - p_0}{2\mu} \qquad [E.1.54]$$

It can easily be verified that the two expressions give the same value when the plastic region starts to develop.

$$p_i + a = \frac{2}{1+m}(p_0 + a) \;:\; \frac{u_i}{r_i} = \frac{p_0 + a}{2\mu}\frac{1-m}{1+m} \qquad [E.1.55]$$

For the construction of a graphical representation of the displacement of the cavity boundary as a function of the pressure in the cavity, the equations can be written in dimensionless form by the introduction of the variables;

$$P = \frac{p_i + a}{p_0 + a} \qquad [E.1.56]$$

$$U = \frac{u_i}{r_i}\frac{2\mu}{p_0 + a} \qquad [E.1.57]$$

The solution can then be written as

$$P < \frac{2}{1+m} : U = P - \qquad [E.1.58]$$

$$P = \frac{2}{1+m} : U = \frac{1-m}{1+m} \qquad [E.1.59]$$

$$P > \frac{2}{1+m} : U = \frac{1-m}{1+m}\left[\frac{1+m}{2}P\right]^{(k+1)/(1-m)} \qquad [E.1.60]$$

It is recalled that the parameters are defined as follows;

$$a = c\cot\varphi \qquad [E.1.61]$$

$$m = \frac{1-\sin\varphi}{1+\sin\varphi} \qquad [E.1.62]$$

$$k = \frac{1-\sin\psi}{1+\sin\psi} \qquad [E.1.63]$$

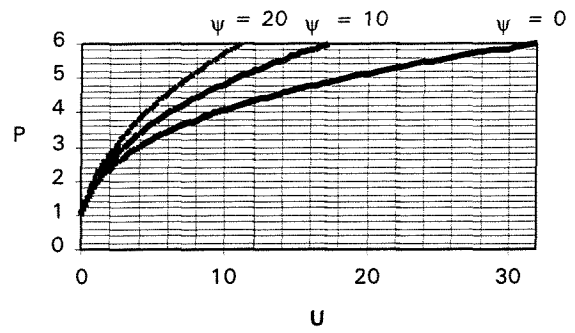

Figure 14: Expansion versus pressure, cylindrical cavity in infinite space

Figure 14 shows the relation between the dimensionless pressure P and the *dimensionless displacement U, for the case that* $\varphi = 30^0$, *and for three values of* dilatancy angle ψ.

Stresses

To give a graphical representation of the stresses, distinction must be made between the pressure in the cavity below the limit that produces plastic deformations, and above that limit. The limiting value of the pressure is $P = 2/(1+m)$. Below this limit all deformations will be elastic, and the stresses are given by [E.1.25] and [E.1.26], with $r_e = r_{li}$ and $p_e = p_i$.

The parameters $s_{rr} = -\sigma_{rr}$ and $s_{tt} = -\sigma_{tt}$ are introduced to ensure positive parameters for pressure.

In dimensionless form the equations become;

$$1 < P < \frac{2}{1+m} : \frac{s_{rr} + a}{p_0 + a} = 1 + (P-1)\frac{r_i^2}{r^2} \qquad [E.1.64]$$

$$1 < P < \frac{2}{1+m} \;:\; \frac{s_{tt}+a}{p_0+a} = 1-(P-1)\frac{r_i^2}{r^2} \qquad \text{[E.1.65]}$$

Above this limit there will be two regions, a plastic region immediately around the cavity, and an elastic region outside, up to infinity. The boundary between these two regions is the radius r_e, which is determined by [E.1.43];

$$P > \frac{2}{1+m} \;:\; (\frac{r_e}{r_i})^{(1-m)} = \frac{1+m}{2}\frac{p_i+a}{p_0+a} \qquad \text{[E.1.66]}$$

Using the definition [E.1.56] of P;

$$P > \frac{2}{1+m} \;:\; \frac{r_e}{r_i} = [\frac{P}{2/(1+m)}]^{1/(1-m)} \qquad \text{[E.1.67]}$$

In the elastic region the stresses are given by [E.1.25] and [E.1.26];

$$P > \frac{2}{1+m},\ r > r_e \;:\; \frac{s_{rr}+a}{p_0+a} = 1+(\frac{p_e+a}{p_0+a}-1)\frac{r_e^2}{r^2} \qquad \text{[E.1.68]}$$

$$P > \frac{2}{1+m},\ r > r_e \;:\; \frac{s_{tt}+a}{p_0+a} = 1-(\frac{p_e+a}{p_0+a}-1)\frac{r_e^2}{r^2} \qquad \text{[E.1.69]}$$

Substituting the value of $p_e + a$ from [E.1.42] into these equations gives;

$$P > \frac{2}{1+m},\ r > r_e \;:\; \frac{s_{rr}+a}{p_0+a} = 1+\sin\varphi\frac{r_e^2}{r^2} \qquad \text{[E.1.70]}$$

$$P > \frac{2}{1+m},\ r > r_e \;:\; \frac{s_{tt}+a}{p_0+a} = 1-\sin\varphi\frac{r_e^2}{r^2} \qquad \text{[E.1.71]}$$

The value of r_e/r_{li} in these equations is given by [E.1.67], which shows that r_e will increase if the pressure in the cavity increases.

In the plastic region the stresses are given by [E.1.36] and [E.1.37];

$$P > \frac{2}{1+m},\ r < r_e \;:\; \frac{s_{rr}+a}{p_0+a} = P(\frac{r}{r_i})^{-(1-m)} \qquad \text{[E.1.72]}$$

$$P > \frac{2}{1+m},\ r < r_e \;:\; \frac{s_{tt}+a}{p_0+a} = mP(\frac{r}{r_i})^{-(1-m)} \qquad \text{[E.1.73]}$$

For the case $\varphi = 30^0$ the radial stresses are shown in Figure 15 for increasing values of the stress inside the cavity. The radial stress at the cavity boundary increases from p_0 to $6p_0$. The quantity S shown in this figure has been defined as;

$$S = \frac{s_{rr}+a}{p_0+a} \qquad \text{[E.1.74]}$$

The tangential stresses for the same values of the radial stress at the cavity boundary are shown in Figure 16. The quantity T shown in this figure has been defined as;

$$T = \frac{s_{tt}+a}{p_0+a} \qquad \text{[E.1.75]}$$

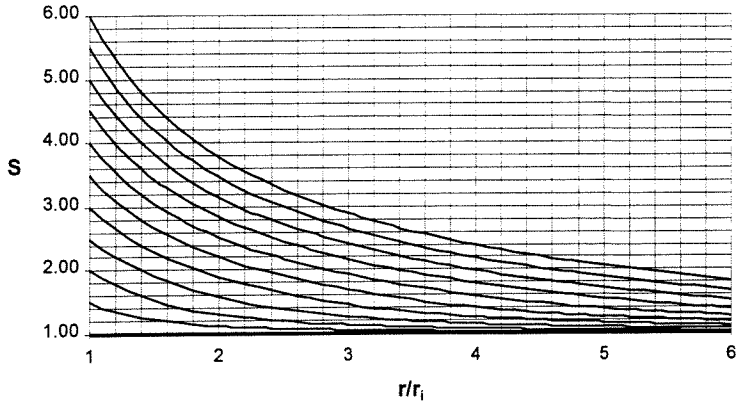

Figure 15: Cylindrical cavity in infinite space: radial stresses: S

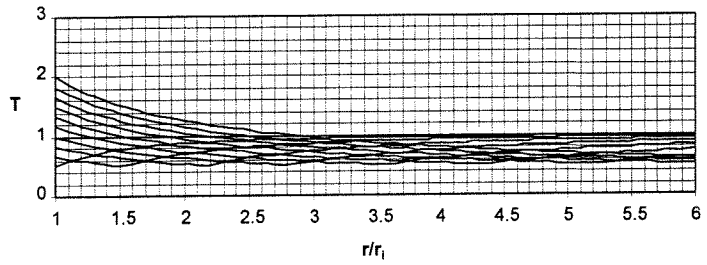

Figure 16: Cylindrical cavity in infinite space: tangential stresses: T

The stresses at the interface between the plastic and elastic zone, i.e. for $r = r_e$, are $S = 2/(1+m)$ and $T = 2m/(1+m)$. These values are always positive, and they are independent of the pressure in the cavity.

E.2 Spherical cavity

This represents injection of mud or another heavy fluid into a spherical inclusion in a soil mass of infinite extent, under high pressure.

E.2.1 Basic equations

Figure 12 shows an element of material in a spherical co-ordinate system. If the radial co-ordinate is denoted by r and the angle in the x,y-plane by θ, and the angle with the vertical axis by ψ, then the volume of the element is $r^2 \cdot dr \cdot d\theta \cdot d\psi \cos(\psi)$. It is assumed that the displacement field is spherical symmetrical, so that there are no shear stresses acting upon the element, and the tangential stress $d\sigma_{tt}$ is independent of the orientation of the plane. The stresses acting upon the element are indicated in Figure 17.

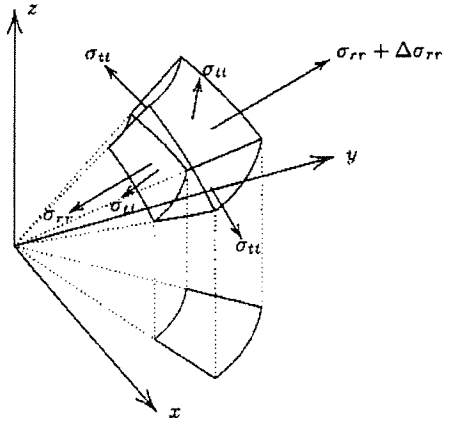

Figure 17: Element, spherical cavity

The only non-trivial equation of equilibrium now is the one in radial direction;

$$\frac{d\sigma_{rr}}{dr} + 2\frac{\sigma_{rr} - \sigma_{tt}}{r} = 0 \qquad [E.2.1]$$

This equation must be satisfied in the elastic region and in the plastic region. The two regions will be considered separately.

E.2.2 Elastic region

Differential equation

In the elastic region the stresses can be related to the strains by Hooke's law;

$$\sigma_{rr} = \lambda e + 2\mu\varepsilon_{rr} \qquad [E.2.2]$$

$$\sigma_{tt} = \lambda e + 2\mu\varepsilon_{tt} \qquad [E.2.3]$$

Where e is the volume strain;

$$e = \varepsilon_{rr} + \varepsilon_{tt} \qquad [E.2.4]$$

and λ and μ are the elastic coefficients (Lamé constants);

$$\lambda = \frac{\nu E}{(1+\nu)(1-2\nu)} \qquad [E.2.5]$$

$$\mu = \frac{E}{2(1+\nu)} \qquad [E.2.6]$$

Stresses are considered *positive for tension*.
Strains are considered *positive for extension*.

The strains ε_{rr} and ε_{tt} can be related to the radial displacement u_r by the relations;

$$\varepsilon_{rr} = \frac{du_r}{dr} \qquad [E.2.7]$$

$$\varepsilon_{tt} = \frac{u_r}{r} \qquad [E.2.8]$$

The volume strain can now be written as;

$$e = \frac{du_r}{dr} + 2\frac{u_r}{r} \qquad [E.2.9]$$

Substitution of equations [E.2.2] till [E.2.8] into [E.2.1] gives;

$$\frac{d^2u}{dr^2} + \frac{2}{r}\frac{du}{dr} - 2\frac{u}{r^2} = 0 \qquad [E.2.10]$$

This is the basic differential equation for spherically symmetric elastic deformations. The elastic properties of the material do not appear in this equation.

General solution

The general solution of the differential equation [E.2.10] is;

$$u = Ar + \frac{B}{r^2} \qquad [E.2.11]$$

Where A and B are integration constants, to be determined from the boundary conditions. The general expression for the volume strain, corresponding to the solution [E.2.11] is;

$$e = 3A \qquad [E.2.12]$$

The stresses σ_{rr} and σ_{tt} can be expressed as;

$$\sigma_{rr} = (3\lambda + 2\mu)A - 4\mu\frac{B}{r^3} \qquad [E.2.13]$$

$$\sigma_{tt} = (3\lambda + 2\mu)A + 4\mu\frac{B}{r^3} \qquad [E.2.14]$$

This solution will be elaborated in the next section.

Elastic region

The solution for a cavity in an infinite elastic field applies to the cavity expansion problem in the outer region, for $r_e < r < \infty$ (see Figure 13)

The solution is considered to consist of two parts;

- The initial state, uniform stresses in the entire medium
- Solution for the increase of the stresses due to expansion of the cavity (incremental)

The first part, the initial stress, is supposed to be;

$$\sigma_{rr} = -p_0 \qquad [E.2.15]$$

$$\sigma_{tt} = -p_0 \qquad [E.2.16]$$

The second part of the solution, increase due to expansion, is supposed to have the following boundary condition;

$$r \to \infty \; : \; \sigma_{rr} = 0 \qquad \text{[E.2.17]}$$

$$r = r_e \; : \; \sigma_{rr} = -(p_e - p_0) \qquad \text{[E.2.18]}$$

Where p_e is the final pressure at the boundary of the elastic region, which is supposed to be greater than the initial pressure p_o.

The constants A and B of the elastic solution are now found to be;

$$A = 0 \qquad \text{[E.2.19]}$$

$$B = \frac{(p_e - p_0) r_e^{\,3}}{4\mu} \qquad \text{[E.2.20]}$$

The stresses for this part of the solution are;

$$\sigma_{rr} = -(p_e - p_0)\frac{r_e^{\,3}}{r^3} \qquad \text{[E.2.21]}$$

$$\sigma_{tt} = \frac{1}{2}(p_e - p_0)\frac{r_e^{\,3}}{r^3} \qquad \text{[E.2.22]}$$

The displacement field corresponding to this part of the solution is;

$$u = \frac{(p_e - p_0) r_e^{\,3}}{4\mu r^2} \qquad \text{[E.2.23]}$$

The displacement field [E.2.23] represents the total displacements due to stress increase caused by the expansion of the cavity.
The displacement at the boundary of the cavity is of particular interest;

$$u_e = \frac{(p_e - p_0) r_e}{4\mu} \qquad \text{[E.2.24]}$$

The total stresses are the *sum* of the *initial* stresses and the *incremental* elastic stresses;

$$\sigma_{rr} = -p_0 - (p_e - p_0)\frac{r_e^{\,3}}{r^3} \qquad \text{[E.2.25]}$$

$$\sigma_{tt} = -p_0 + \frac{1}{2}(p_e - p_0)\frac{r_e^{\,3}}{r^3} \qquad \text{[E.2.26]}$$

It can easily be verified that this solution satisfies the boundary conditions;

$$r \to \infty \; : \; \sigma_{rr} = -p_0 \qquad \text{[E.2.27]}$$

$$r = r_e \; : \; \sigma_{rr} = -p_e \qquad \text{[E.2.28]}$$

The values of r_e and p_e are still unknown at this stage.

E.2.3 Plastic region

Differential equation

The interior region, $r_i < r < r_e$, the soil may be in the plastic state (see Figure 13). It is assumed that in this region the radial stress σ_{rr} is the major principal stress, and the tangential stress σ_{tt} is the minor principal stress. The basis of this assumption is the notion that the cause for stress increase is the fact that the radial pressure at the cavity boundary is increased.

In this case the Mohr-Coulomb criterion can be written as;

$$\sigma_{tt} - a = m(\sigma_{rr} - a) \qquad [E.2.29]$$

Where;

$$a = c\cot\varphi \qquad [E.2.30]$$

And;

$$m = \frac{1-\sin\varphi}{1+\sin\varphi} \qquad [E.2.31]$$

This is the active soil pressure coefficient (K_a). It should be noted that both σ_{rr} and σ_{tt} are negative (pressure), with $\sigma_{rr} < \sigma_{tt} < 0$

Substitution of [E.2.29] into the general equation [E.2.1] now gives;

$$\frac{d(\sigma_{rr} - a)}{dr} + 2(1-m)\frac{\sigma_{rr} - a}{r} = 0 \qquad [E.2.32]$$

This is the differential equation in the plastic region.

Solution in the plastic region

The differential equation [E.2.32] can be solved by;

$$\sigma_{rr} - a = Cr^{-2(1-m)} \qquad [E.2.33]$$

Where C is an unknown integration constant. Using the boundary condition;

$$r = r_i \;:\; \sigma_{rr} = -p_i \qquad [E.2.34]$$

It follows that;

$$-(p_i + a) = Cr_i^{-2(1-m)} \qquad [E.2.35]$$

Elimination of C now gives the final solution in the plastic region;

$$\sigma_{rr} - a = -(p_i + a)\left(\frac{r}{r_i}\right)^{-2(1-m)} \qquad [E.2.36]$$

The tangential stress then is, with [E.2.29];

$$\sigma_{tt} - a = -m(p_i + a)\left(\frac{r}{r_i}\right)^{-2(1-m)} \qquad [E.2.37]$$

If the value of the pressure p_i is given, the stresses in the plastic region are completely determined. However, how far the plastic region extends is not yet known.

E.2.4 Completion of the solution

Determination of constants

To complete the solution the plastic and elastic region must be linked. The conditions are;

$$r = r_e : \sigma_{rr|pl} = \sigma_{rr|el} \qquad [E.2.38]$$

$$r = r_e : \sigma_{tt|pl} = \sigma_{tt|el} \qquad [E.2.39]$$

The first condition is a direct consequence of radial equilibrium at the interface between the plastic and elastic regions. The second condition follows from the usual assumption in elasto-plastic problems that the stresses in the elastic region must approach the Mohr- Coulomb yield condition at the interface.

The first condition [E.2.38], gives with [E.2.28] and [E.2.36];

$$p_e + a = (p_i + a)(\frac{r_e}{r_i})^{-2(1-m)} \qquad [E.2.40]$$

Similarly, the second condition, equation [E.2.39], gives with [E.2.26] and [E.2.37];

$$\frac{3}{2}(p_0 + a) - \frac{1}{2}(p_e + a) = m(p_i + a)(\frac{r_e}{r_i})^{-2(1-m)} \qquad [E.2.41]$$

From these two equations it follows that;

$$p_e + a = \frac{3}{1+2m}(p_0 + a) \qquad [E.2.42]$$

This determines the radial stress at the boundary between the plastic and the elastic regions.

Furthermore, it follows from [E.2.42] and [E.2.40] that;

$$(\frac{r_e}{r_i})^{2(1-m)} = \frac{1+2m}{3}\frac{p_i + a}{p_0 + a} \qquad [E.2.43]$$

This determines the radius of the plastic region.

A plastic region will develop when the right hand side of this equation is greater than 1.

$$p_i + a > \frac{3}{1+2m}(p_0 + a) = \frac{1+\sin\varphi}{1-\frac{1}{3}\sin\varphi}(p_0 + a) \qquad [E.2.44]$$

For smaller values of the pressure at the cavity boundary the entire field will be elastic.

Displacements

The displacements can be determined by starting from the solution in the elastic region, see 2.23;

$$r > r_e : u = \frac{(p_e - p_0)r_e^3}{4\mu r^2} \qquad [E.2.45]$$

This is an isochoric displacement (displacement without volume change – volume $= 4\pi r^2 u$, radial displacement u [E.2.45] is inversely proportional to r^2).

The displacement at the inner boundary of the elastic region is;

$$u_e = \frac{(p_e - p_0)r_e}{4\mu} \qquad \text{[E.2.46]}$$

With [E.2.42] and [E.2.43] this can also be written as;

$$u_e = \frac{(p_0 + a)r_i}{2\mu}\frac{1-m}{1+2m}\left[\frac{1+2m}{3}\left(\frac{p_i + a}{p_0 + a}\right)\right]^{1/2(1-m)} \qquad \text{[E.2.47]}$$

For the deformations in the plastic region it is assumed that there can be a certain volume change (by dilatancy), proportional to the shear strain. It can be expected that in this case of cavity expansion the radial displacement u will be positive, and that its magnitude will decrease as the distance r increases. (u/r- positive; du/dr – negative)

$$|\gamma| = |\varepsilon_{rr} - \varepsilon_{tt}| = \left|\frac{du}{dr} - \frac{u}{r}\right| = \frac{u}{r} - \frac{du}{dr} \qquad \text{[E.2.48]}$$

The volume change is now supposed to be;

$$e = \frac{du}{dr} + 2\frac{u}{r} = \left(\frac{u}{r} - \frac{du}{dr}\right)\sin\psi \qquad \text{[E.2.49]}$$

Where ψ is the dilatancy angle, positive for volume expansion. If $\psi = o$ the deformations will be isochoric. For positive values of ψ the right hand side of [E.2.49] will be positive, indicating a volume expansion.

The differential equation [E.2.49] can be integrated to give;

$$\frac{u}{u_e} = \left(\frac{r_e}{r}\right)^k \qquad \text{[E.2.50]}$$

Where the integration constant has been chosen such that $u = u_e$ for $r = r_e$ and where;

$$k = \frac{2 - \sin\psi}{1 + \sin\psi} \qquad \text{[E.2.51]}$$

The displacement of the cavity boundary now is, with [E.2.43];

$$\frac{u_i}{u_e} = \left(\frac{r_e}{r_i}\right)^k = \left[\frac{1+2m}{3}\frac{p_i + a}{p_0 + a}\right]^{k/2(1-m)} \qquad \text{[E.2.52]}$$

With [E.2.47] this gives finally;

$$\frac{u_i}{r_i} = \frac{p_0 + a}{2\mu}\frac{1-m}{1+2m}\left[\frac{1+2m}{3}\frac{p_i + a}{p_0 + a}\right]^{(k+1)/2(1-m)} \qquad \text{[E.2.53]}$$

This solution applies if the pressure at the cavity boundary is sufficiently high, so that a certain plastic region develops around the cavity. If this is not the case (factor between brackets is <1), the elastic solution remains;

$$p_i + a < \frac{3}{1+2m}(p_0 + a) \;:\; \frac{u_i}{r_i} = \frac{p_i - p_0}{4\mu} \qquad \text{[E.2.54]}$$

It can easily be verified that the two expressions give the same value when the plastic region starts to develop.

$$p_i + a = \frac{3}{1+2m}(p_0 + a) \;:\; \frac{u_i}{r_i} = \frac{p_0 + a}{2\mu}\frac{1-m}{1+2m} \qquad \text{[E.2.55]}$$

For the construction of a graphical representation of the displacement of the cavity boundary as a function of the pressure in the cavity, the equations can be written in dimensionless form by the introduction of the variables;

$$P = \frac{p_i + a}{p_0 + a} \qquad [E.2.56]$$

$$U = \frac{u_i}{r_i}\frac{2\mu}{p_0 + a} \qquad [E.2.57]$$

The solution can then be written as

$$P < \frac{3}{1+2m} : U = \frac{1}{2}(P-1) \qquad [E.2.58]$$

$$P = \frac{3}{1+2m} : U = \frac{1-m}{1+2m} \qquad [E.2.59]$$

$$P > \frac{3}{1+2m} : U = \frac{1-m}{1+2m}\left[\frac{1+2m}{3}P\right]^{(k+1)/2(1-m)} \qquad [E.2.60]$$

It is recalled that the parameters are defined as follows;

$$a = c\cot\varphi \qquad [E.2.61]$$

$$m = \frac{1-\sin\varphi}{1+\sin\varphi} \qquad [E.2.62]$$

$$k = \frac{2-\sin\psi}{1+\sin\psi} \qquad [E.2.63]$$

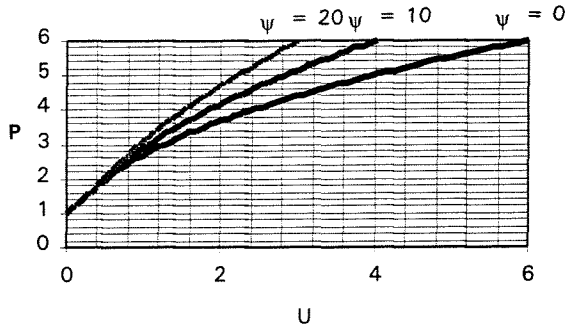

Figure 18: Expansion versus pressure, spherical cavity in infinite space

Figure 18 shows the relation between the dimensionless pressure P and the dimensionless displacement U, for the case that $\varphi = 30^0$, and for three values of dilatancy angle ψ.

Stresses

To give a graphical representation of the stresses, distinction must be made between the pressure in the cavity below the limit that produces plastic deformations, and above that limit. The limiting value of the pressure is $P = 3/(1+2m)$. Below this limit all deformations will be elastic, and the stresses are given by [E.2.25] and [E.2.26], with $r_e = r_{li}$ and $p_e = p_i$.

The parameters $s_{rr} = -\sigma_{rr}$ and $s_{tt} = -\sigma_{tt}$ are introduced to ensure positive parameters for pressure.

In dimensionless form the equations become;

$$1 < P < \frac{3}{1+2m} : \frac{s_{rr} + a}{p_0 + a} = 1 + (P-1)\frac{r_i^3}{r^3} \qquad [E.2.64]$$

$$1 < P < \frac{3}{1+2m} \;:\; \frac{s_{tt}+a}{p_0+a} = 1-(P-1)\frac{r_i^3}{r^3} \qquad \text{[E.2.65]}$$

Above this limit there will be two regions, a plastic region immediately around the cavity, and an elastic region outside, up to infinity. The boundary between these two regions is the radius r_e, which is determined by [E.2.43];

$$P > \frac{3}{1+2m} \;:\; (\frac{r_e}{r_i})^{2(1-m)} = \frac{1+2m}{3}\frac{p_i+a}{p_0+a} \qquad \text{[E.2.66]}$$

Using the definition [E.2.56] of P;

$$P > \frac{3}{1+2m} \;:\; \frac{r_e}{r_i} = [\frac{P}{3/(1+2m)}]^{1/2(1-m)} \qquad \text{[E.2.67]}$$

In the elastic region the stresses are given by [E.2.25] and [E.2.26];

$$P > \frac{3}{1+2m},\ r > r_e \;:\; \frac{s_{rr}+a}{p_0+a} = 1+(\frac{p_e+a}{p_0+a}-1)\frac{r_e^3}{r^3} \qquad \text{[E.2.68]}$$

$$P > \frac{3}{1+2m},\ r > r_e \;:\; \frac{s_{tt}+a}{p_0+a} = 1-\frac{1}{2}(\frac{p_e+a}{p_0+a}-1)\frac{r_e^3}{r^3} \qquad \text{[E.2.69]}$$

Substituting the value of $p_e + a$ from [E.2.43] into these equations gives;

$$P > \frac{3}{1+2m},\ r > r_e \;:\; \frac{s_{rr}+a}{p_0+a} = 1+\frac{2(1-m)}{1+2m}\frac{r_e^3}{r^3} \qquad \text{[E.2.70]}$$

$$P > \frac{3}{1+2m},\ r > r_e \;:\; \frac{s_{tt}+a}{p_0+a} = 1-\frac{1-m}{1+2m}\frac{r_e^3}{r^3} \qquad \text{[E.2.71]}$$

The value of r_e/r_{li} in these equations is given by [E.2.67], which shows that r_e will increase if the pressure in the cavity increases.

In the plastic region the stresses are given by [E.2.36] and [E.2.37];

$$P > \frac{3}{1+2m},\ r < r_e \;:\; \frac{s_{rr}+a}{p_0+a} = P(\frac{r}{r_i})^{-2(1-m)} \qquad \text{[E.2.72]}$$

$$P > \frac{3}{1+2m},\ r < r_e \;:\; \frac{s_{tt}+a}{p_0+a} = mP(\frac{r}{r_i})^{-2(1-m)} \qquad \text{[E.2.73]}$$

For the case $\varphi = 30^0$ the radial stresses are shown in Figure 19 for increasing values of the stress inside the cavity. The radial stress at the cavity boundary increases from p_o to $6p_o$. The quantity S shown in this figure has been defined as;

$$S = \frac{s_{rr}+a}{p_0+a} \qquad \text{[E.2.74]}$$

The tangential stresses for the same values of the radial stress at the cavity boundary are shown in Figure 20. The quantity T shown in this figure has been defined as;

$$T = \frac{s_{tt}+a}{p_0+a} \qquad \text{[E.2.75]}$$

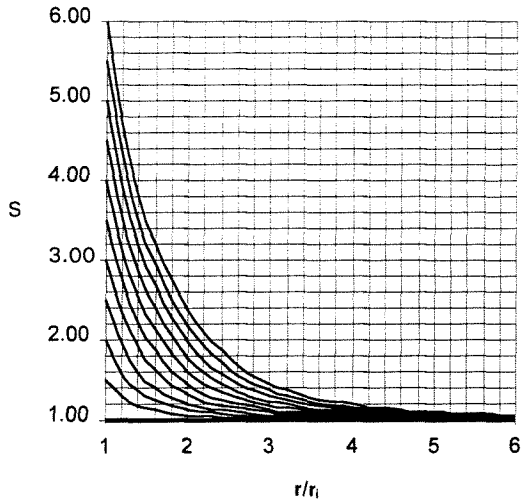

Figure 19: Spherical cavity in infinite space: radial stresses: S

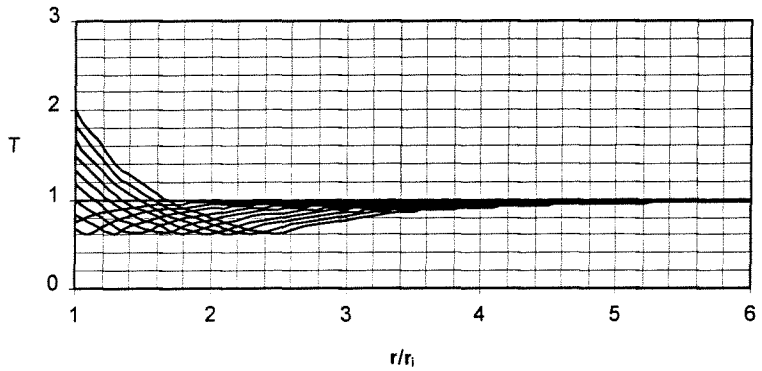

Figure 20: Spherical cavity in infinite space: tangential stresses: T

The stresses at the interface between the plastic and elastic zone, i.e. for $r = r_e$, are $S = 3/(1 + 2m)$ and $T = 3m/(1 + 2m)$. These values are always positive, and they are independent of the pressure in the cavity.

F COMPARING L&H TO STRAIN FAILURE CRITERION

In this appendix results given by the strain failure criterion will be compared to results given by Luger and Hergarden's radius of plastic zone criterion.

In chapter 3 of the report the shortcomings of the soil models at the basis of the criteria are outlined. It is therefore emphasised that the results of the calculations made and the conclusions drawn in this appendix should be treated carefully.

First a general case and a overview of the influence of parameters will be given. Next the results of BTL experiments involving maximum allowable pressures will be compared. For a description regarding these experiments reference is made to appendix C.

The following equations were used;

Luger and Hergarden

Maximum; $$p'_{max} = (p'_f + c \cdot \cot\varphi) \cdot \{(\frac{R_0}{R_{p,max}})^2 + Q\}^{\frac{-\sin\varphi}{1+\sin\varphi}} - c \cdot \cot\varphi$$

Limit; $$p'_{lim} = (p'_f + c \cdot \cot\varphi) \cdot Q^{\frac{-\sin\varphi}{1+\sin\varphi}} - c \cdot \cot\varphi$$

in which; $$p'_f = \sigma'_0(1+\sin\varphi) + c\cos\varphi \qquad \text{and} \qquad Q = \frac{(\sigma'_0 \cdot \sin\varphi + c \cdot \cos\varphi)}{G}$$

Maximum strain

Cylindrical cavity;

$$p_{i,max} = \left\{ \left[\varepsilon_{tt,max} \cdot \frac{2\mu}{p_0 + a} \cdot \frac{1+m}{1-m} \right]^{\frac{1-m}{k+1}} \cdot \frac{2}{1+m} \cdot (p_0 + a) \right\} - a$$

Spherical cavity:

$$p_{i,max} = \left\{ \left[\varepsilon_{tt,max} \cdot \frac{2\mu}{p_0 + a} \cdot \frac{1+2m}{1-m} \right]^{\frac{2(1-m)}{k+1}} \cdot \frac{3}{1+2m} \cdot (p_0 + a) \right\} - a$$

Reference

Reference is made to chapter two of the report and appendix D for the equations of Luger and Hergarden and its symbols. For maximum strain reference is made to chapter three and four of the report and appendix E.

F.1 Standard cases

F.1.1 Standard case

To get a feeling for numerical values, a standard case was defined;

Input values:

φ	$= 30^0$	$\rightarrow$ m = 1/3	σ_{soil}	= 10*20 = 200 kPa	soil stress
ψ	$= 0^0$	$\rightarrow$ k = 0	u	= 10*10 = 100 kPa	water pressure
c	= 0	$\rightarrow$ a = 0	σ'	= 200-100 = 100 kPa	effective stress
ν	= 1/3		p_o	assumed σ' = 100 kPa	
E	= 25000kPa		σ'_0	assumed $p_o = \sigma'$ = 100 kPa	
G	$= E/(2*(1+\nu)) = \mu$	$\rightarrow$ G = 9375kPa	R_0	= 0,2m	radius borehole
γ_{nat}	= 20 kN/m^3		$R_{p,\,max}$	= 10/1,5 = 6 $^2/_3$ m	radius plastic zone
h	= 10m	(depth boring)	$\varepsilon_{tt,\,max}$	2 and 5 %	maximum strain

Table 6: Input values standard case

With these values the maximum allowable stresses are calculated according to maximum allowable strain criterion (cylindrical and spherical) and according to Luger and Hergarden's failure criterion.

Output values:

Tangential strain – cylindrical – $p'_{i,\,max}$ (2%)	= 294	kPa $\rightarrow$	2.9	*p_o
Tangential strain – cylindrical – $p'_{i,\,max}$ (5%)	= 398	kPa $\rightarrow$	4.0	*p_o
Tangential strain – spherical – $p'_{i,\,max}$ (2%)	= 487	kPa $\rightarrow$	4.9	*p_o
Tangential strain – spherical – $p'_{i,\,max}$ (5%)	= 731	kPa $\rightarrow$	7.3	*p_o
Luger& Hergarden – p'_{max}	= 815	kPa $\rightarrow$	8.2	*p_o
Luger& Hergarden – p'_{lim}	= 860	kPa $\rightarrow$	8.6	*p_o

Table 7: Output values standard case

Conclusions

The values calculated with the strain criterion are much more conservative. This is a result of the possibility to introduce a more conservative upper limit by changing the maximum strain.

F.1.2 Variation of parameters

To give an impression of the importance of different parameters in the failure criterion as defined by Luger and Hergarden and as defined for maximum strain the parameters are varied. A standard case is defined (Table 8) and one parameter (one at a time) is enlarged with 25%.

Parameters varied

Parameter	standard	variation
p'_o or σ'_0	75 kPa	not varied directly
depth	10m	10-12.5
φ	30^0	30-37.5
E	10 000 kPa	10 000-12500
ψ	0^0	10-12.5
c	0 kPa	10-12.5
R_o	0.075m	0.075-0.094
γ	(20-10) kPa	18-22.5

Table 8: Standard case and variation

Graph and Table

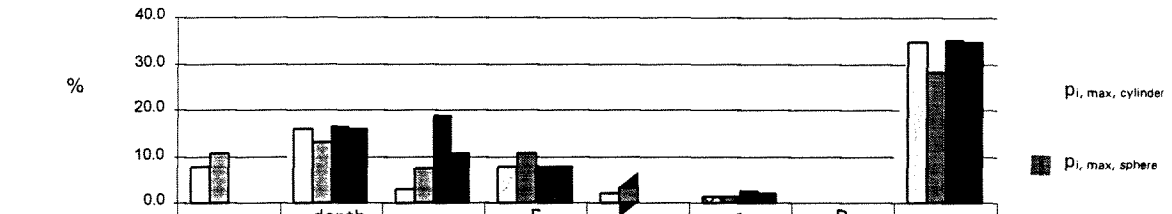

	ε	depth	φ	E	ψ	c	R_0	γ
$p_{i,\ max,\ cylinder}$	7.7	16.0	2.7	7.7	2.0	1.1	0.0	34.7
$p_{i,\ max,\ sphere}$	10.4	13.2	7.5	10.4	3.1	1.3	0.0	28.1
L&H - p'_{max}	0.0	16.3	18.7	7.6	0.0	2.5	-0.2	34.9
L&H - p'_{lim}	0.0	16.0	10.7	7.7	0.0	2.1	0.0	34.7

Figure 21: Variation of parameters

Conclusions

Though the results in Figure 21 should be treaded carefully as the parameters are not linear, one can see that almost all parameters have more or less the same influence in the compared criteria. The same can be seen later on in paragraph F.5 'BTL 46 – Monitoring projects HDD' where for the compared failure criteria graphs are presented (Figure 24, Figure 26, Figure 28).

F.2 BTL 21 – Sight experiment*

In the sight experiment in the dredging flume of Delft Hydraulics a blow out was enforced in sand. It could not be enforced in clay. In clay a blockage failed as each time the return flow restarted.

The fluid pressures in the borehole were registered with a pressure meter, penetrated in the borehole from the surface. The sand was densified and therefore very solid and firm. The drilling was performed rather shallow (but still ten times the diameter of the drill head). The fluid pressures were higher than expected. It was measured that the pressure was higher than 3.5 bar. It was estimated that the failure pressure was 4.5 bar at the moment that the blow out actually occurred.

The drill head was not moved anymore, but the drilling fluid flow was maintained, the return flow was blocked. Therefore the values found with the equation for a sphere should match best.

F.2.1 Numerical values BTL 21

Default values

Default-values sand assumed in BTL21 (based on table 6.6 – BTL21)

Default value	value	unit
Diameter borehole	100	mm
Angle of internal friction - φ	35	^{0}
Poisson's ratio - ν	0.30	-
Elasticity modulus – E	100 000	kPa
Cohesion – c	0	kPa
Cover	1000	mm
Maximum radius plastic zone - $R_{p,\,max}$	1000	mm
Unit weight soil – γ	20	kN/m^3
tangential strain (assumed) – $\varepsilon_{tt,\,max}$	2	%
Dilatancy angle (assumed) – ψ	0	^{0}

Table 9: Default values BTL21

$R_{p,\,max}$ was taken until ground surface instead of 2/3 of the depth

* Reference is made to appendix C, in which the research performed within the framework of BTL is discussed more extensively.

Results

Results default-values sand (based on table 6.9 – BTL21):

Default value	value	unit
$\sigma'_{vertical}$	10	kPa
$\sigma'_{horizontal}$	4.26	kPa
$\sigma'_{average}$	7.13	kPa
G	38 460	kPa
P'_f	11.22	kPa
P'_{max}	59.90	kPa
P'_{lim}	315.04	kPa
$P'_{i,\ max,\ sphere}$	272	kPa
$P'_{i,\ max,\ cylinder}$	97	kPa

Table 10: Results default values BTL21

All values of allowable pressures were calculated with $\sigma'_{average}$.

Sensitivity analysis

Sensitivity analysis parameters sand (based on table 6.10 – BTL21):

Varied parameter		P'_f kPa	P'_{max} kPa	P'_{lim} kPa	$P'_{i,\ sphere}$ kPa	$P'_{i,\ cyl}$ kPa
Angle of internal friction	40	11.15	67.27	389.88	335	110
θ	45	11.04	73.98	466.21	400	125
Elasticity modulus – E	80000	11.22	59.84	290.43	244	90
kPa	120000	11.22	59.94	336.69	297	105
Cohesion – c	0.5	11.63	65.16	334.02	285	103
kPa	1	12.04	70.41	352.56	297	108
Cover	800	8.98	40.80	273.39	243	85
mm	1200	13.47	81.87	353.74	299	109
$\varepsilon_{tt,\ max}$	0.5	-	-	-	139	59
%	5	-	-	-	425	113
ψ	5	-	-	-	353	80
^{0}	10	-	-	-	456	67

Table 11: Sensitivity analysis parameters BTL 21

Conclusion

The results of the equation for maximum strain, spherical cavity matches best for this experiment compared to the results of the other equations. Although it seems that a larger strain than 2% and / or some dilatancy should be introduced.

F.2.2 Volume calculations

During the experiment a volume of mud was pumped into the soil, which was measured with a flow meter. In the following subparagraph it is tried to compare this volume to the strain of the 'balloon'. It was measured in experiment 27 of BTL 21 that approximately 75litre mud was pumped into the soil. To calculate the dimensions of the sphere, which represent this volume, the following is assumed:

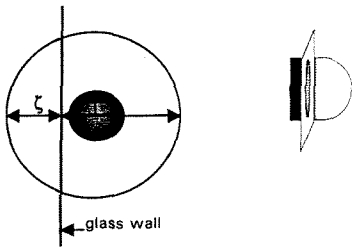

Figure 22: Representation of partial sphere

(1) the volume is a partial sphere (see Figure 22), (2) the infiltration of the mud into the surrounding sand is not hindered (about 50mm), (3) the wall of the borehead is neglected. The volume is assumed to be a perfect partial sphere, (4) the diameter of the borehead is 70mm, (5) the distance between the borehead and the glass wall is assumed to be 15mm

Calculation (iterative): Assuming a sphere of 620mm gives a volume of 125l - the value of ζ -> 620/2-70/2-15 = 260mm. Volume of 'dome' than is 48l - the volume of the partial sphere = 125l-48l = 77l

The radius of this sphere would therefor be 310mm. The part of the soil hydraulically excavated is assumed to be at maximum 200mm around the borehead. With this the tangential strain becomes approximately: (310-50*-200)/200mm*100% = 30%

This gives excessive values. Nevertheless in this experiment very large strain rates occurred before failure due to fracturing actually took place. This maybe due to the exceptional test conditions, therefore the test results cannot be transferred reliably to practice.

* distance that the mud has infiltrated

F.3 BTL 48 – Blow out experiments*

Scale tests were performed at GeoDelft Laboratory in which the main parameter, fluid pressure, was not scaled. The purpose of these tests was to examine how sand fails and to get more quantitative results regarding this failure process.

Fracturing was observed again. The peak pressure was more or less the same in each test, after that the pressure developed differently. It was concluded that the first crack develops at the measured peak pressure. This peak pressure was in the range of 370-400kPa. The initial stress was estimated to be in the range of 120-200kPa. (the pressure at the upper plate was 200kPa – friction could be a reason for a smaller pressure at the inside of the soil volume).

In the test situation a cylindrical cavity was introduced. Therefore the values of the L&H-equations can be better compared, since these are derived for a cylindrical cavity.

Default values (assumed in BTL48)

Default value	value	unit
Diameter borehole	30	mm
Angle of internal friction - φ	40	^{0}
Poisson's ratio - ν	0.26	-
Elasticity modulus – E	15000	kPa
Cohesion – c	0	kPa
σ'_0	160	kPa
Maximum radius plastic zone - $R_{p,\,max}$	300	mm
tangential strain (assumed) – $\varepsilon_{tt,\,max}$	2	%
dilatancy angle (assumed) – ψ	0	^{0}

Table 12: Default values BTL48

The calculations presented in BTL 48 only showed the results found using the equation for 0.9*limit pressure of L&H.

Results default values

Default value	Value	unit	
G	5938	kPa	
P'_f	263	kPa	
P'_{max}	1075	kPa	
P'_{lim}	780	kPa	
$0.9*P'_{lim}$	700	kPa	
$P'_{i,\,max,\,sphere}$	564	kPa	not relevant – cylinder mechanism
$P'_{i,\,max,\,cylinder}$	365	kPa	

Table 13: Results default values BTL48

* Reference is made to appendix C, in which the research performed within the framework of BTL is discussed more extensively.

Sensitivity analysis

Varied parameter		P'_f kPa	P'_{max} kPa	P'_{lim} kPa	$0.9*P'_{lim}$ kPa	$P'_{i,\ cyl}$ kPa
Angle of internal friction	35	250	950	725	650	350
°	45	275	1200	835	750	375
Elasticity *modulus* – E	10000	263	965	667	600	310
Kpa	20000	263	1150	875	790	410
Cohesion – c	0.5	263	1075	780	705	365
Kpa	1	264	1080	785	710	365
σ'_0	120	197	860	660	590	306
Kpa	200	330	1270	895	805	415
$\varepsilon_{tt,\ max}$	0.5	-	-	-	-	212
%	5	-	-	-	-	523
ψ	5	-	-	-	-	375
°	10	-	-	-	-	386

Table 14: Sensitivity analysis parameters BTL 48

Conclusions

The pressure computed with the equation for maximum strain gives results that are comparable to the measured values for maximum allowable pressure (2% strain). Some dilatancy could play a role, but does not have a large influence.

F.4 BTL 47 – Attempt to enforce blow out*

On the site of a contractor (Visser & Smit Hanab) a few tests have been done. The results where published in BTL 47. A blow out at great depth (10m) was not achieved. In each test the drill head (after having drilled until more or less to the right depth) was pushed further in the soil without pumping drilling fluid to block the return flow (as in BTL 21). Therefore the mechanism should resemble most the mechanism for a spherical cavity.

In BTL 54 additional calculations where made for these tests and the tests of BTL 21. Parameters mentioned in this paragraph have been derived from this report (BTL 54).

In the following soil was drilled (from surface down):
1. Terrain was raised with about 3m of sand in the past (top layer)
2. Clay-peat layer - 1 to 2 metres
3. Sand layer with clay – 2 to 3 metres
4. Clay-peat layer – 1 to 2 metres
5. From about 8m minus ground surface - sand

The ground water level is about 3.7m minus the surface

F.4.1 Calculations experiment 1 and 2

First experiment:
In the first test the return flow was successfully blocked at a depth of over 9 metres. However, in spite of the large volume of drilling fluid enforce, a blow-out to the ground surface did not occur. A volume of 4.88 m^3 was pumped in the ground. The measured fluid pressure in the borehole was 2.1 bar.
Second experiment:
During the second test a block of the return flow was not achieved (depth over 9 metres); at 2 bar return flow.

In these calculations it is assumed that the measured fluid pressures represent the soil failure pressure.

Default values

Default value	Value	unit
Depth drill head (ground level)	-9.4	m
Diameter borehole	0.075	m
Maximum radius plastic zone - $R_{p,\,max}$	9.4	m
Angle of internal friction - φ	30	^{0}
Poisson's ratio - ν	0.33	-
Elasticity modulus – E	10 000	kPa
Cohesion – c	0	kPa
effective soil pressure - σ'_0	63.4	kPa
Water tension – u_0	55	kPa
tangential strain (assumed) – $\varepsilon_{tt,\,max}$	2	%
dilatancy angle (assumed) – ψ	0	^{0}

Table 15: Default values BTL 47 – experiment 1&2

* Reference is made to appendix C, in which the research performed within the framework of BTL is discussed more extensively.

Results default values

Default value	value	unit
G	3750	kPa
P'_f	150	kPa
P_{max}	520	kPa
P_{lim}	366	kPa
$P_{i, max, sphere}$	251	kPa
$P_{i, max, cylinder}$	215	kPa

Table 16: Results default values BTL 47 – experiment 1&2

Sensitivity analysis parameters

Varied parameter		P_{max} kPa	P_{lim} kPa	$P_{i, sphere}$ kPa	$P_{i, cyl}$ kPa
Angle of internal friction	35	600	429	273	225
°	40	680	435	293	232
Elasticity modulus – E	8 000	488	345	228	203
kPa	12 000	550	386	273	225
Cohesion – c	0.5	525	368	252	215
kPa	1	527	370	254	216
σ'_0	50	505	355	244	209
kPa	70	555	385	266	225
$\varepsilon_{tt, max}$	0.5	-	-	136	155
%	5	-	-	377	217
ψ	5	-	-	269	167
°	10	-	-	288	175

Table 17: Sensitivity analysis parameters BTL 47– experiment 1&2

Conclusions

The results found are comparable to the measured values.

F.4.2 Calculations experiment 3

In the third test (depth 3.35m) the return flow was blocked as in the first test. No large pressure increase was registered. Probably the soil was pushed aside (soil displacement) at the measured pressure of 0.5bar.

In these calculations it is assumed that the measured fluid pressures represent the soil failure pressure.

Default values

Default value	Value	unit
Depth drill head (ground level)	-3.35	M
Diameter borehole	0.075	M
Maximum radius plastic zone - $R_{p, max}$	3.35	M
Angle of internal friction - φ	25	°
Poisson's ratio - ν	0.37	-
Elasticity modulus – E	5000	kPa
Cohesion – c	5	kPa
effective soil pressure - σ'_0	42.7	kPa
water tension – u_0	0	kPa
tangential strain (assumed) – $\varepsilon_{tt, max}$	2	%
dilatancy angle (assumed) – ψ	0	°

Table 18: Default values BTL 47 – experiment 3

Results default values

Default value	Value	unit
G	1830	kPa
P'_f	65	kPa
P_{max}	270	kPa
P_{lim}	166	kPa
$P_{i,\ max,\ sphere}$	144	kPa
$P_{i,\ max,\ cylinder}$	97	kPa

Table 19: Results default values BTL 47 – experiment 3

Sensitivity analysis parameters:

Varied parameter		P_{max} kPa	P_{lim} kPa	$P_{i,\ sphere}$ kPa	$P_{i,\ cyl}$ kPa
Angle of internal friction	20	224	165	136	92
°	30	310	206	151	101
Elasticity modulus – E	4000	249	174	131	90
kPa	7500	300	212	171	111
Cohesion – c	0	236	168	135	92
kPa	15	320	218	158	105
σ'_0	35	237	166	131	86
kPa	50	293	205	157	107
$\varepsilon_{tt,\ max}$	0.5	-	-	79	61
%	5	-	-	212	130
ψ	5	-	-	152	100
°	10	-	-	160	103

Table 20: Sensitivity analysis parameters BTL 47– experiment 3

Conclusions

The results found are too high compared to the measured values. However if a smaller strain is allowed the measured pressures can be better approached.

F.4.3 Calculations experiment 5

In this last test a blow-out was achieved. However this was a "shallow" blow out (depth 1m). In this case the cavity expansion theory is not valid. The measured pressure was 0.2bar.

Default values:

Default value	Value	unit
Depth drill head (ground level)	-1.04	m
Diameter borehole	0.075	m
Maximum radius plastic zone - $R_{p,\ max}$	1,0	m
Angle of internal friction - φ	30	°
Poisson's ratio - ν	0.33	-
Elasticity modulus – E	3000	kPa
Cohesion – c	0	kPa
effective soil pressure - σ'_0	12.8	kPa
water tension – u_0	0	kPa
tangential strain (assumed) – $\varepsilon_{tt,\ max}$	2	%
dilatancy angle (assumed) – ψ	0	°

Table 21: Default values BTL 47 – experiment 5

Results default values

Default value	value	unit
G	1125	kPa
P'_f	19	kPa
P_{max}	86	kPa
P_{lim}	72	kPa
$P_{i,\ max,\ sphere}$	61	kPa
$P_{i,\ max,\ cylinder}$	37	kPa
P_{wedge}	51	kPa

Table 22: Results default values BTL 47 - experiment 5

For 'shallow' parts of the drilling the proposed failure mechanism is a wedge that is 'pushed out the soil'. The following calculation can be made.

$$p_{wedge,max} = u_0 + \gamma' \cdot H \cdot (1 + 0.3\frac{H}{D})$$

$$p_{wedge,max} = 0 + 17{,}1 \cdot (1 + 0.3\frac{1}{0.15}) = 51\,kN/m^2$$

$p_{wedge,\ max}$	maximum allowable pressure according to 'wedge' approach
u_0	initial water pressure
γ'	effective soil density
H	depth of drilling (height soil above drilling)
D	diameter drill head

Sensitivity analysis parameters

Varied parameter		P_{max} kPa	P_{lim} kPa	$P_{i,\ sphere}$ kPa	$P_{i,\ cyl}$ kPa
Angle of internal friction	35	101	81	67	39
°	40	117	90	73	42
Elasticity modulus - E	2500	83	67	56	35
KPa	3500	88	75	65	39
Cohesion - c	0.5	89	74	62	38
KPa	1	93	76	63	38
σ'_0	10	69	61	53	31
KPa	15	97	80	66	41
$\varepsilon_{tt,\ max}$	0.5	-	-	33	23
%	5	-	-	91	50
ψ	5	-	-	66	39
°	10	-	-	72	41

Table 23: Sensitivity analysis parameters BTL 47- experiment 5

Conclusions

The results found are too high compared to the measured values. However if a smaller strain is allowed the measured pressures can be better approached (even better than the 'wedge').

F.4.4 Conclusions BTL 47 - Attempt to enforce blow out

It seems possible to approach the measured fluid pressures with the strain criterion for a sphere. However it seems that a smaller strain than 2% is justifiable. However during the experiment probably soil stratification was the cause that in spite of the large quantities of fluid applied, no deep blow out could be achieved. Instead internal fluid losses occurred. It is therefore difficult to draw conclusions.

F.5 BTL 46 – Monitoring projects HDD*

monitoring three projects – Noordzeekanaal, Ringvaart and Blerick

In the framework of BTL three drilling projects were monitored to evaluate developed theory with measured values. As a hind cast using the actual applied operational parameters, calculations where made with the computer program, Geboor (BTL51). In this paragraph the results of Geboor, regarding maximum allowable pressures and occurring pressures during the drilling, are presented graphical, as a function of drilling distance, next to the calculations made with the new developed failure-criterion.

For the parameters the following assumptions are used;

- The soil pressure for σ'_0 or p_0 is assumed to be $\sigma'_{average} = (\sigma'_{vert} + \sigma'_{hor})/2$
- The other characteristics needed for the equation are chosen depending on the layer in which is drilled. (local, no averaging soil parameters)

Values of parameters were based on soil investigation done by Geodelft.

* Reference is made to appendix C, in which the research performed within the framework of BTL is discussed more extensively.

F.5.1 Noordzeekanaal

Soil

The following soil profile has been imported into the computer program Geboor:

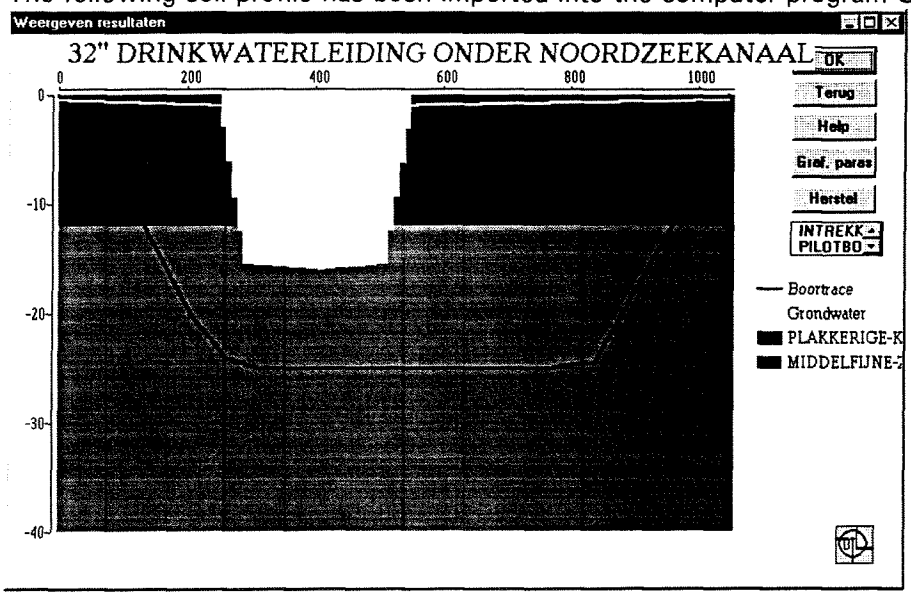

Figure 23: Soil profile Noordzeekanaal (Geboor)

Graph

This results in the following graph for the drilling fluid pressures;

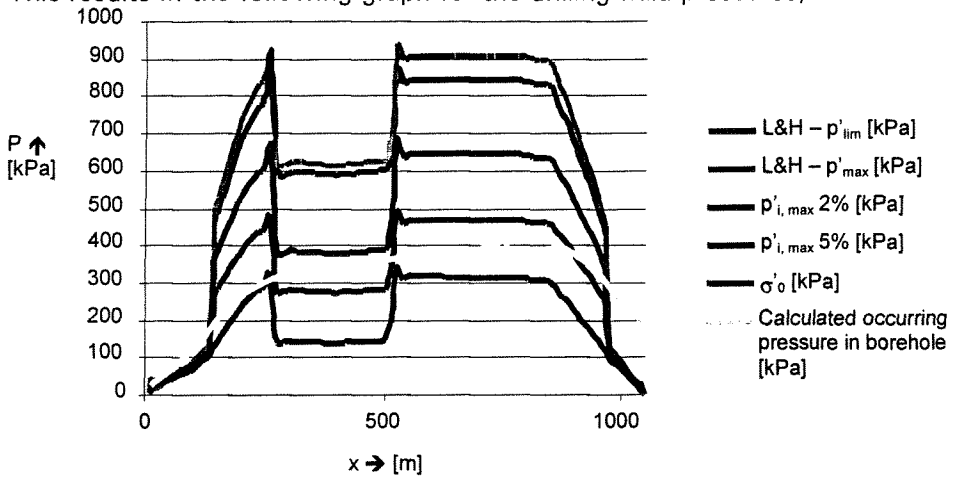

Figure 24: Maximum allowable pressures Noordzeekanaal

Conclusions

Both graphs computed for maximum strain (2% and 5%) seem to be above the calculated occurring pressure in the borehole, except for the part under the Noordzeekanaal (2%). However the fluid pressures during this drilling, were not measured.

F.5.2 Ringvaart

Soil

The following soil profile has been imported into the computer program Geboor:

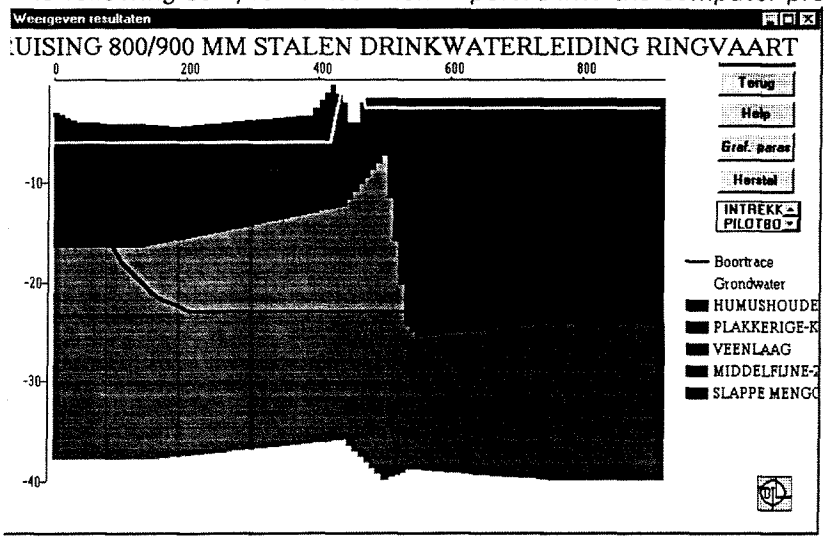

Figure 25: Soil profile Ringvaart (Geboor)

Graph

This results in the following graph for the drilling fluid pressures;

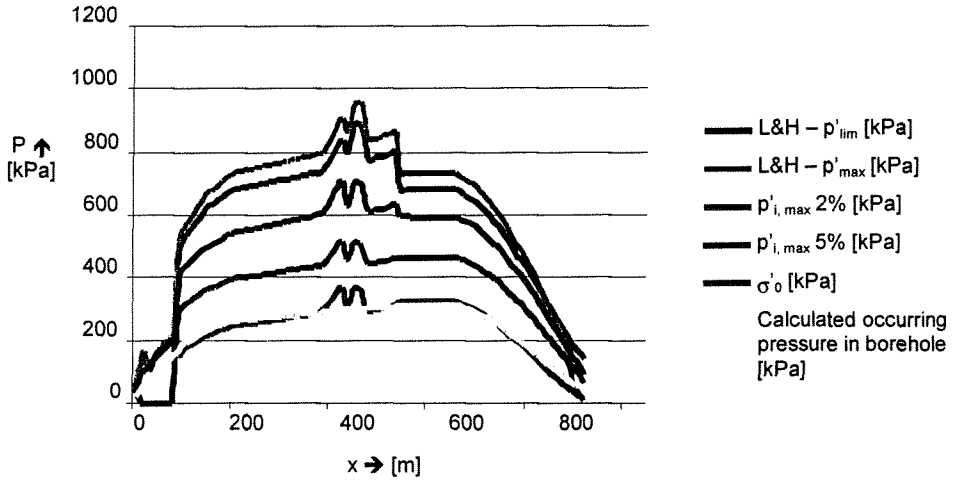

Figure 26: Maximum allowable pressures Ringvaart

Conclusions

Both graphs computed for maximum strain (2% and 5%) seem to be above the calculated occurring pressure in the borehole. However the maximum measured pressure was 5 bar. The 'grey' line should probably be 'higher'. The calculated occurring pressure in the borehole can probably better match the measured pressure if a smaller borehole had been assumed in the calculations for occurring pressure (0.15m instead of 0.3m). In that case the strain criterion of 2% would be too conservative.

F.5.3 Blerick

Soil

The following soil profile has been imported into the computer program Geboor:

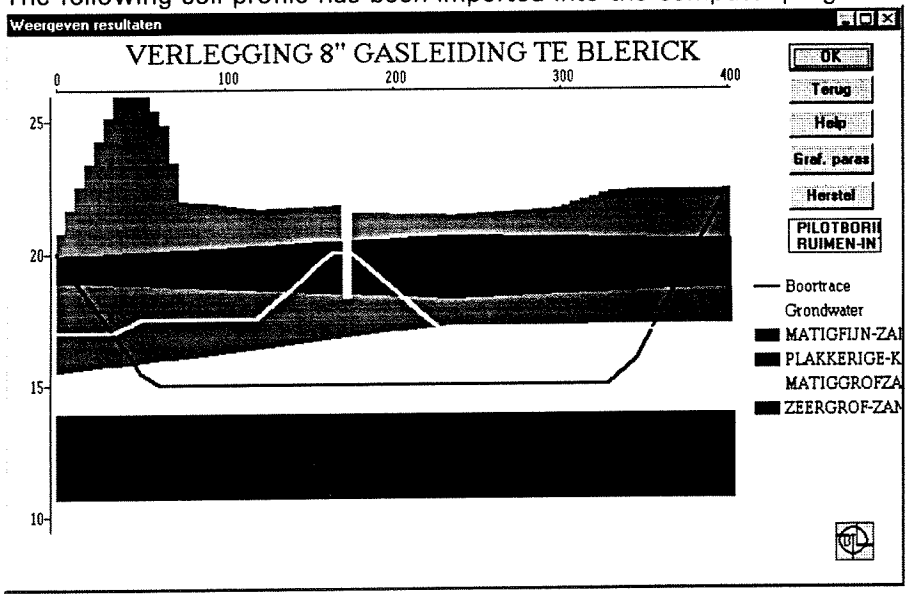

Figure 27: Soil profile Blerick (Geboor)

Graph

This results in the following graph for the drilling fluid pressures;

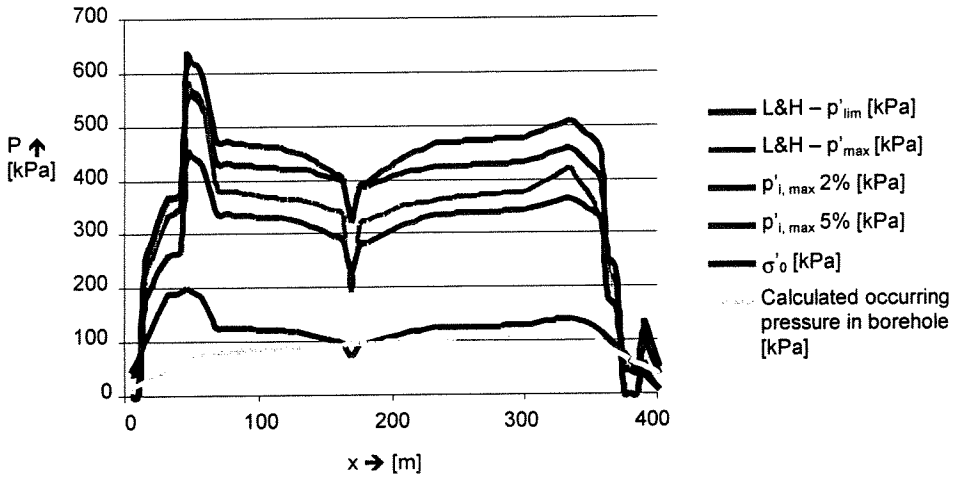

Figure 28: Maximum allowable pressures Blerick

Conclusions

Both graphs computed for maximum strain (2% and 5%) seem to be above the calculated occurring pressure in the borehole. However the maximum measured pressure was 2 bar. The 'grey' line should probably be 'higher'. The calculated occurring pressure in the borehole can probably better match the measured pressure if a smaller borehole had been assumed in the calculations for occurring pressure (0.15m instead of 0.3m).